



جمهورية العراق  
وزارة التعليم العالي والبحث العلمي  
جامعة بابل  
كلية التربية للعلوم الصرفة  
قسم الفيزياء

## استقصاء بعض الخواص الفيزيائية للمترابكات النانوية (PVA-PVP-CO<sub>2</sub>O<sub>3</sub>) وتطبيقها المضاد للبكتريا

رسالة مقدمة

الى مجلس كلية التربية للعلوم الصرفة في جامعة بابل  
وهي جزء من متطلبات نيل درجة الماجستير  
في التربية / فيزياء

من قبل الطالب

**احمد هاشم محمد رشك**

بكالوريوس تربية فيزياء  
جامعة بابل 2002 م

بإشراف

**أ. د. مجيد علي حبيب**

2022م

1444هـ

**Republic of Iraq  
Ministry of Higher Education  
& Scientific Research  
University of Babylon  
College of Education for Pure Sciences  
Department of Physics**



# **Investigation of Some Physical Properties of (PVA-PVP-Co<sub>2</sub>O<sub>3</sub>) Nanocomposites with Antibacterial Application**

A Thesis

Submitted to The Council of The College of Education  
For Pure Sciences, University of Babylon in Partial  
Fulfillment of Requirements for The Degree  
of Master in Education / Physics

By

**Ahmed Hashim Mohammad Reshaq**

B.Sc. in physics  
University of Babylon (2002)

Supervised by

**Prof. Dr. Majeed Ali Habeeb**

**2022 A.D**

**1444 A.H**

بِسْمِ اللَّهِ الرَّحْمَنِ الرَّحِيمِ

﴿شَهِدَ اللَّهُ أَنَّهُ لَا إِلَهَ إِلَّا هُوَ

وَالْمَلَائِكَةُ وَأُولُو الْعِلْمِ قَائِمًا بِالْقِسْطِ لَا

إِلَهَ إِلَّا هُوَ الْعَزِيزُ الْحَكِيمُ﴾

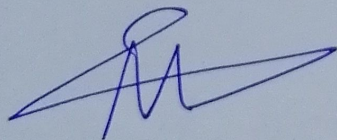
صدق الله العلي العظيم

سورة آل عمران  
(الآية 18)

# Scientific Supervisor Certification

This is to certify that I have read this thesis entitled " Investigation of Some Physical Properties of (PVA-PVP-Co<sub>2</sub>O<sub>3</sub>) Nanocomposites with Antibacterial Application" and I found that this thesis is qualified for debate.

Signature:



Name: Dr.

Adel H. Omran AlKhyatl

Title: Professor

Address: University of Kufa

Date: / / 2022

## Scientific Supervisor Certification

This is to certify that I have read this thesis entitled " Investigation of Some Physical Properties of (PVA-PVP-Co<sub>2</sub>O<sub>3</sub>) Nanocomposites with Antibacterial Application" and I found that this thesis is qualified for debate.

Signature: S. A. Hussain

Name: Dr. Prof. Dr. Saleem Azava Hussain

Title: Professor

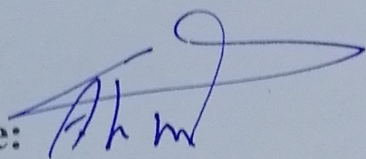
Address: University of Qadisiyah

Date: / / 2022

# Linguistic Supervisor Certification

This is to certify that I have read this thesis entitled " **Investigation of Some Physical Properties of (PVA-PVP-Co<sub>2</sub>O<sub>3</sub>) Nanocomposites with Antibacterial Application**" and I found that this thesis is qualified for debate.

Signature:



**Name: Dr. Ahmed Rawdhan Salman**

**Title: Assitant Professor**

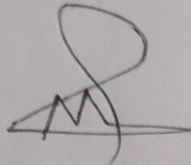
**Address: University of Babylon**

**Date: / / 2022**

## *Supervisor Certificate*

I certify that this thesis entitled " **Investigation of Some Physical Properties of (PVA-PVP-Co<sub>2</sub>O<sub>3</sub>) Nanocomposites with Antibacterial Application**" is prepared by the student (**Ahmed Hashim Mohammad**) under my supervision at the College of Education for Pure Sciences , University of Babylon as partial fulfillment of the requirements for the degree of **Master in Education/Physics**.

Signature :



Name : Dr. Majeed Ali Habeeb

Title : Professor

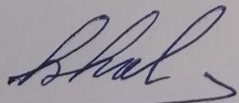
(Supervisor)

Date : / /2022

## *Head of the Department Certification*

In view of the available recommendation , I forward this thesis for debate by the examining committee .

Signature :



Name :

Title : Professor

(Head of Physics Department)

Date : / /2022



**Dedication**

*To mesopotamia(Iraq) with honour and dignity...  
To those, Who lost their lives in a war without committing any  
crime...*

*To my first and dearest teacher my father...  
To my mother whose love is planted in my heart...*

*To my brothers and sisters...*

*To my close friends*

*To my teachers*

*Who provide me the keys of success*

*Ahmed*



## *Acknowledgements*

First of all thanks to my God for helping me to complete this thesis, then, I would like to express my sincere appreciation and deep gratitude to my supervisor, Prof .**Dr. Majeed Ali Habeeb** for suggesting the topic of this thesis, guidance, suggestions and continuous encouragement throughout the research work.

A word of thanks is due to staff members of the physics department in the college of education for pure sciences and to the dean of the college of education for pure sciences at university of babylon for their help and kind assistance. I want to thank my family and all those who helped me, even if a word. I would like to thank Prof. **Dr. Ahmed Hashim Mohaisen** for encouragement and support.

Finally, I would like to express my thanks to all my friends and to all the people who helped me, in one way or another to complete this study and I ask Allah to help them all.

*Ahmed*

## *Abstract*

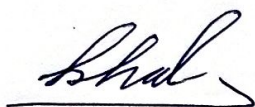
In this study, (PVA-PVP-Co<sub>2</sub>O<sub>3</sub>) nanocomposites have been prepared using casting method with different weight percentages of cobalt oxide nanoparticles (1.6, 3.2, 4.8, and 6.4) wt.%. The (PVA-PVP-Co<sub>2</sub>O<sub>3</sub>) nanocomposites have been diagnosed by different methods such as optical microscope images, Fourier transform infrared rays (FTIR) and scanning electron microscope (SEM) images. The experimental results for photos of optical microscope show distribution of cobalt oxide nanoparticles atoms for all nanocomposites films, it is also show a continuous network of ions inside the polymers in ratio of (6.4 wt.%) of cobalt oxide nanoparticles. Also, the experimental results (FTIR) showed increasing the value of the absorbance of the (PVA-PVP-Co<sub>2</sub>O<sub>3</sub>) nanocomposites with increase in the proportion of cobalt oxide nanoparticles. All peak characteristics remain the same and the most bond in the same wavenumber. The morphology of the (PVA-PVP-Co<sub>2</sub>O<sub>3</sub>) nanocomposites films has been studied using (SEM) technique, which showed a good distribution and homogeneous in surface morphology with increasing of cobalt oxide nanoparticles. The results of optical properties of the nanocomposites show that the absorbance increases when increasing the concentration of cobalt oxide nanoparticles. The (PVA-PVP-Co<sub>2</sub>O<sub>3</sub>) nanocomposites have high absorbance in the (UV-Region) and low absorbance in the (Vis-Region) and (IR-Region), the electronic transitions in the films are indirect (allowed and forbidden) at all concentrations. The refractive index, extinction coefficient, and the dielectric constant (real and imaginary part) increase with increasing the concentration of the cobalt oxide nanoparticles. The energy gap decreases with the increase of the

concentration of the cobalt oxide nanoparticles. The optical conductivity increase with the increasing concentration of  $\text{Co}_2\text{O}_3$  nanoparticles. The A.C electric properties show that the dielectric constant and dielectric loss of the nanocomposites decrease with increasing the frequency of applied electrical field and they increase with the increase of the concentration of cobalt oxide nanoparticles, the A.C electrical conductivity increases with increasing the concentration of cobalt oxide nanoparticles, frequency, and almost constant at high frequency. The antibacterial properties of the (PVA-PVP-  $\text{Co}_2\text{O}_3$ ) nanocomposites were tested against gram positive (*S. aureus*) and gram negative (*E. coli*). The results showed the inhibition zone was increased with increase the concentrations of  $\text{Co}_2\text{O}_3$  nanoparticles.

## Examining Committee Certification

We certify that we have read this thesis entitled (**Investigation of Some Physical Properties of (PVA-PVP-Co<sub>2</sub>O<sub>3</sub>) Nanocomposites with Antibacterial Application**) and as committee , examined the student (**Ahmed Hashim Mohammad**) its contents and that in our opinion it meets the standards of a thesis for the degree of Master in Education/Physics.

Signature :



Name : **Dr. Khalid Haneen Abass**

Title : Professor

Date : / /2022

(Chairman)

Signature :



Name : **Dr. Ali R. Abdulridha**

Title : Professor

Date : / /2022

(Member)

Signature :



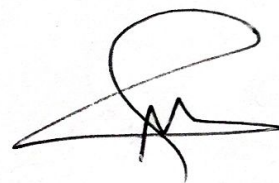
Name : **Dr. Abdulhussain Abbas Khadayeir**

Title : Professor

Date : / /2022

(Member)

Signature :



Name : **Dr. Majeed Ali Habeeb**

Title : Professor

Date : / /2022

(Member/Supervisor)

**I hereby certify the decision of the examining committee**

Signature :

Name : **Dr. Bahaa Hussein Salih Rabee**

Title : Professor

Address : Dean of the College of Education for Pure Sciences .

Date : / /2022

## الخلاصة

في هذه الدراسة، تم تحضير المترابك النانوي (PVA-PVP-CO<sub>2</sub>O<sub>3</sub>) باستخدام طريقة الصب مع نسب وزنية مختلفة من اوكسيد الكوبلت النانوي (1.6, 3.2, 4.8, and 6.4) wt%. وقد تم تشخيص أغشية المترابك النانوية (PVA-PVP-CO<sub>2</sub>O<sub>3</sub>) وبطرق مختلفة مثل المجهر الضوئي والتحليل الطيفي للأشعة تحت الحمراء (FTIR) وصور المجهر الإلكتروني الماسح (SEM). أظهرت النتائج التجريبية بأن صور المجهر الضوئي توضح توزيع ذرات اوكسيد الكوبلت النانوية لجميع أغشية المترابك النانوي. ويبين تكون شبكة مستمرة من الأيونات داخل البوليمرين عند النسبة (6.4 wt.%) من اوكسيد الكوبلت النانوي. كذلك بينت النتائج التجريبية بالنسبة (FTIR) زيادة في قيمة الامتصاصية للمترابك النانوي (PVA-PVP-CO<sub>2</sub>O<sub>3</sub>) مع زيادة في نسبة جسيمات اوكسيد الكوبلت النانوية ولا تلاحظ تكون قمم جديدة وأغلب أواصر البوليمرات لا تتغير مع تغير نسب المضاف أو مع العدد الموجي. وقد تمت دراسة مورفولوجية السطح لأغشية المترابك النانوي باستخدام تقنية المجهر الإلكتروني الماسح (SEM)، و الذي أظهر التوزيع الجيد والمتجانس للجسيمات النانوية على مورفولوجية السطح. أظهرت نتائج الخصائص البصرية للمترابك النانوي زيادة الامتصاصية عند زيادة تركيز جسيمات اوكسيد الكوبلت النانوي للمترابك المحضر وامتصاصية عالية في منطقة الموجات فوق البنفسجية (UV-Region) وامتصاصية قليلة في منطقة الضوء المرئي (Vis-Region) والمنطقة تحت الحمراء (IR-Region) ، والانتقالات الالكترونية في الاغشية تكون غير مباشرة (مسموحة و ممنوعة) في جميع التراكيز. أما الثوابت البصرية معامل الانكسار، معامل الخمود، و ثابت العزل (الجزء الحقيقي والخيالي) تزداد مع زيادة تركيز جسيمات اوكسيد الكوبلت النانوية. فجوة الطاقة تقل بزيادة تركيز اوكسيد الكوبلت النانوي. التوصيلية البصرية تزداد بزيادة تركيز اوكسيد الكوبلت النانوي. النتائج التي تم الحصول عليها تشير الى أن الخصائص الكهربائية المتناوبة (A.C) تبين ان ثابت العزل الكهربائي والفقدان العزلي للمترابك تتناقص مع زيادة تردد المجال الكهربائي المسلط و أنها تزداد مع زيادة تركيز جسيمات اوكسيد الكوبلت النانوي، و تزداد التوصيلية الكهربائية المتناوبة مع زيادة تركيز جسيمات اوكسيد الكوبلت النانوي و التردد وثابتة تقريبا في الترددات العالية. اختبرت المترابكات النانوية (PVA-PVP-CO<sub>2</sub>O<sub>3</sub>) كمضادات لبكتريا موجبة غرام (المكورات العنقودية الذهبية) وسالبة غرام (الاشريكية القولونية). بينت النتائج أن منطقة التنشيط ازدادت بزيادة تراكيز الجسيمات النانوية .

. CO<sub>2</sub>O<sub>3</sub>

## ***Contents***

<b><i>Section</i></b>	<b><i>Subject</i></b>	<b><i>Page</i></b>
	<b><i>Dedication</i></b>	<b><i>I</i></b>
	<b><i>Acknowledgements</i></b>	<b><i>II</i></b>
	<b><i>Abstract</i></b>	<b><i>III</i></b>
	<b><i>Contents</i></b>	<b><i>V</i></b>
	<b><i>List of Symbols</i></b>	<b><i>X</i></b>
	<b><i>List of Abbreviations</i></b>	<b><i>XIII</i></b>
	<b><i>List of Figures</i></b>	<b><i>XIV</i></b>
	<b><i>List of Tables</i></b>	<b><i>XVII</i></b>
<b><i>Chapter One (Introduction and Literature Survey)</i></b>		
<b><i>1.1</i></b>	<b><i>Introduction</i></b>	<b><i>1</i></b>
<b><i>1.2</i></b>	<b><i>Polymer Structure</i></b>	<b><i>2</i></b>
<b><i>1.3</i></b>	<b><i>Chemical Classification of Polymers</i></b>	<b><i>2</i></b>
<b><i>1.3.1</i></b>	<b><i>Linear Polymers</i></b>	<b><i>2</i></b>
<b><i>1.3.2</i></b>	<b><i>Branched Polymers</i></b>	<b><i>3</i></b>
<b><i>1.3.3</i></b>	<b><i>Cross Linked Polymers</i></b>	<b><i>3</i></b>
<b><i>1.4</i></b>	<b><i>Thermal Classification of Polymers</i></b>	<b><i>4</i></b>
<b><i>1.4.1</i></b>	<b><i>Thermoplastic Polymers</i></b>	<b><i>4</i></b>
<b><i>1.4.2</i></b>	<b><i>Thermoset Polymers</i></b>	<b><i>5</i></b>
<b><i>1.4.3</i></b>	<b><i>Elastomers Polymers</i></b>	<b><i>6</i></b>
<b><i>1.5</i></b>	<b><i>Classification Based on Sources Polymers</i></b>	<b><i>7</i></b>
<b><i>1.5.1</i></b>	<b><i>Natural Polymers</i></b>	<b><i>7</i></b>
<b><i>1.5.2</i></b>	<b><i>Synthetic Polymers</i></b>	<b><i>7</i></b>
<b><i>1.6</i></b>	<b><i>Classification of polymers dependent on homogeneity</i></b>	<b><i>8</i></b>

<i>Section</i>	<i>Subject</i>	<i>Page</i>
1.6.1	<i>Homopolymers</i>	8
1.6.2	<i>Copolymers</i>	8
1.6.3	<i>Composite Polymers</i>	8
1.7	<i>Polymer Blend</i>	8
1.8	<i>Nanomaterials</i>	9
1.9	<i>Composite Materials</i>	9
1.10	<i>Nanocomposites</i>	10
1.11	<i>Physical Properties of the Used Materials</i>	10
1.11.1	<i>Polyvinyl Alcohol (PVA)</i>	10
1.11.2	<i>Polyvinyl Pyrrolidone (PVP)</i>	12
1.12	<i>Additive Material</i>	14
1.13	<i>Literature Review</i>	15
1.14	<i>The Aim of The Study</i>	19
<b><i>Chapter Two (Theoretical Part)</i></b>		
2.1	<i>Introduction</i>	20
2.2	<i>Optical Properties of Polymers</i>	20
2.2.1	<i>Absorbance (A)</i>	20
2.2.2	<i>Transmittance (T)</i>	21
2.2.3	<i>Fundamental Absorption Edge</i>	21
2.2.4	<i>The Electronic Transitions</i>	22
2.2.5	<i>Optical Constants</i>	25
2.2.5.1	<i>Absorption Coefficient (<math>\alpha</math>)</i>	25
2.2.5.2	<i>Refractive Index (n)</i>	27
2.2.5.3	<i>Extinction Coefficient (k)</i>	27
2.2.5.4	<i>Dielectric Constant (<math>\epsilon</math>)</i>	28

<b>Section</b>	<b>Subject</b>	<b>Page</b>
2.2.5.5	<i>Optical Conductivity (<math>\sigma_{op}</math>)</i>	29
2.3	<i>Electrical Properties</i>	29
2.4	<i>The Electrical Polarization</i>	30
2.5	<i>The A.C Electrical Conductivity</i>	33
2.6	<i>Antibacterial Activity</i>	36
<b>Chapter Three (Experimental Part)</b>		
3.1	<i>Introduction</i>	38
3.2	<i>The Utilized Materials</i>	38
3.2.1	<i>Matrix Material</i>	38
3.2.2	<i>Additive Nanomaterial</i>	38
3.3	<i>Preparation of Nanocomposites</i>	38
3.4	<i>Measurements of Structural Properties</i>	41
3.4.1	<i>Optical Microscope</i>	41
3.4.2	<i>FTIR Spectral Characterization</i>	41
3.4.3	<i>Scanning Electron Microscope</i>	42
3.5	<i>Optical Properties Measurements</i>	43
3.6	<i>Measurement of A.C. Electrical Conductivity</i>	44
3.7	<i>Antibacterial Activity Application Measurements of Nannocomposites</i>	45
<b>Chapter Four (Results, Discussions and Conclusion)</b>		
4.1	<i>Introduction</i>	46
4.2	<i>The Structural Properties</i>	46
4.2.1	<i>The Optical Microscope</i>	46
4.2.2	<i>Fourier Transform Infrared Rays</i>	48
4.2.3	<i>Scanning Electron Microscopy (SEM)</i>	53

<b>Section</b>	<b>Subject</b>	<b>Page</b>
<b>4.3</b>	<i>The Optical Properties</i>	<b>55</b>
<b>4.3.1</b>	<i>The Absorbance (A)</i>	<b>55</b>
<b>4.3.2</b>	<i>Transmittance Spectrum</i>	<b>56</b>
<b>4.3.3</b>	<i>Absorption Coefficient (<math>\alpha</math>)</i>	<b>57</b>
<b>4.3.4</b>	<i>Optical Energy Gaps of The (Allowed and Forbidden) Indirect Transition</i>	<b>58</b>
<b>4.3.5</b>	<i>Refractive Index (n)</i>	<b>60</b>
<b>4.3.6</b>	<i>Extinction Coefficient (k)</i>	<b>61</b>
<b>4.3.7</b>	<i>Real and Imaginary Part of Dielectric Constant (<math>\epsilon_1</math>, <math>\epsilon_2</math>)</i>	<b>62</b>
<b>4.3.8</b>	<i>Optical Conductivity (<math>\sigma_{op}</math>)</i>	<b>64</b>
<b>4.4</b>	<i>The A.C Electrical Properties of (PVA-PVP-<math>Co_2O_3</math>) Nanocomposites</i>	<b>64</b>
<b>4.4.1</b>	<i>The Dielectric Constant for (PVA-PVP-<math>Co_2O_3</math>) Nanocomposites</i>	<b>65</b>
<b>4.4.2</b>	<i>The Dielectric Loss of (PVA-PVP-<math>Co_2O_3</math>) Nanocomposites</i>	<b>67</b>
<b>4.4.3</b>	<i>The A.C Electrical Conductivity of (PVA-PVP-<math>Co_2O_3</math>) Nanocomposites</i>	<b>69</b>
<b>4.5</b>	<i>Application of (PVA-PVP-<math>Co_2O_3</math>) nanocomposites for antibacterial activity</i>	<b>70</b>
<b>4.6</b>	<i>Conclusions</i>	<b>72</b>
<b>4.7</b>	<i>Future work</i>	<b>73</b>
	<b>References</b>	<b>74-86</b>

## *List of Figures*

<i>No.</i>	<i>Title</i>	<i>Page</i>
<b>1.1</b>	Constructivism Authority for (a- Linear polymer, b- Branched polymer , c-Cross linked polymer)	<b>4</b>
<b>1.2</b>	Configuration of thermoplastic polymers	<b>5</b>
<b>1.3</b>	Configuration of thermoset polymers	<b>6</b>
<b>1.4</b>	Configuration of elastomer polymers	<b>7</b>
<b>1.5</b>	The chemical structure of polyvinyl alcohol	<b>11</b>
<b>1.6</b>	The chemical structure of polyvinyl pyrrolidone	<b>13</b>
<b>2.1</b>	The variation of absorption edge with absorption regions	<b>22</b>
<b>2.2</b>	The transition types (a) allowed direct transition. (c) allowed indirect transition.(b) forbidden direct transition. (d) forbidden indirect transition	<b>25</b>
<b>2.3</b>	The electrical conductivity of material	<b>29</b>
<b>2.4</b>	The four types of polarization	<b>33</b>
<b>2.5</b>	The four types of polarization	<b>36</b>
<b>3.1</b>	The preparation condition of (PVA-PVP- $\text{Co}_2\text{O}_3$ ) films and the structural, electrical and optical measurements.	<b>40</b>
<b>3.2</b>	Image of optical microscope	<b>41</b>
<b>3.3</b>	Image of (FTIR) spectroscopy	<b>42</b>
<b>3.4</b>	Diagram for system of SEM device	<b>43</b>
<b>3.5</b>	Image of UV spectrophotometer	<b>44</b>
<b>3.6</b>	Diagram for system of A.C electrical measurement	<b>45</b>

<b>4.1</b>	Photomicrographs (10×) for (PVA-PVP- Co <sub>2</sub> O <sub>3</sub> ) nanocomposites: (A) for (PVA-PVP), (B) for 1.6 wt% Co <sub>2</sub> O <sub>3</sub> , (C) for 3.2 wt% Co <sub>2</sub> O <sub>3</sub> , (D) for 4.8 wt% Co <sub>2</sub> O <sub>3</sub> , (E) for 6.4 wt% Co <sub>2</sub> O <sub>3</sub>	<b>47</b>
<b>4.2</b>	FTIR spectra for (PVA-PVP-Co <sub>2</sub> O <sub>3</sub> ) nanocomposites film : (A) PVA-PVP, (B) 1.6 wt% Co <sub>2</sub> O <sub>3</sub> , (C) 3.2 wt% Co <sub>2</sub> O <sub>3</sub> , (D) 4.8 wt% Co <sub>2</sub> O <sub>3</sub> , (E) 6.4 wt% Co <sub>2</sub> O <sub>3</sub>	<b>50-52</b>
<b>4.3</b>	SEM images for (PVA-PVP-Co <sub>2</sub> O <sub>3</sub> ) nanocomposites : (A) for (PVA-PVP), (B) for 1.6 wt% Co <sub>2</sub> O <sub>3</sub> , (C) for 3.2 wt% Co <sub>2</sub> O <sub>3</sub> , (D) for 4.8 wt% Co <sub>2</sub> O <sub>3</sub> , (E) for 6.4 wt% Co <sub>2</sub> O <sub>3</sub>	<b>54</b>
<b>4.4</b>	The absorption of (PVA-PVP-Co <sub>2</sub> O <sub>3</sub> ) nanocomposites as a function of wavelength.	<b>56</b>
<b>4.5</b>	The transmittance of (PVA-PVP-Co <sub>2</sub> O <sub>3</sub> ) nanocomposites as a function of wavelength.	<b>57</b>
<b>4.6</b>	The absorption coefficient of (PVA-PVP-Co <sub>2</sub> O <sub>3</sub> ) nanocomposites as a function of photon energy	<b>58</b>
<b>4.7</b>	The relationship between $(\alpha h\nu)^{1/2}$ (cm-1.eV) <sup>1/2</sup> and photon energy of (PVA-PVP-Co <sub>2</sub> O <sub>3</sub> ) nanocomposites	<b>59</b>
<b>4.8</b>	The relationship between $(\alpha h\nu)^{1/3}$ (cm-1.eV) <sup>1/3</sup> and the photons energy of the (PVA-PVP-Co <sub>2</sub> O <sub>3</sub> ) nanocomposites	<b>60</b>
<b>4.9</b>	Refractive index of (PVA-PVP-Co <sub>2</sub> O <sub>3</sub> ) nanocomposites as a function of wavelength.	<b>61</b>
<b>4.10</b>	Extinction coefficient of (PVA-PVP-Co <sub>2</sub> O <sub>3</sub> ) nanocomposites as a function of wavelength	<b>62</b>
<b>4.11</b>	The real dielectric constant as a function of wavelength for (PVA-PVP-Co <sub>2</sub> O <sub>3</sub> ) nanocomposites	<b>63</b>

<b>4.12</b>	Imaginary dielectric constant as a function of wavelength for (PVA-PVP-Co <sub>2</sub> O <sub>3</sub> ) nanocomposites	<b>63</b>
<b>4.13</b>	The optical conductivity as a function of wavelength for (PVA-PVP-Co <sub>2</sub> O <sub>3</sub> ) nanocomposites	<b>64</b>
<b>4.14</b>	Variation of dielectric constant with a concentration of (Co <sub>2</sub> O <sub>3</sub> ) nanoparticles of (PVA-PVP-Co <sub>2</sub> O <sub>3</sub> ) nanocomposites	<b>66</b>
<b>4.15</b>	Variation of the dielectric constant with frequency for (PVA-PVP-Co <sub>2</sub> O <sub>3</sub> ) nanocomposites	<b>67</b>
<b>4.16</b>	Variation of the dielectric loss with frequency for (PVA-PVP-Co <sub>2</sub> O <sub>3</sub> ) nanocomposites	<b>68</b>
<b>4.17</b>	Variation of dielectric loss with a concentration of (Co <sub>2</sub> O <sub>3</sub> ) nanoparticles for (PVA-PVP-Co <sub>2</sub> O <sub>3</sub> ) nanocomposites	<b>68</b>
<b>4.18</b>	Variation of the A.C electrical conductivity with different concentrations for (PVA-PVP-Co <sub>2</sub> O <sub>3</sub> ) nanocomposites	<b>69</b>
<b>4.19</b>	Variation of the A.C electrical conductivity with frequency for (PVA-PVP-Co <sub>2</sub> O <sub>3</sub> ) nanocomposites	<b>70</b>
<b>4.20</b>	Image for inhibition zones of (PVA-PVP-Co <sub>2</sub> O <sub>3</sub> ) nanocomposite films on <i>S. aureus</i> and <i>E. coli</i>	<b>71</b>
<b>4.21</b>	Variation inhibition zone diameter of (PVA-PVP-Co <sub>2</sub> O <sub>3</sub> ) nanocomposite films on <i>E. coli</i> with Co <sub>2</sub> O <sub>3</sub> concentration	<b>72</b>
<b>4.22</b>	Variation inhibition zone diameter of (PVA-PVP-Co <sub>2</sub> O <sub>3</sub> ) nanocomposite films on <i>S. aureus</i> with Co <sub>2</sub> O <sub>3</sub> concentration	<b>72</b>

## *List of Symbols*

<i>Symbol</i>	<i>Physical Meanings</i>
<i>n</i>	<i>Refractive index</i>
<i>k</i>	<i>Extinction coefficient</i>
<i>A</i>	<i>Absorption</i>
<i>I<sub>o</sub></i>	<i>Incident intensity of light</i>
<i>I<sub>A</sub></i>	<i>Absorbed intensity of light</i>
<i>T</i>	<i>Transmittance</i>
<i>I<sub>T</sub></i>	<i>Intensity of transmitted</i>
<i>k</i>	<i>Wave vector</i>
<i>α</i>	<i>Absorption coefficient</i>
<i>h</i>	<i>Planck constant</i>
<i>ν</i>	<i>Photon frequency</i>
<i>E<sub>g</sub><sup>opt.</sup></i>	<i>Optical energy gap</i>
<i>r</i>	<i>Value determines the type of electronic transitions</i>
<i>E<sub>ph</sub></i>	<i>Energy phonon</i>
<i>c</i>	<i>Velocity of light</i>
<i>λ</i>	<i>Wavelength of light</i>
<i>R</i>	<i>Reflectance</i>
<i>d</i>	<i>Thickness</i>
<i>N</i>	<i>Complex refractive index</i>
<i>ε'</i>	<i>Dielectric constant</i>
<i>ε</i>	<i>Complex dielectric constant</i>
<i>ε<sub>1</sub></i>	<i>Real dielectric constant</i>

$\epsilon_2$	<i>Imaginary dielectric constant</i>
$\sigma_{op}$	<i>Optical Conductivity</i>
$\sigma$	<i>Electrical conductivity</i>
$\mu_o$	<i>Mobility</i>
$P$	<i>Polarization</i>
$N_m$	<i>Number of molecules</i>
$\mu$	<i>Electrical dipole moment</i>
$\alpha_o$	<i>Polarizability</i>
$E$	<i>Electrical field intensity</i>
$D$	<i>Electrical displacement</i>
$\epsilon_o$	<i>Vacuum permittivity</i>
$P_e$	<i>Electronic polarization</i>
$P_i$	<i>Ionic polarization</i>
$P_d$	<i>Rotational polarization</i>
$P_o$	<i>Space charge polarization</i>
$V_m$	<i>Maximum voltage</i>
$I$	<i>Current</i>
$i$	<i>Imaginary number</i>
$\omega$	<i>Angular frequency</i>
$C$	<i>Capacitance</i>
$f$	<i>Frequency</i>
$I_p$	<i>Conduction current</i>
$I_q$	<i>Capacitance current</i>
$\epsilon''$	<i>Dielectric loss</i>
$R_p$	<i>Parallel resistance</i>

$C_P$	<i>Parallel capacitance</i>
$z$	<i>Impedance</i>
$C_o$	<i>Vacuum capacitor</i>
$\sigma_{A.C}$	<i>A.C electrical conductivity</i>

### *List of Abbreviations*

<i>Abbreviations</i>	<i>Physical Meanings</i>
<i>PVA</i>	<i>Polyvinyl alcohol</i>
<i>PVP</i>	<i>Polyvinyl pyrrolidone</i>
<i>Co<sub>2</sub>O<sub>3</sub></i>	<i>Cobalt oxide nanoparticles</i>
<i>FTIR</i>	<i>Fourier transformation infrared ray</i>
<i>SEM</i>	<i>Scanning electron microscope</i>
<i>UV</i>	<i>Ultra violet</i>
<i>A.C</i>	<i>Alternating current</i>
<i>IR</i>	<i>Infrared</i>
<i>C.B.</i>	<i>Conduction Band</i>
<i>V.B</i>	<i>Valence Band</i>

## *List of Tables*

<i>No.</i>	<i>Title</i>	<i>Page</i>
<b>1.1</b>	Physical and chemical properties of polyvinyl alcohol (PVA)	<b>12</b>
<b>1.2</b>	Physical and chemical properties of polyvinyl pyrrolidone (PVP)	<b>13</b>
<b>1.3</b>	Physical and chemical properties of cobalt oxide	<b>14</b>
<b>3</b>	Weight percentage for nanocomposites	<b>39</b>
<b>4.1</b>	FTIR Transmittance bands positions and their assignments for pure PVA	<b>49</b>
<b>4.2</b>	FTIR Transmittance bands positions and their assignments for pure PVP	<b>50</b>
<b>4.3</b>	The values of energy gap for the allowed and forbidden indirect transition for (PVA-PVP-Co <sub>2</sub> O <sub>3</sub> ) nanocomposites	<b>60</b>

**1.1 Introduction**

Nanotechnology is a new technology that can be used in many different fields. It has become very popular in a number of different fields over the last 10 years, including the mechanics, electronics, materials sciences, medicine, optics, airspace and oil. Its societal impact has been recognized as a significant factor. The prefix "nano" originates from the Greek word for "dwarf." "Nano" is a term that refers to extremely small objects. A nanometer (nm) is one billionth of a meter, or 10 angstroms. As example, a nanometer is ten thousand times less than the diameter of a human hair at  $10^{-9}$  meter. A human hair is around 50 microns in diameter [1].

Nanotechnology will enable the development of new materials providing the basis for the design and development of new properties and structures, which will result in increased performance, reduced cost of maintenance, and enhanced functionality [ 2]. Nanotechnology is a relatively new field of study that developed as a result of the observation that materials exhibit dramatically different characteristics at nanoscale than at bigger particle sizes [3]. The researcher Feynman in 1959, pointed to the presence of something in the depths, there is plenty of room at the bottom. Norio Taniguchi coined the word "nanotechnology" in 1974 in Japan, as follows; Nanotechnology mainly consists of the processing of separation, consolidation and deformation of materials by one atom or one molecule [4].

Nanotechnology involves work from top-down, i.e. reducing the size of large structures to the minor design, such as photonic applications in nanoelectronics and nanoengineering , or bottom-up, involving the transformation of individual atoms or molecules in to the nanostructures and so more closely resembling biology [5]. Nanotechnologies are vital technologies for the twenty-first century, and significant research is being conducted in this subject. Soon, new applications can also become

accessible. Due to the fact that applications with nanoscale structural characteristics exhibit significantly different , chemical,biological and physical characteristics than their macroscopic equivalents, nanotechnology can be helpful on a variety of levels [6].

## **1.2 polymers structure**

Polymers are composed of huge organic molecules (macro molecules) composed of repeated small structural (monomer units) that are joined together through a process known as polymerization. [7]. Molecules in polymers are made up of thousands of atoms that are linked together by covalent chemical bonds. The forces that hold the molecules together depend on the type of polymer they are made of. Due to the large, coupled molecules in polymers that are difficult to manage, there are only a few crystal connections in polymers at low temperatures. It is only in limited regions that a linear chain of molecules can arrange themselves in an organized form. In the solid state, polymers are comprised of crystalline and non-crystalline regions [8].

## **1.3 Chemical Classification of Polymers**

Polymers can be classified according to their chemical structure:

### **1.3.1 Linear Polymers**

The main structural unit of these polymers is a single molecular series for certain lengths that is linked together in a linear shape. It doesn't have any branches except for the twisted totals that are part of the monomer, as shown in figure (1.1.a).

Van der Waals and hydrogen bonding between the chains may be extensive in linear polymers. Polyethylene, poly (vinyl chloride),

polystyrene, poly (methyl methacrylate), nylon, and fluorocarbons are some of the more prevalent polymers that form linear shapes [9].

### **1.3.2 Branched Polymers**

The reaction between poly-functional molecules results in structural units that can be connected in such a way as to form non-linear structures. In certain situations, the side growth of each polymer chain can be stopped before the chain has a chance to link up with another chain. The resulting polymer molecules are said to be branched. Branching can produce several physical properties in a polymer, such as a decrease in solvent solubility, a rise in the softening point and also a decrease in thermoplastic properties.

For instance, while high density polyethylene (HDPE) is predominantly a linear polymer, low density polyethylene (LDPE) has small chain branching [10], as shown in the figure (1.1.b)

### **1.3.3 Cross linked Polymers**

There are a lot of chemical bonds that connect to each other in a complicated way in this type of thing. The format string is composed of three-dimensional polymer chains connected by a slew of than one site, or when monomers with effective totals are used rather than being contained two effective totals, as seen in the figure (1.1.c) [11,12].

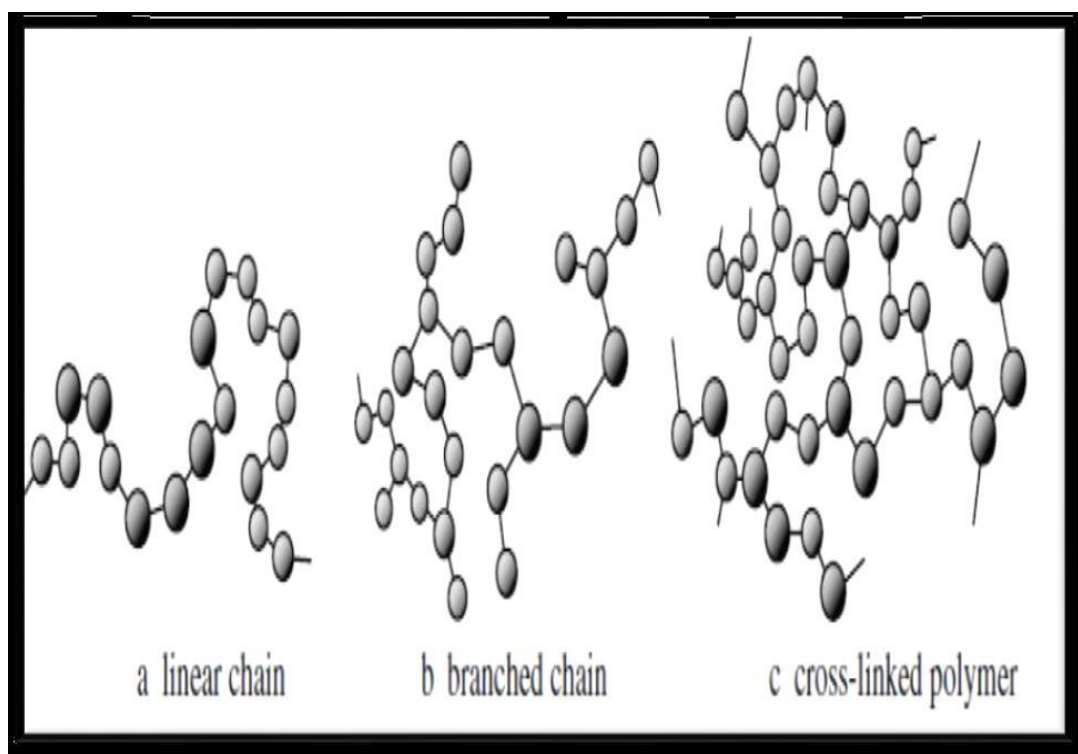


**Figure (1.1):** Constructivism Authority for (a- Linear polymer, b- Branched polymer , c-Cross linked polymer) [12].

## 1.4 Thermal Classification of Polymers

Polymers are divided into groups based on how temperature affects them [13,14]:

### 1.4.1 Thermoplastic Polymers

Temperature has an effect on these polymers' characteristics. The polymers degrade as the temperature increases. Possess a sticky and malleable nature; polymers revert to their solid state as the temperature decreases. Due to the fact that the molecules of the thermoplastic polymers are bound together via Intermolecular forces are weak (Van der Waals forces). When heated, these molecules slide over one another, which includes polyethylene, polystyrene, polyvinyl chloride, and polypropylene, as depicted in figure (1.2).

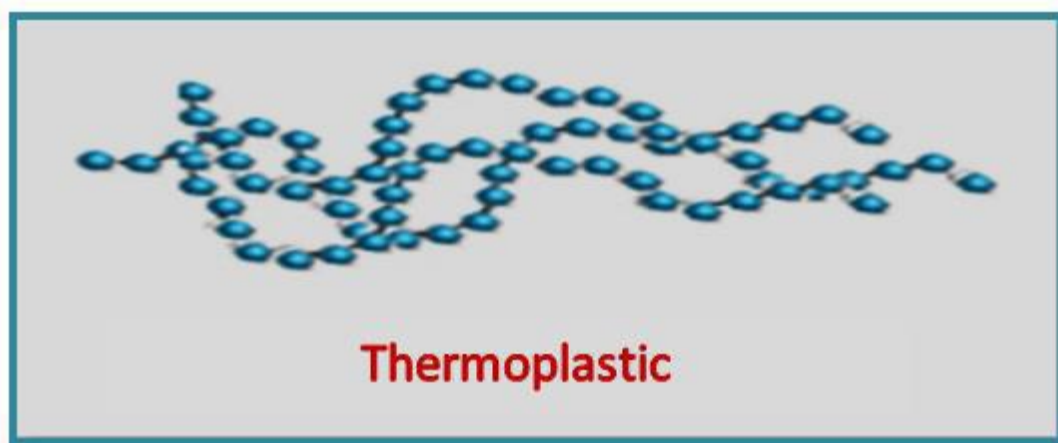


**Figure (1.2 ) Thermoplastic polymer configuration [14]**

### **1.4.2 Thermoset Polymers**

Thermosets are typically three-dimensional networked polymers with a large degree of polymer chain crosslinking. When these polymers are heated, they change in a chemical way. These polymers become insoluble after being heated, do not conduct heat or electricity, and difficult since these polymers' molecules are connected via covalent solid chemical connections. This type of polymer includes urea-formaldehyde resin and phenol formaldehyde resin.

The arrangement of thermoset polymers is illustrated in this figure.

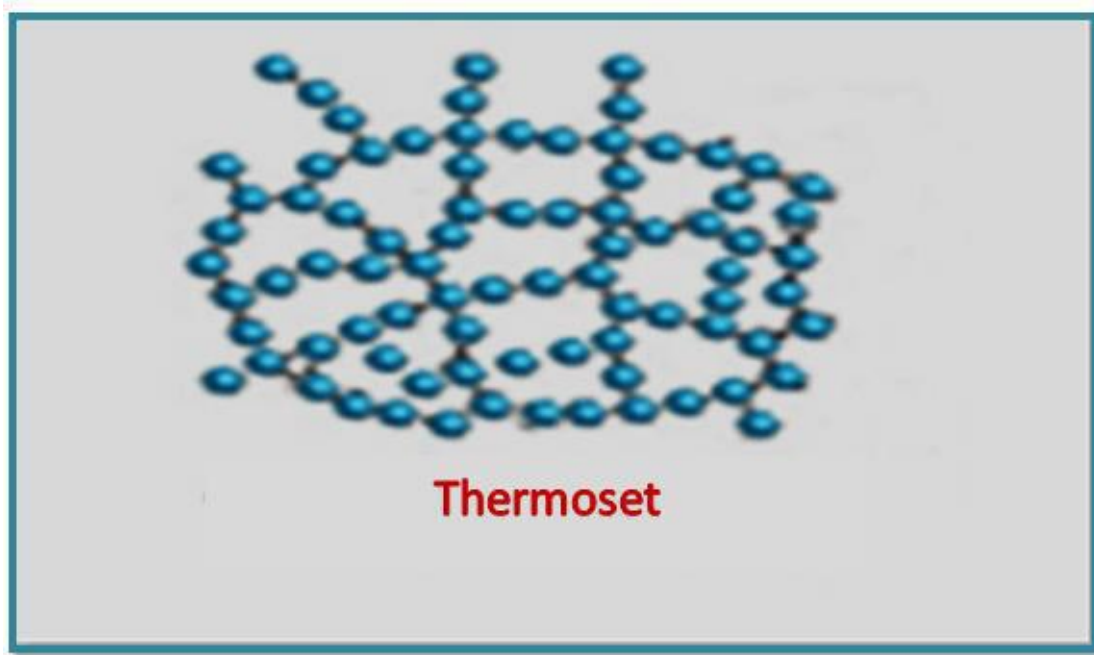
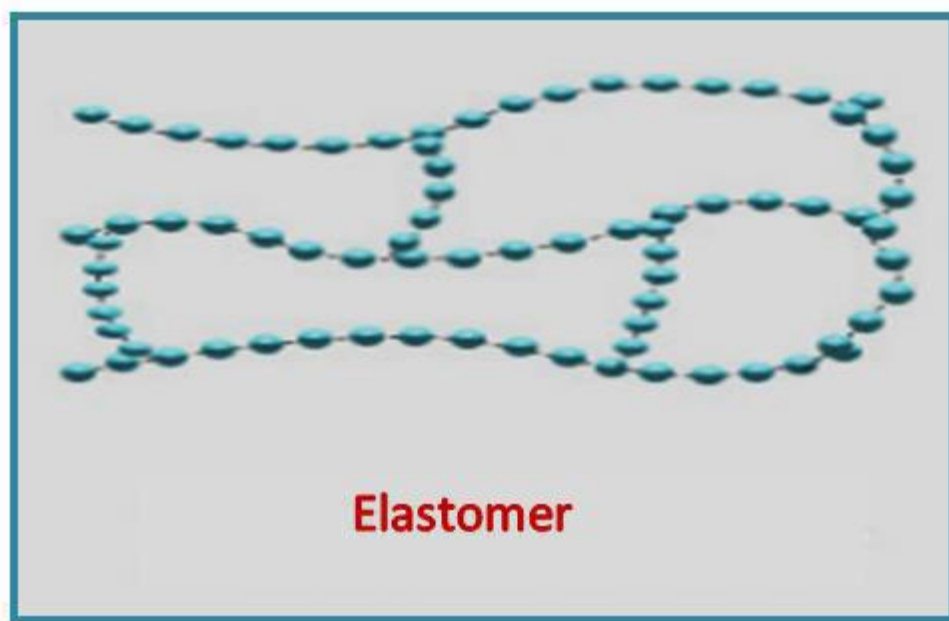


Figure (1.3) Thermoset polymer configuration [14]

### 1.4.3 Elastomers Polymers

Elastomers are a type of network polymer that is lightly cross-linked and may be reversibly stretched to extraordinary lengths. They have very tightly randomly coiled molecules when not stressed, but when they are stretched, they become a lot bigger and bend. This lowers the randomization of the chains, resulting in a decrease in the entropy of the material, which is caused by the retrospective force observed.

Cross-links prohibit molecules from moving past one another when a material is expanded. When the rubber cools (partially), it becomes crystal clear or glassy transparent. They do not flow when heated in the conventional sense due to cross-links. Neoprene and vulcanized rubber neoprene are as illustrated in figure (1.4).



**Figure (1.4): Elastomer polymer configuration [14]**

## **1.5 Classification Based on Sources Polymers**

Two major sources of polymers are as follows[15]:

### **1.5.1 Natural polymers**

It is naturally occurring substance found in plants and animals, such as lumber, cotton, silk, natural rubber, and wool. Starch, protein, and cellulose are all natural foods that are composed of natural polymers.

### **1.5.2 Synthetic Polymers**

The polymer is synthesized from simple chemical components and accounts for the great majority of industrially important polymers, including rubber, plastics, synthetic leather, and nylon textiles. Other qualities of synthetic polymers include physical and mechanical properties, as well as heat stability.

## **1.6 Classification of Polymers dependent on homogeneity**

Polymers are divided according to the homogeneity for their repeating units into the following categories:

### **1.6.1 Homopolymers:**

Homopolymers are materials composed entirely of one monomer [16].

### **1.6.2 Copolymers:**

If their components have more than one monomer type, they are referred to as copolymers [16].

### **1.6.3 Composite Polymers:**

It is the addition of materials to homogeneous polymers in order to modify certain of their properties and the incorporation of new recipes [17].

## **1.7 Polymer Blend**

Over the last several decades, polymer blends have been the subject of major technological and polymer science [18]. The term "polymer blend" refers to the process of physically blending two or more different polymers with or without chemical interaction [19].

Polymer blends can be composed of amorphous or crystalline polymers [20]. Two or many types of polymers can be mixed together to make new materials that have better properties than their parts alone. [21]. There are numerous reasons why polymer blending is regarded as a critical field of polymer development and research, one of which is that polymer blends provide a rapid and cost-effective means of obtaining new polymeric materials. These materials typically exhibit a range of characteristics that are dependent on the characteristics of their constituents, and polymer blends

enable a variety of industrial applications via property enhancement and cost savings [22,23].

Three important criteria influence the performance of polymer blends: compatibility, miscibility, and morphology. Numerous attempts have been made to comprehend these three variables in polymer mix systems [24,25].

### **1.8 Nanomaterials**

Nanomaterials studies is a discipline that approaches nanotechnology from a materials science perspective. A nanometer (nm) is a unit of measurement equal to one billionth of a meter. A single unit of a nanomaterial is between (1-100) nanometers in size.

These materials frequently exhibit exceptional qualities as a result of their shape, size, and chemical composition [26]. Two major causes contribute to nanoparticles' characteristics being notably different from those of ordinary materials: greater relative surface area and quantum effects [27].

### **1.9 Composite Materials**

When two or more materials are combined in a way that is different in shape or material composition, the resulting composite has qualities that are distinct from the individual materials , this is referred to as a composite material system [28]. Additionally, it has a robust structure. The composite is composed of two primary components: the matrix (the fundamental material) and the additives. The matrix serves to encapsulate and bulk up the composite. It encircles and strengthens other components, forming a "compact system." Additives are substances that are added to polymers to give them specific properties and improve their basic properties. These substances can be added in granular form or as small particles. Additives can

improve the overall conductivity, reduce porosity, improve friction, and some magnetic properties [28,29,30].

### **1.10 Nanocomposites**

Nanocomposites are materials composed of at least one component with a nanometric size of ( $10^{-9}$  m) [31]. Nanocomposites are made up of polymers (natural and manufactured) and nanomaterials, which are materials having a nanoscale topography or are built of nanoscale building components [32].

The main concept of nanocomposites is based on the creation of a large interface between both the nano-sized building components and the polymer matrix [33]. The mechanical, thermal, electrical, optical, catalytic, and electrochemical properties of nanocomposites will be significantly different from those of their constituent materials [34].

### **1.11 Physical Properties of the Used Materials**

#### **1.11.1 Polyvinyl alcohol (PVA)**

Polyvinyl alcohol possesses a number of unique qualities, including biodegradability, chemical stability, high abrasion resistance, eco-friendliness, tensile strength, elongation, thermal stability, ease of processing, flexibility, and low manufacturing cost. Polyvinyl alcohol is a water-soluble artificial polymer with low toxicity with superior wounds dressing bioreactor characteristics [35,36]. Polyvinyl alcohol is notable for its semi-crystalline nature, which consists of both crystalline and amorphous regions, resulting in interfacial effects that enhance the physical qualities [37,38].

When exposed to high temperatures, it decomposes swiftly. Different additives, such as salts, polymers, ions, and nanocomposites, are commonly used to enhance and improve the characteristics of PVA [39]. PVA is a poor

electrical insulator by nature, but when doped with conductive inorganic fillers, it becomes conductive [40]. Polyvinyl alcohol is often used as a polymer matrix to make different composites at a low cost technique [41].

Due to its unique physical and chemical properties, polyvinyl alcohol (PVA) is a significant polymer [42]. It is used in the industry for adhesives as well as biomedical materials such as drug delivery systems and membranes. Additionally, PVA can be used in medical applications such as the fabrication of artificial blood vessels, contact lenses, and artificial intestines. Because of its compatibility with the live body, it has been identified as a medical substance [43,44].

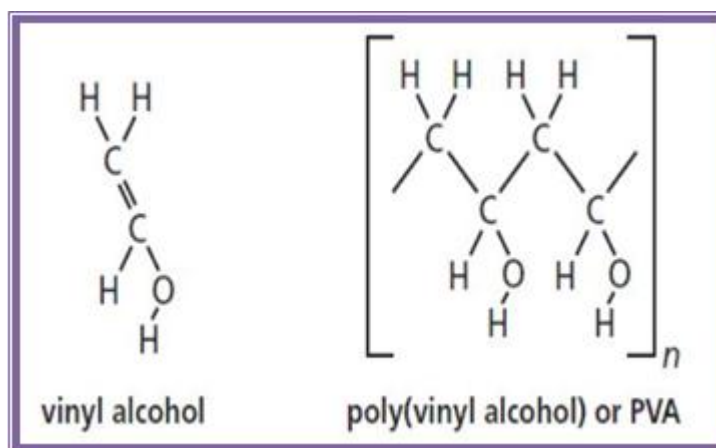


Figure (1.5): The chemical structure of polyvinyl alcohol [43]

**Table (1.1): Physical and chemical properties of polyvinyl alcohol (PVA) [44].**

Property	Value
Appearance	White to ivory white granular powder
Molecular formula	$(C_2H_4O)_n$
Density $g/cm^3$	1.19-1.39
Solution PH	5-6.5
Refractive index	1.55
Glass transition temperature $(T_g) ^\circ C$	85
Melting temperature $(T_m) ^\circ C$	230 for fully hydrolyzed grades, 180-190 for partially hydrolyzed grades.

### 1.11.2 Polyvinyl pyrrolidone (PVP)

Polyvinyl pyrrolidone is a biocompatible polymer that is hydrophilic and is used in a many of biomedical applications [45]. And separation processes to improve the hydrophilic properties of blended polymeric materials [46]. Due to its water solubility and exceptionally low cytotoxicity [47]. PVP has garnered particular interest among conjugated polymers due to its good environmental stability, easy process situation and excellent transparency. PVP is a potential material with a high charge storage capacity as well as electrical and optical properties that depend on the dopant used.

A chemical study says that PVP is inert, non-toxic, and interestingly [48]. Polyvinyl pyrrolidone's chemical structure is shown in figure (1.6) [48].

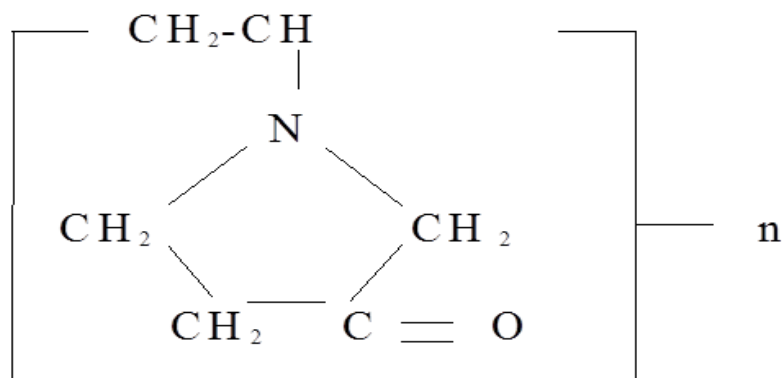


Figure (1.6) The chemical structure of polyvinyl pyrrolidone[48]

Table (1.2): Physical and chemical properties of polyvinyl pyrrolidone (PVP) [48].

Property	Value
Appearance	White to creamy-white
Molecular formula	$(C_6H_9NO)_n$
Density $g/cm^3$	1.25
Solution PH	3-7
Refractive index	1.53
Glass transition temperature ( $T_g$ ) $^{\circ}C$	109
Melting temperature ( $T_m$ ) $^{\circ}C$	150

### 1.12 Additive Material (Cobalt Oxide $\text{Co}_2\text{O}_3$ )

Cobalt Oxide ( $\text{Co}_2\text{O}_3$ ) is a highly insoluble and thermally stable source of Cobalt that is suited for glass production ceramic and optic applications. Compounds made of oxides are not electrically conducting. However, some perovskite-structured oxides are electrically conductive, so they can be used in the cathode of solid oxide fuel cells and systems that generate oxygen. A metallic cation and at least one oxygen anion are present in these compounds. Due to the fact that they are typically insoluble in aqueous solutions (water) and extremely stable, they can be used for everything from simple ceramic structures like clay bowls to advanced electronics and light weight structural components in aerospace and electrochemical applications such as fuel cells, in which they demonstrate ionic conductivity. There is an increasing need for metal oxide materials in the scientific community because of their environmental friendliness and stability, natural abundance, ease of synthesis, and expanded application reasons [49].

**Table (1.3): Different characteristics of  $\text{Co}_2\text{O}_3$  [49]**

Chemical formula	$\text{Co}_2\text{O}_3$
Molar mass	165.8646 g/mol
Appearance	Black solid
Density	5.18 g/cm <sup>3</sup>
Melting point	895 °C (1.643 °F, 1.168 K)
Solubility in water	negligible
Magnetic susceptibility ( $\chi$ )	$+4560 \times 10^{-6} \text{ cm}^3/\text{mol}$

### 1.13 Literature Review

Recent years have seen an increase in interest in polymer composites research in general and nanocomposites research in particular, due to their potential uses in optical, mechanical, electrical, ablative, and thermal applications. A short summary of recent advances in the fields above is shown below:

**In (2010) R.J. Sengwa, *et al.* [50]** have studied the dielectric properties of solution intercalation and melted intercalation. Films of poly(vinyl alcohol)-poly(vinyl pyrrolidone)-montmorillonite clay nanocomposites. The complex impedance, alternating current A.C electrical conductivity, and Complex dielectric function of these films were studied as a function of clay concentration in the frequency range (20Hz-1MHz) at 30 degrees celsius. The D.C conductivity of these films differs atypically as the clay concentration increases. The complex impedance spectrum indicates that the dielectric characteristics of these nanocomposite films were not affected by electrode polarization in the investigated frequency range.

**In (2011) K. Sivaiah, *et al* [51]** have studied optical and structural properties of Li+:PVP & Ag+:PVP polymer films. PVP polymers including Li+ or Ag+ ions have also a been synthesized intransparency and good stability by using solution casting process. Their optical, structural, electrical and thermal properties have been examined from the measurements of SEM , XRD, optical absorption spectra and FTIR. The silver particles are spherical in shape, have a uniform distribution in solution, and have an average size of about 3  $\mu\text{m}$ , as determined by SEM micrographs.

**In (2012),Xiushan Zhu , *et al.* [52]** in this study, thin films were formed using the spin coating process from a composite of polyvinyl alcohol and cobalt oxide ( $\text{Co}_3\text{O}_4$ ) nanoparticles.The nonlinear and linear optical

properties of nanocomposites with thicknesses of hundreds of nanometers were examined. The absorption spectra found two direct band gaps ( $E_g = 1.38$  eV and 2.0 eV) when the absorption coefficient and refractive index were determined.

**In 2013, M. Ghanipour and D. Dorrnian [53]** have studied the optical properties of nano-Ag doped and undoped PVA films. They discovered that as silver nanoparticles' weight percentages increased, the absorbance increased and the value of the optical energy gap decreased.

**In (2013), M.A. Habeeb [54]** have studied the thermal and A.C electrical properties for (PVA/PVP/Ag) nanocomposites. He discovered that as the concentration of nanosilver and the temperature increase, the thermal conductivity increases, The dielectric loss, dielectric constant, and alternating current electrical conductivity all increases as the concentrations of nanosilver increases. With increasing frequency, dielectric loss and dielectric constant decrease, while (A.C) electrical conductivity of nanocomposites increases as the frequency increases.

**In (2014), H. Chandrakala et. al [55]** this study indicated that as the concentrations of nanoparticles increased, the dielectric loss and dielectric constant increased as well, while decreases as the frequency increases. With greater frequency, the AC conductivity of PVA-ZnO-Ce<sub>2</sub>O<sub>3</sub> nanocomposites was increased. The optical characteristics indicate that charge transfer complexes between the hydroxyl groups of PVA and NPs.

**In (2016), K.J.Kadhim, et al.[ 56]** this work studied optical characteristics for (PVA-PEG-PVP) blend by adding of the titanium oxide nanoparticles for biological applications. The experimental results indicate that as the concentration of titanium oxide nanoparticles increases, the absorbance increases. The energy band gap decreasing and the other optical constants of

the (PVA-PEG-PVP) blend increased when the titanium oxide nanoparticles concentration increases.

**In (2017), M. Karpuraranjith and S.Thambidurai [57]** have studied produced the (cesium/zinc oxide-polyvinyl pyrrolidone) nanocomposites by using precipitation process. Antibacterial activity of chitosan,(cesium/zinc-oxide polyvinyl pyrrolidone),and (polyvinyl pyrrolidone–zinc oxide) nanocomposites was examined versus gram negative bacteria *Escherichia coli* (E.coil) and gram positive bacteria *Staphylococcus aureus* (S.aureus).The results indicated that gram positive bacteria are more susceptible to inhibition than gram negative bacteria.

**In (2018),F.M. Ali *et al.* [58]** tested the Polymer blend samples based on Polyvinyl pyrrolidone (PVP)/ Polyvinyl alcohol (PVA) doped with various concentrations of cerium ions [(PVA/PVP)-x wt.% Ce<sup>3+</sup>] (x = 3%, 5%, 10% and 15%). In the ultraviolet and visible range, the absorption spectra displays that the fundamental absorption edge of (PVA/PVP)-x wt. percent Ce<sup>3+</sup> composites had a wide red shift. By gradually increasing the Ce<sup>3+</sup> ion concentration, the optical gap  $E_g$  was reduced from 4.54 eV for the undoped PVA/PVP film to 3.10 eV. The doping of cerium ions has a major effect on the static refractive indices. Adding cerium ions to PVA/PVP blend films causes a considerable rise in the refractive index while simultaneously decreasing the optical gap. These findings are likely to have a significant impact on a wide range of applications, including organic semiconductors, polymer waveguides, optoelectronic devices , and polymer solar cells.

**In (2019), H. Khalid *et al.* [59]** the researcher investigated the fabrication of new nanocomposites (carboxymethylcellulose–polyvinylalcohol–polyvinylpyrrolidone–leadoxide nanoparticles).The influence of (PbO<sub>2</sub>) nanoparticles on the optical characteristics of a (CMC–PVP–PVA) blend has

been studied. The (PbO<sub>2</sub>) nanoparticles were introduced at doses of 2, 4, 6, and 8 wt % to a polymer blend (polyvinyl alcohol 30%, polyvinyl pyrrolidone 30%, and carboxy methyl cellulose 40%). The optical characteristics of (CMC–PVP–PVA–PbO<sub>2</sub>) nanocomposites, The results of the experiments indicate that the absorption coefficient ( $\alpha$ ), absorbance (A), extinction coefficient (k), refractive index (n), optical conductivity ( $\sigma_{op}$ ), and (real and imaginary) dielectric constants ( $\epsilon_1$  and  $\epsilon_2$ ) of the (CMC–PVP–PVA) blend increase as the weight percentages of lead oxide nanoparticles increase. With increasing lead oxide nanoparticle concentrations, the energy gap ( $E_g$ ) of the (CMC–PVP–PVA) blend decreases.

**In (2020), Q. Jebur, et al. [60]** have studied the dielectric and structural characteristics of (PVA-PEO-Fe<sub>2</sub>O<sub>3</sub>) nanocomposites. The results indicate that when the frequency of the applied electric field increases, the dielectric loss and dielectric constant decreased while the electrical conductivity increases. The optical experiments revealed that the absorbance for (PVA-PEO-Fe<sub>2</sub>O<sub>3</sub>) increases with increasing iron oxide nanoparticle concentrations. With increasing concentrations for iron oxide nanoparticles, the indirect ( $E_g$ ) energy gap for the (PVA-PEO) blend reduces. The optical constants of (PVA-PEO) blend, such as , extinction coefficient, absorption coefficient, refractive index, real and imaginary dielectric constants, and optical conductivity, altered as the weight percentage of iron oxide nanoparticles increased.

**In (2021), A. Abid, et al. [61]** the present work examined polymer blend (PVA-PVP)-carbon black (C.B N375) nanocomposites. The nanocomposites (PVA-PVP-C.B) are prepared by the use of a casting method. The dielectric constant and dielectric loss of the samples decreased as the frequency of the applied electric field increased, however the A.C electrical conductivity results increased as the frequency increased. With increasing carbon black

concentrations, the dielectric constant, dielectric loss, and electrical conductivity (A.C) of all films increased.

**In (2022), Y.Cao *et al.* [62]** in this study, the solution blow spinning (SBS) technique was used to rapidly create polyvinyl pyrrolidone (PVP), polycaprolactone (PCL), and PCL/PVP nanofibrous films to encapsulate chlorogenic acid (CGA). The PVP nanofibrous film did not show any inhibition activity against *E. coli* or *S. aureus*, while the PCL/PVP and PCL films showed will antimicrobial activity. In summary, the above findings indicated that PCL and PCL/PVP nanofibrous films containing CGA had interesting applications in food packaging.

#### **1.14 The Aim of The Study**

- 1- After preparing the samples (PVA-PVP  $\text{Co}_2\text{O}_3$ ), we expect the physical properties to improve.
- 2- Studying the effect of ( $\text{Co}_2\text{O}_3$ ) nanoparticles on the, optical, dielectric and structural properties of ( PVA-PVP- $\text{Co}_2\text{O}_3$ ) nanocomposites.
- 3- The application of (PVA-PVP- $\text{Co}_2\text{O}_3$ ) nanocomposites with antibacterial activity .

## 2.1 Introduction

This chapter includes a general description of the study's theoretical part, including physical concepts, relationships, scientific clarifications, and laws applied to explain the study's findings.

## 2.2 The Optical Properties

The variations electronic characteristics with size resulting in major variations in the optical characteristics of nanoscale materials[63]. When particles are reduced to an enough small size, quantum effects limiting the energies where the holes and electrons can be exist in the particles, due to the fact that energy is proportional to wavelength, the optical properties of the particles can be finely tuned depending on its size. Thus, by changing the size of particles, it is possible to cause them to absorb or emit light at specific wavelengths [64]. The study of polymer optical characteristics advances our understanding of the internal structure of the polymer, the type of the bonds, and the application possibilities of polymers. Knowing the transmittance and absorption spectra of a polymer enables the identification of numerous optical properties over a wide range of wavelengths. By examining the ultra - violet spectra, we can determine the type of bonds, energy beams and orbitals. The visible light spectrum gives adequate information about a material's behavior for solar applications. The infrared spectrum is necessary in order to determine the overall structure of a polymers and the elements that consisting its chemical structures [65].

### 2.2.1 Absorbance (A)

Absorbance can be defined as the ratio between the absorbed intensity ( $I_A$ ) by material and the incident intensity of light ( $I_0$ ) [66].

$$A = I_A/I_0 \dots\dots\dots (2.1)$$

### 2.2.2 Transmittance (T)

The transmittance ( $T$ ) of a film is defined as the ratio for the intensity of rays that pass through it ( $I_T$ ) to the intensity of incident rays ( $I_0$ ) [67].

$$T = I_T / I_0 \dots\dots\dots ( 2.2)$$

### 2.2.3 Fundamental Edge of Absorption

The fundamental edge of absorption is defined as a rapid increase in absorption when the amount of energy absorbed is nearly equalize to the energy gap between the bands. As a result, the fundamental absorption edge denotes the region where there is the least amount of energy differential between the top points in the valence bands and bottom points in the conduction bands [68]. The regions of absorption can be divided into three distinct regions [69]:

#### A. High absorption region

This region is represented in figure (2.1) portion (A), in the region of high absorption, where  $(\alpha \geq 10^4) \text{ cm}^{-1}$ . In this region, the absorption coefficient correlates to transitions between stretched states in the valence and conduction band.

#### B. Exponential region

This region can be seen in the figure (2.1) portion (B). The absorption coefficient for this region is between  $(1 \leq \alpha \leq 10^4) \text{ cm}^{-1}$ . The absorption in this region is caused by transitions between extended states and localized states in the band tail. This is referred to it as the Urbach edge.

### C. Low absorption region

There is an extremely low absorption coefficient ( $\alpha$ ) in this region, which is about ( $\alpha < 1\text{cm}^{-1}$ ). The transition occurs in this region as a result of state density within space motion caused by structural defects. As showed in figure (2.1), the portion (C).

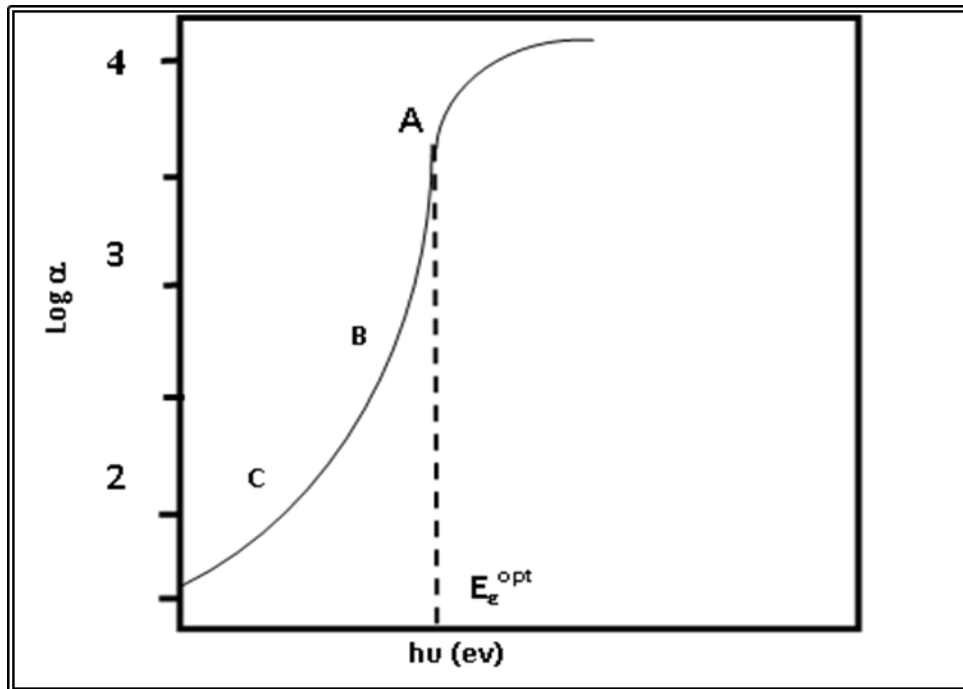


Figure ( 2.1 ): The relationship between the absorption edge and the absorption regions [61].

### 2.2.4 The Electronic Transitions

There are two main types of electrical transitions [70].

#### 1. Direct transition

This transition occurs in semiconductors if the bottom for (C.B) is directly above the top for (V.B.). This indicates that their wave vectors are equal, i.e. ( $\Delta K = 0$ ). Absorption happens at this stage when ( $h\nu = E_g^{opt}$ ). This type of

transition requires the conservation laws of momentum and energy. There are two types of direct transitions [71].

**a- Direct allowed transition:**

This transition occurs between the highest points in ( $V.B$ ) and the bottom points in ( $C.B$ ), as observe in the fig (2.2-a)

**b- Direct forbidden transition:**

These transitions occur between points adjacent to the lowest point in the conduction band ( $C.B$ ) and the highest point in the valence band ( $V.B$ ) [72], as showed in the fig (2.2.b). Absorption coefficient of this type of transition is calculated as follows:

$$\alpha h\nu = B(h\nu - E_g^{opt})^r \dots\dots\dots (2.3)$$

Where  $E_g^{opt}$  : The energy gap between direct transitions.

$B$ : Constant varies with different materials.

$r$ : is exponential constant, and its amount depends on the nature of the transition

$r = 1/2$  for allowed direct transition.

$r = 3/2$  for forbidden direct transition

$\alpha$ : is the absorption coefficient.

$h$ : is the Planck's constant.

$\nu$ : is the photon frequency.

## 2. Indirect transitions

In this form of transition, the bottom for (*C.B.*) doesn't over the peak for (*V.B.*), as shown in the curve (E-K), and the electron moves from the (*V.B.*) to the (*C.B.*) in a way that isn't perpendicular where the values of the waves vectors of the electrons before and after this transition are not the same ( $\Delta K \neq 0$ ). This type of transition occurs with the assistance of a particle termed a "Phonon," which is necessary for conservation of the momentum and energy law. Indirect transitions are classified into two types [72]:

### c- Allowed indirect transitions:

These transitions occur between the lowest point in (*C.B.*) and the highest point in (*V.B.*), which are located in the (K-space's) difference region, as showed in the figure (2.2.c).

### d- Forbidden indirect transitions:

These transitions occur between points adjacent the top for (*V.B.*) and points adjacent the bottom for (*C.B.*) [73], as shown in fig (2.2.d). Absorption coefficient of a transition involving phonon absorption calculated by:

$$\alpha_{\text{ph}} = B(\hbar\nu - E_g^{\text{opt}} \pm E_{\text{ph}})^r \dots\dots\dots (2.4)$$

When:  $E_{\text{ph}}$ : Phonon energy, is (+) phonon emission, and (-) phonon absorption.

( $r = 2$ ) for allowed indirect transition.

( $r = 3$ ) for forbidden indirect transition.

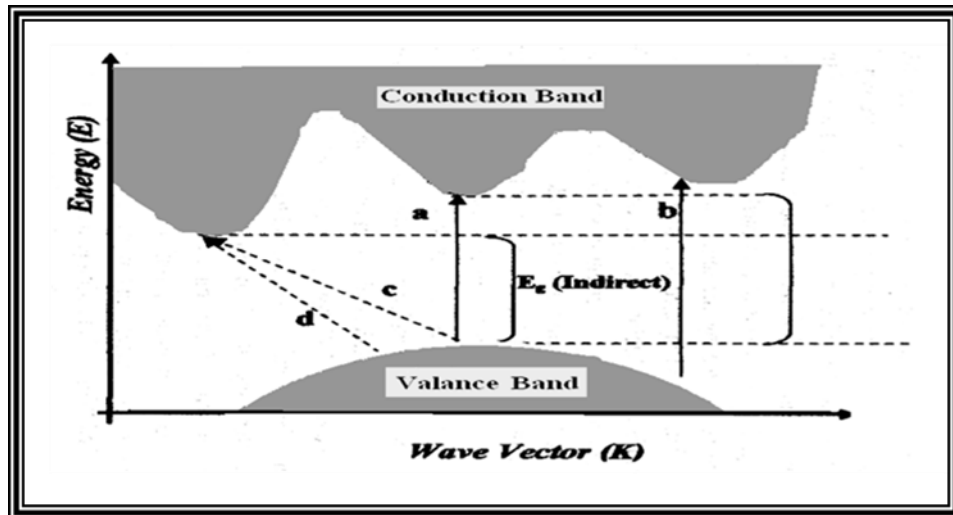


Figure ( 2.2 ): Types of transition [59]

a- allowed direct transition.

c- allowed indirect transition

b- forbidden direct transition.

d- forbidden indirect transition

### 2.2.5 The optical constants

There are many important reasons for studying the optical constants of materials. Firstly, the usage of materials at optical applications like interference filters, reflective coatings, and optical fiber necessitates an accurate understanding of their optical constants over a broad wavelength range. Secondly, all materials' optical properties can be connected to their electronic band structure, atomic structure, and electrical properties [74].

#### 2.2.5.1 Absorption coefficient ( $\alpha$ )

The absorption coefficient is defined as the decrease in the ratio of incident wave relative to unit length in the direction of a wave propagation within the medium [75]. The absorption coefficient ( $\alpha$ ) is proportional to the energy of the incident photon ( $h\nu$ ).

Photon energy calculated by Planck's law [76] :

$$E = h\nu = hc / \lambda \quad \dots\dots\dots(2.5)$$

Where:  $c$ : is the light's velocity and  $\lambda$ : is the light's wavelength.

The transmittance of an absorbent medium with a thickness of ( $d$ ) is calculated by this equation:

$$T = (1 - R)^2 \exp(-\alpha d) \dots\dots\dots (2.6)$$

Where:  $T$ : transmittance,  $R$ : is the reflectance.

If a light of intensity ( $I_0$ ) is incident on a film of thickness ( $d$ ), the transmitted intensity ( $I_T$ ) can be calculated as follows [78]:

$$I_T = I_0 \exp(-\alpha d) \dots\dots\dots(2.7)$$

$$I_T / I_0 = \exp(-\alpha d) \dots\dots\dots (2.8)$$

where :  $T = I_T / I_0$

$$T = \exp(-\alpha d) \dots\dots\dots(2.9)$$

$$1/T = \exp(\alpha d) \dots\dots\dots (2.10)$$

Then:

$$\alpha d = 2.303 \log_s (I_0 / I_T) \dots\dots\dots (2.11)$$

But  $A = \log (I_0 / I_T)$

$$\alpha d = 2.303 \times A \dots\dots\dots(2.12)$$

Then:

$$\alpha = (2.303 \times A) / d \dots\dots\dots(2.13)$$

Where: ( $d$ ) is the thickness of the sample in centimeters, ( $A$ ) is the absorbance of the material.

### 2.2.5.2 Refractive Index ( $n$ )

The refractive index is the ratio of the velocity of light in a vacuum ( $C$ ) to its velocity through a material. The refractive index ( $n$ ) was determined using equation (2.16) depending on the extinction coefficient ( $k$ ) and reflectance as described in the following equation [79]:

$$R = \frac{(n-1)^2+k^2}{(n+1)^2+k^2} \dots\dots\dots(2.14)$$

where ( $k$ ) is the extinction coefficient.

Additionally, the following equation can be used to calculate the transmittance ( $T$ ) and absorbance ( $A$ ):

$$R + A + T = 1 \dots\dots\dots(2.15)$$

The following equation can be used to calculate the refractive index ( $n$ ) [80]:

$$n = \sqrt{\frac{4R-k^2}{(R-1)^2}} - \frac{(R+1)}{(R-1)} \dots\dots\dots(2.16)$$

### 2.2.5.3 Extinction coefficient ( $k$ )

The extinction coefficient ( $k$ ) denotes the amount of attenuation of an electromagnetic wave passing through a material, with its values dependent on the structure of free electrodes and the material density [81]. It denotes the imaginary value of the refractive index that is complex ( $N$ ):

$$N = n - ik \dots\dots\dots(2.17)$$

when:  $n$  : is the real value for refractive index.

The extinction coefficient ( $k$ ) can be calculated by using equation [83]:

$$k = \alpha \lambda / 4\pi \dots\dots\dots (2.18)$$

Where  $\lambda$  : is the wavelength of photon beams that are incident.

#### 2.2.5.4 Dielectric Constant ( $\epsilon$ )

The dielectric constant demonstrates matter's possibility to polarize, it can respond very difficultly with multiple frequencies. At optical frequencies, which are expressed by waves of light, electronic polarity is more dominates than other types of polarization. real and Imaginary dielectric constants can be computed using the equation [84]:

$$\epsilon = \epsilon_1 - i\epsilon_2 \dots\dots\dots (2.19)$$

where:  $\epsilon$  is the complex dielectric constant and  $(\epsilon_1, i\epsilon_2)$  are the real and the imaginary parts of the dielectric constant, respectively. The imaginary and real parts of the dielectric constant are related to  $(n)$  and  $(k)$  values [84].

$$\epsilon = N^2 \dots\dots\dots (2.20)$$

$$(n - ik)^2 = \epsilon_1 - i\epsilon_2 \dots\dots\dots (2.21)$$

From equation (2.19) real and the imaginary complex dielectric coefficient can be written as following [85]:

$$\epsilon_1 = (n^2 - k^2) \dots\dots\dots (2.22)$$

$$\epsilon_2 = (2nk) \dots\dots\dots (2.23)$$

#### 2.2.5.5 Optical Conductivity ( $\sigma_{op}$ )

Optical conductivity ( $\sigma_{op}$ ) is directly related to absorption coefficient ( $\alpha$ ) and refractive index ( $n$ ) by the following relation [86]:

$$\sigma_{op} = \alpha n c / 4\pi \dots\dots\dots (2.24)$$

### 2.3 Electrical properties

It is possible to classify matter into conductors, semiconductors, and insulators depending on its electrical conductivity. Conductivities of some polymers ( $10^{-12} \text{ ohm}^{-1} \text{ cm}^{-1}$ ) for polyamides and ( $\sim 10^{-17} \text{ ohm}^{-1} \text{ cm}^{-1}$ ) ( $10^{-16} \text{ ohm}^{-1} \text{ cm}^{-1}$ ) for polystyrene [87]. The electrical conductivity of materials and their range is depicted ( 2.3 ).

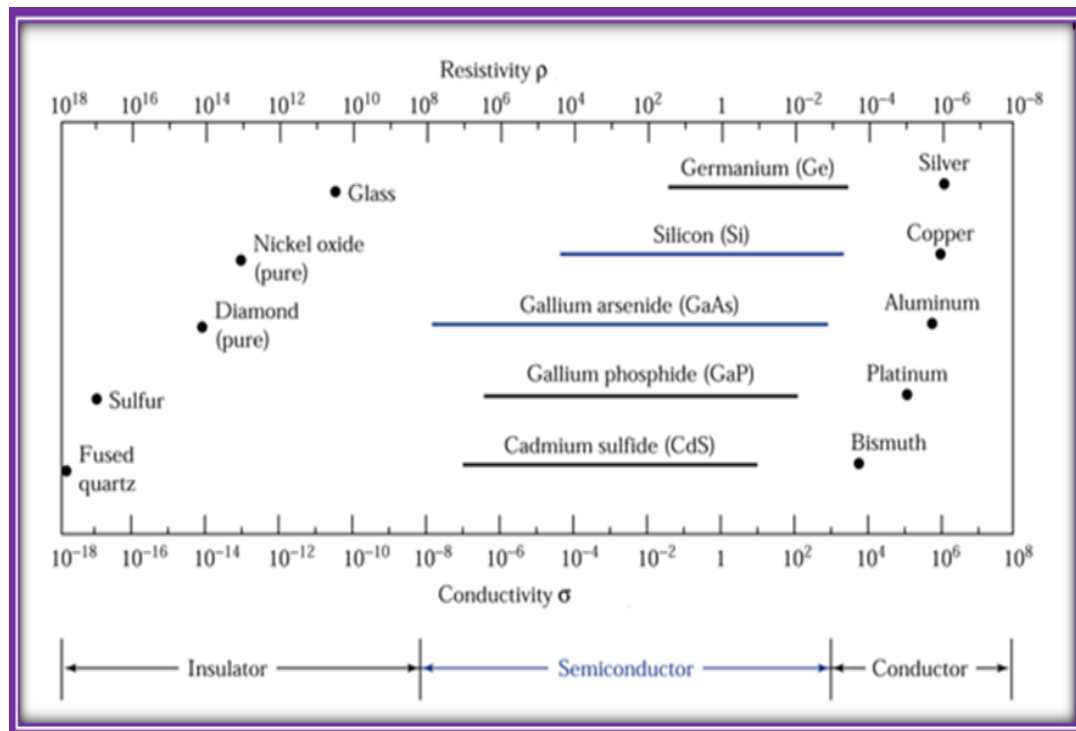


**Figure (2.3): The electrical conductivity for materials [87].**

The electrical properties of a material are determined by its chemical composition, its atomic arrangement, and the presence for energy gap flaws. This flaw can be decreased in a many of ways, like annealing. The electrical properties are also significantly reliant on the technique used for preparation and the deposition conditions[88].

## 2.4 The Electrical polarization

Electric polarization is a phenomena that occurs when the centers of negative and positive charges don't coincide. When an electric field is applied to a dielectric material, this phenomenon usually appears. Because an electric field is applied during electrical resistivity measurements, polarization in a material can happen during electrical resistivity measurements[89]. It's worth noting that this polarized surface charge density (formerly represented by  $(P)$  and also referred to as simply polarization or induced polarization) is perfectly equal to the value of the dipole moment for each unit volume [90]:

$$P = N_m \mu \quad \dots\dots\dots (2.25)$$

Where :  $N_m$  is the number of molecules. We can make the following assumption about the dipole moment being proportionate to the electrical field [91]:

$$\mu = a_o E \quad \dots\dots\dots (2.26)$$

where:  $a_o$ : is a constant named the polarizability.

$E$ : is an electrical field intensity.

The relation between the electrical displacement (flux density) ( $D$ ) and ( $E$ ) is shown by [92]:

$$D_o = \varepsilon_o E \quad \dots\dots\dots (2.27)$$

where:  $\varepsilon_o = 8.854 \times 10^{-12} F/m$  is the permittivity of a vacuum.

The electric flux density in the dielectric part is proportional to that in vacuum by [93]:

$$D = \epsilon_0 E + P \quad \dots\dots\dots (2.28)$$

As:

$$D = \epsilon' \epsilon_0 E \quad \dots\dots\dots (2.29)$$

$$\text{But, } \epsilon' = D / \epsilon_0 E$$

Then:

$$\epsilon' = 1 + P / (\epsilon_0 E) \quad \dots\dots\dots (2.30)$$

The polarizability and dielectric constant are related by the Clausius-Mossotti equation [91]:

$$(N_m a_o) / (3\epsilon_0) = (\epsilon' - 1) / (\epsilon' + 2) \quad \dots\dots\dots (2.31)$$

Polarization of material can be detected by the components of this polarization so that the total polarization can be calculated, figure (2.4) depicts the several types of polarization [94]:

$$P = P_e + P_i + P_d + P_o \quad \dots\dots\dots (2.32)$$

#### **A- Electronic Polarization ( $P_e$ ):**

Electronic polarization arises as a result of a distortion in the charge distribution caused by an external electric field. A separation arises between the positive charge of the nucleus and the center of the negative charge, resulting in the generation of induced dipoles [95]. Electronic polarization occurs in a relatively short period of time ( $10^{-15}$  seconds) and is not affected by temperature [96], as shown in figure 1. (2.4-a).

**B- Ionic Polarization ( $P_i$ ):**

It was generated as an ionic compound with ionic properties. It occurred when matter was subjected to an electric field, which altered the lengths of the ionic bonds, resulting in the formation of a net dipole moment in the molecule that did not exist previously [95]. It only lasts for about  $10^{-11}$ – $10^{-13}$  seconds [96]. The temperature has no effect on this type of polarization, as showed in the figure (2.4-b).

**C- Rotational or Orientation Polarization ( $P_d$ ) :**

It's also called as molecular polarization [94]. This occurs in molecules with a perpetual dipole moment [97]. When the electric field is applied, the dipoles revolve around of the axis , also arrange themselves in direction of the field. This type of polarization is dependent on temperature and takes a long time to occur [95], as showed in the figure (2.4-c).

**D- Space Charge or Interfacial Polarization ( $P_o$ ):**

It occurs when a matter contains impurities, a vacuum, or a structural fault, which results in a concentration of opposing charges on the impurities terminals, this refers to the formation of dipoles within an molecule ,atom, or zone of material. This type of polarization is dependent on homogeneity of matter and the rate of being free from impurities. It occurs mostly in radios frequency and can be expand to frequencies beneath audio and depending on flaws that produces the polarization [95], as illustrated in figure (2.4-d).

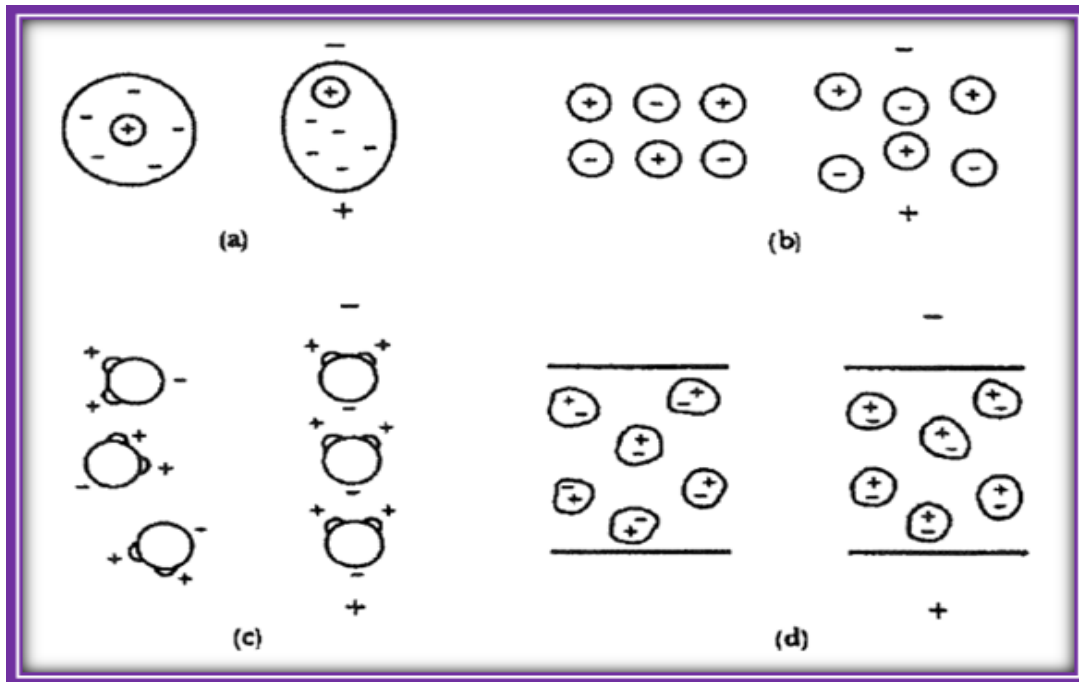


Figure (2.4): Four different types of polarization [94]

**a: Electronic polarization c: Orientation polarization d:Space charge b: Ionic polarization**

## 2.5 The (A.C) Electrical Conductivity

(A.C) conductivity isn't the same as (D.C) conductivity, which is when the frequency of an electric field doesn't change during (D.C) conductivity, while the frequency of the electric field will change through (A.C) conductivity [98]. It is very common to use dielectric spectroscopy to study at the dielectric characteristics of polymers like ( $\epsilon'$ ,  $\tan\delta$ ,...), it is based on measuring the voltage and current (phase and amplitude of the A.C. system) [99].

The dielectric constant represents the ratio of the capacitance of the capacitor in the presence of the insulation between its plates to its capacitance in the presence of the vacuum, Its amount varies from material to another depending on the amount of polarization in the material [100].

When the voltage is alternating  $V = V_m e^{i\omega t}$  [100], is applied through a capacitor ( $C$ ) contains insulator, therefore, the currents moving through the capacitor ( $C$ ) precedes the voltage by the phase ( $\pi/2$ ) [101]:

$$I = i \omega C V \quad \dots\dots\dots (2.33)$$

where ( $i$ ) is an imaginary number ( $i = \sqrt{-1}$ ), ( $\omega$ ) represent the angular frequency of the applied electric field ( $\omega = 2\pi f$ ), ( $V_m$ ) is the maximum voltage and ( $f$ ) is the frequency.

This demonstrates that an electronic current ( $I$ ) is the total of a conduction current ( $I_p$ ), which is a same phase with ( $V$ ), and the capacitance current ( $I_q$ ), which has a phase changes of ( $\pi/2$ ), as follows [102]:

$$I = I_p + i I_q \quad \dots\dots\dots (2.34)$$

The capacitance of a capacitor made up of two parallel surfaces is determined by the following equation:

$$C = \epsilon \epsilon_o A_r / d \quad \dots\dots\dots (2.35)$$

Where : ( $d$ ) is the thickness and ( $A_r$ ) is the area.

Substituting equation (2.35) into equation (2.33), obtain:

$$I = i \omega \epsilon \epsilon_o V A_r / d \quad \dots\dots\dots (2.36)$$

After then, the dielectric constant is considered as a complex quantity ( $\epsilon$ ). The difference of the complex dielectric constant's real and imaginary portions is described by equation [103]:

$$\epsilon = \epsilon' - i \epsilon'' \quad \dots\dots\dots (2.37)$$

where:  $\epsilon''$  is the dielectric loss.

Therefore, obtain

$$I = i \omega \varepsilon_o (\varepsilon' - i \varepsilon'') V A_r/d \quad \dots\dots\dots (2.38)$$

When equation (2.34) is compared to equation (2.38), then:

$$I_p = \omega \varepsilon_o \varepsilon'' V A_r/d \quad \dots\dots\dots (2.39)$$

$$I_q = \omega \varepsilon_o \varepsilon' V A_r/d \quad \dots\dots\dots (2.40)$$

Figure (2.5) shows that the loss factor ( $\tan\delta$ ) is determined by the equation [101]:

$$\tan \delta = I_p / I_q = \varepsilon'' / \varepsilon' \quad \dots\dots\dots (2.41)$$

At low frequencies, the capacitor can be expressed by an ideal capacitor and resistance  $R_p$  linked in parallel, so [102]:

$$I = I_p + iI_q = V/R_p + i \omega C_p V \quad \dots\dots\dots (2.42)$$

As a result, the impedance ( $Z$ ) is then equal to [100]:

$$1/Z = 1/R_p + i \omega C_p \quad \dots\dots\dots (2.43)$$

Using the equations (2.39), (2.40) and (2.42), one can get the following [100]:

$$R_p = d / \omega A_r \varepsilon_o \varepsilon'' \quad \dots\dots\dots (2.44)$$

$$\varepsilon'' = 1 / \omega R_p C_o \quad \dots\dots\dots (2.45)$$

$$C_p = \varepsilon_o \varepsilon' A_r / d \quad \dots\dots\dots (2.46)$$

$$\varepsilon' = C_p / C_o \quad \dots\dots\dots (2.47)$$

The dissipated power at an insulator is expressed by the existence of an alternating voltage as a function with alternating conductivity, as shown in equation (2.48):

$$\sigma_{A.C} = \omega \varepsilon_0 \varepsilon'' \dots\dots\dots (2.48)$$

$\sigma_{A.C}$  is a temperature measurement in an insulating material caused by the dipoles rotating in their places (or the charges vibrating) as a result of the field alternating [104].

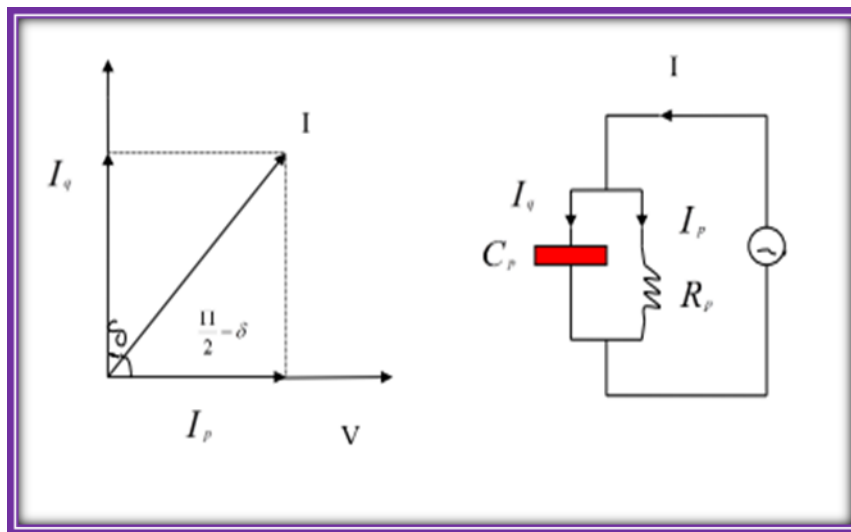


Figure (2.5): The circuit equivalent of a non-ideal capacitor. [101].

### 2.6 Anti-Bacterial Activity

Infectious disease development in general poses a severe threat to public health worldwide, particularly with the emergence of antibiotic-resistant bacterial species. As a result, there is an incentive to develop new bactericidal [105]. In general, both gram-negative and gram-positive bacterial strains are considered to be a significant public health threat. Antibiotics are used to control infections caused by both community and hospital environments pathogens for many years [106,107].

Recent advancements in the domain of nano bio technology, especially the ability to prepare metal oxide nanoparticles with precise size and shape specifications, are anticipated to result in the development of new antibacterial agents. The size of nanoparticles has a major effect on their functional properties. As a result of their unique chemical, physical, and biological characteristics, nanoparticles have garnered considerable attention in various fields, including medicine [108,109,110].

Due to the wide spread use of the antibiotics in prevention and treatment of bacterial infections, resistant microorganisms have developed, necessitating the creation of new active molecules against bacteria. The size of nanoparticles is approximately the same as that of biological molecules and less than that of human cells. Nanotreatment strategies could be used to improve medical treatments [111,112].

### **3.1 Introduction**

This chapter includes the preparation process, instrumentation and measurement techniques. A general description of materials (polyvinyl alcohol, polyvinyl pyrrolidone and cobalt oxide) used in this work are given by (optical microscopic, Fourier Transform Infrared Rays (FTIR), Scanning Electron Microscope (SEM)) and also contains images and includes diagrams of some of electrical circuits.

### **3.2 The Utilized Materials**

The used materials in this study are:

#### **3.2.1 Matrix Material**

Polymers: two types of polymers are used in this work:

- **Polyvinyl Alcohol (PVA)**

The polymer is used as granular form and could be obtained from local markets, and high purity (99.99 %).

- **Polyvinyl Pyrrolidone (PVP)**

It was obtained as powder form and could be obtained from local markets, and high purity (99.99 %).

#### **3.2.2 Additive Nanomaterial**

Cobalt oxide ( $\text{Co}_2\text{O}_3$ ) nanoparticles: It was obtained as powder form and could be obtained from local markets, with radius (30-80) nm and high purity (99.999 %).

### **3.3 Preparation of Nanocomposites**

The (PVA-PVP- $\text{Co}_2\text{O}_3$ ) nanocomposites are prepared by the following:

1. Polymers nanocomposites films have been prepared by mixing 58 % of PVA with (42%) of PVP in (40) mL of distilled water in a glass beaker by using magnetic stirrer, for the maxing process for 15 minutes to obtain more homogenous solution with temperature of (70 C°). Then wait for the solution to be cooled.
2. Adding the weight percentages of additives (1.6,3.2,4.8 and 6.4) wt. % of (Co<sub>2</sub>O<sub>3</sub>), we get the films from this mixture using the casting process, which involves placing the mixture in a template (Petri dish has a diameter of 5cm), and then left for 3 -7days to dry mixture, then taken from template quietly to conducting the necessary tests, using micrometer to measure thickness, it is (120)µm. Figure (3.1) shows The preparation condition of (PVA-PVP-Co<sub>2</sub>O<sub>3</sub>) films and the structural, electrical and optical measurements.

**Table (3): Weight percentage for nanocomposites**

<b>PVA wt.%</b>	<b>PVP wt.%</b>	<b>CO<sub>2</sub>O<sub>3</sub> wt.%</b>
0.58	0.42	0
0.57072	0.41328	0.016
0.56144	0.40656	0.032
0.55216	0.39984	0.048
0.54288	0.39312	0.064

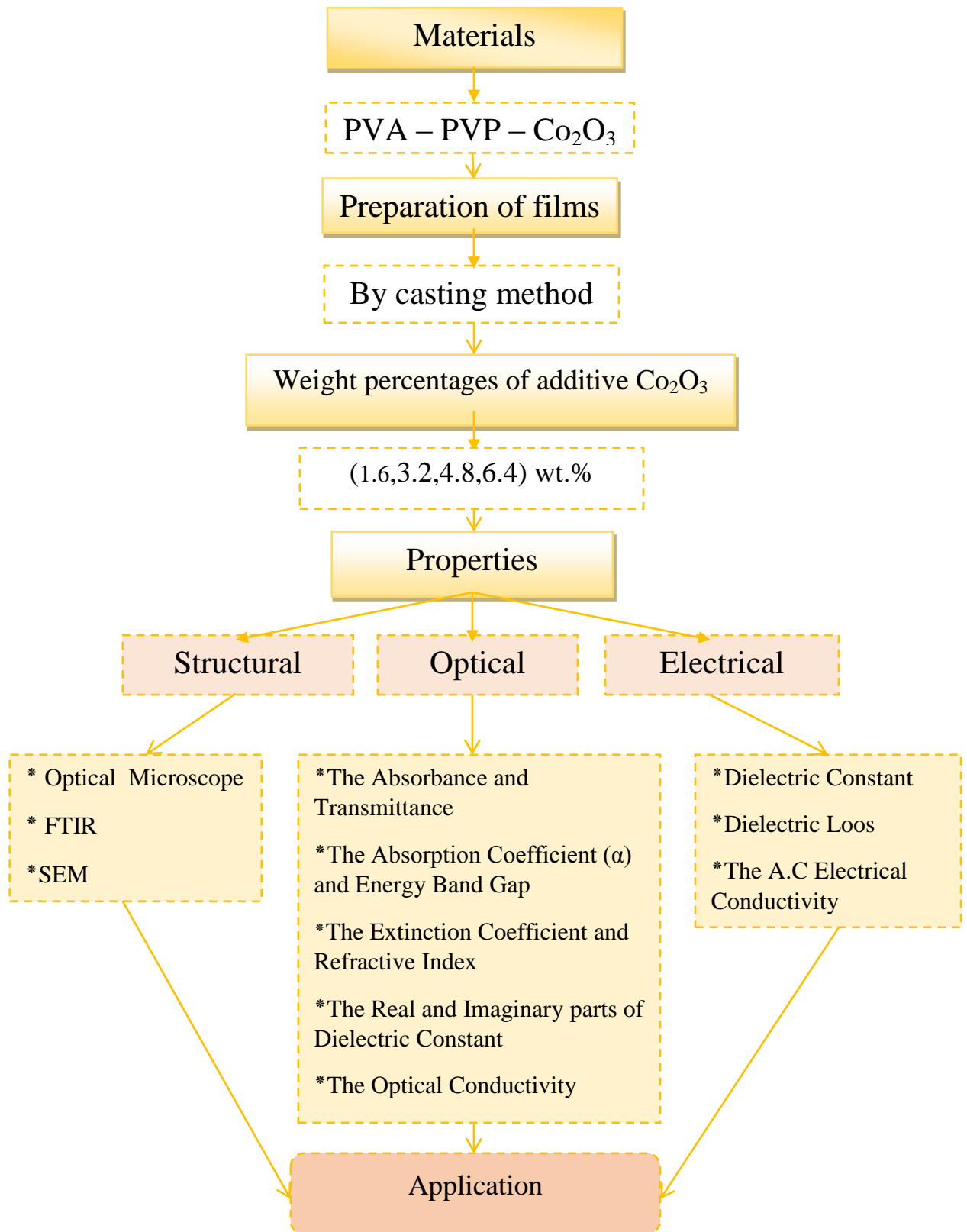


**Figure (3.1): The preparation condition of (PVA-PVP-Co<sub>2</sub>O<sub>3</sub>) films and the structural, electrical and optical measurements.**

### 3.4 Measurements of Structural Properties

#### 3.4.1 Optical Microscope

The sample of (PVA-PVP-Co<sub>2</sub>O<sub>3</sub>) nanocomposites are examined by using the optical microscope, which is supplied from Olympus name (Toup View) type (Nikon -73346) as shown in figure (3.2) and equipped with light intensity automatic controlled camera. Under magnification (10x), exited in Babylon University/College of Education for Pure Sciences.



Figure (3.2): Image of optical microscope.

#### 3.4.2 FTIR Spectral Characterization

FTIR spectra were recorded by FTIR (Bruker company, German origin, type vertex -70) Fourier Transform Infrared Rays exited in Babylon University/College of Education for Pure Sciences/Department of Physics. The wave number range (400-4000) cm<sup>-1</sup> as shown in figure (3.2).



**Figure (3.3): Image of (FTIR) spectroscopy.**

### 3.4.3 Scanning Electron Microscope

The scanning electron microscope (SEM) is an electron microscope that images the sample surface by scanning it with a high -energy beam of electrons in a raster scan pattern .The specimens for an SEM testing must be electrically conductive, at least at the surface, and electrically grounded to prevent the accumulation of electrostatic charge at the surface. Small part of ( $1\text{cm}^2$ ) was taken from the sample to examine it by SEM. In this work ,low vacuum scanning electron microscope was used.The surface morphology of (PVA-PVP- $\text{Co}_2\text{O}_3$ ) nanocomposites was observed using Tescan mira3 SEM microscope. equipped with dual Bruker XFlash EDS detectors and Bruker eFlash HD EBSD( Czech Tescan Instrument Co.) for analytical studies at the University of Tehran as shown in figure (3.4). The advantage was observed using this technique (Low vacuum SE detecto) is beam deceleration technology (BDT) for high resolution imaging and high surface sensitivity at very low kv and variable pressure operation, Fully integrated active anti-vibration system.

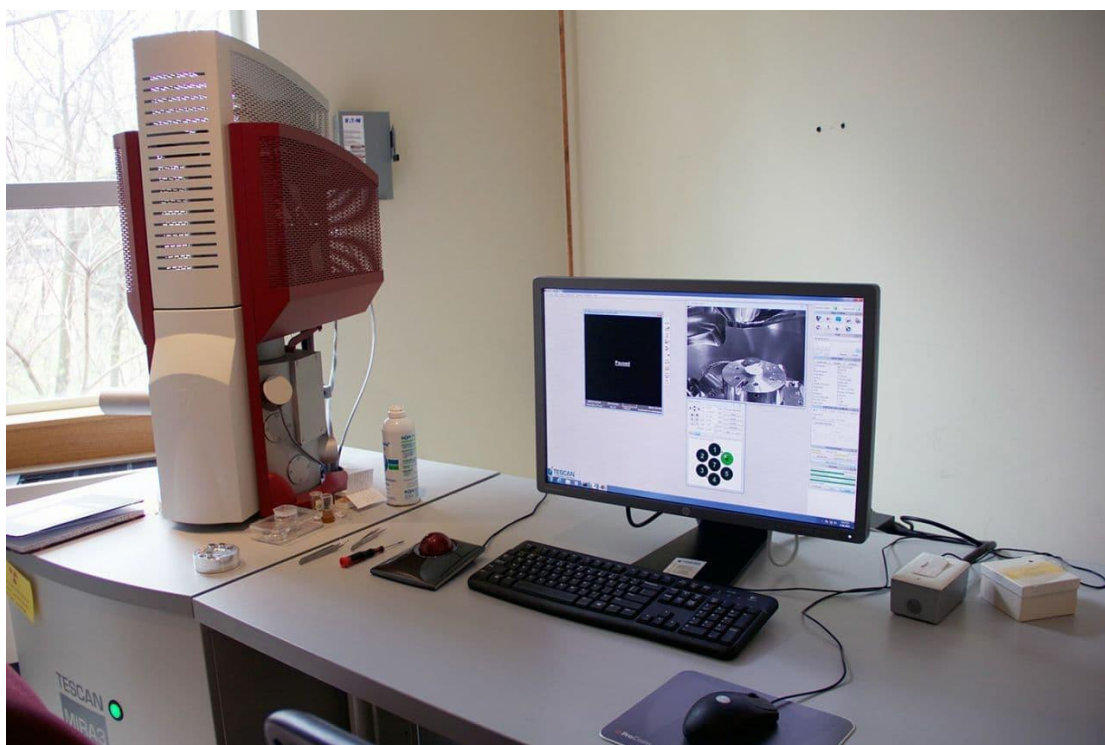


Figure (3.4): Diagram for system of SEM device.

### 3.5 Optical Properties Measurements

The absorption spectrum of (PVA-PVP-  $\text{Co}_2\text{O}_3$ ) nanocomposites films have been recorded in the wavelength range (190-1100) nm by using the double beam spectrophotometer (Shimadzu model UV-1800 A° (JAPAN)) as shown in figure (3.5). It found in Babylon University/College of Education for Pure Sciences/Department of Physics. The absorption spectrum have been recorded at room temperature. A computer program was employed to obtain the optical constants, absorption coefficient, extinction coefficient, refractive index and energy gaps.



**Figure (3.5): Image of UV spectrophotometer.**

### **3.6 Measurement of A.C. Electrical Properties**

The A.C. Electrical Properties have been measured by LCR meter type (HIOKI 3532-50 LCR Hi TESTER (Japan)). It is found in Babylon University, College of Education for Pure Sciences/Department of physics, as shown in figure (3.7). Only (1cm) from each one of the samples have been taken and put between two electrodes and by different frequencies from (100Hz-5MHz) at room temperature which shows a diagram of A.C circuit. The capacity and dissipated factor have been recorded for all samples. Dielectric constant, dielectric loss and conductivity have been calculated from this data by using the special equation of A.C electrical properties.

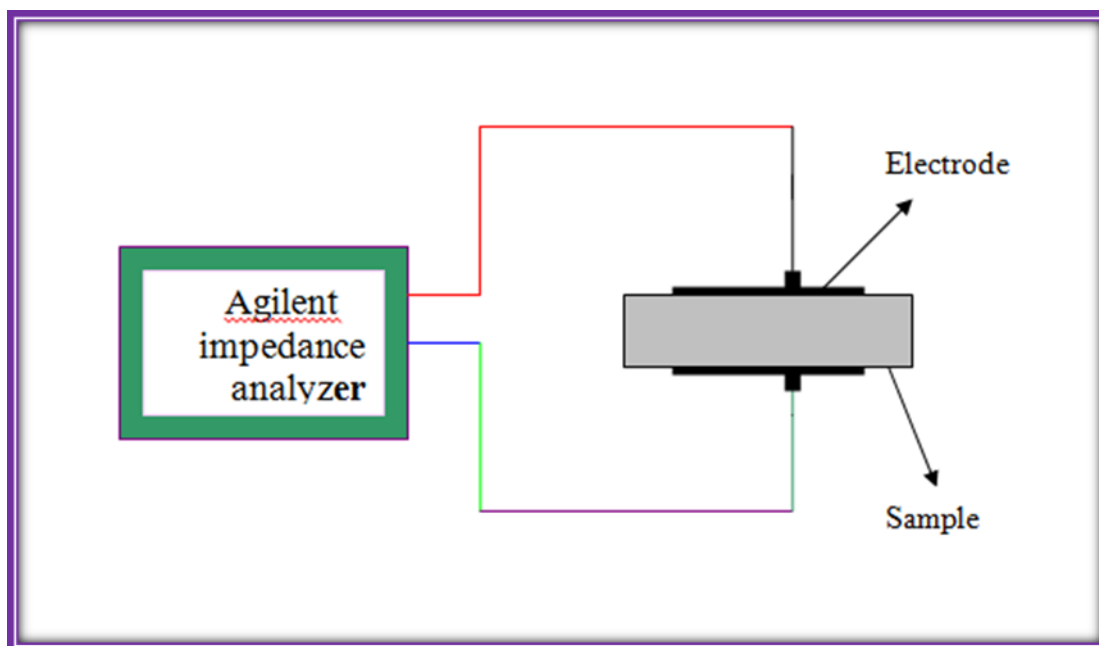


Figure (3.6): Diagram for system of A.C electrical measurement

### 3.7 Antibacterial Activity Application Measurements of Nanocomposites

Antimicrobial activity of the (PVA-PVP- $\text{Co}_2\text{O}_3$ ) nanocomposites tested samples were determined using a disc diffusion method. The antibacterial activities were done by using gram positive organisms (*Staphylococcus aureus*) and gram negative organisms, *Escherichia coli*, Bacteria (*Staphylococcus aureus* and *Escherichia coli*) were cultured in Muller-Hinton agar. The films of the (PVA-PVP- $\text{Co}_2\text{O}_3$ ) nanocomposites were placed over the media and incubated at  $37^\circ\text{C}$  for 24 hours. The inhibition zone diameter was measured.

## **4.1 Introduction**

This chapter included the results and its discussion of the structural ,optical and (A.C) electrical measurements for (PVA-PVA-Co<sub>2</sub>O<sub>3</sub>) nanocomposites . It will also discuss the effect of different concentrations additive nanoparticles (Co<sub>2</sub>O<sub>3</sub>) in the optical microscope, fourier transform infrared rays (FTIR), scanning electron microscope (SEM) and antibacterial activity applications of (PVA-PVP-Co<sub>2</sub>O<sub>3</sub>) nanocomposites are also discussed.

## **4.2The Structural Properties**

### **4.2.1 The Optical Microscope**

Figure (4.1) shows the images of (PVA-PVP-Co<sub>2</sub>O<sub>3</sub>) nanocomposites films taken for samples of different concentrations at magnification power (10x). However, there is a clear difference between the samples as shown in the pictures (A, B, C, D, and E). When the Cobalt oxide nanoparticles concentration in films (polyvinyl alcohol and polyvinyl Pyrrolidone) reaches (6.4 wt.%) for (PVA-PVP-Co<sub>2</sub>O<sub>3</sub>) nanocomposites, the nanoparticles form a continuous network inside the polymers. This network is made up of paths that run through the nanocomposites and enable charge carriers to pass through them [113,114].

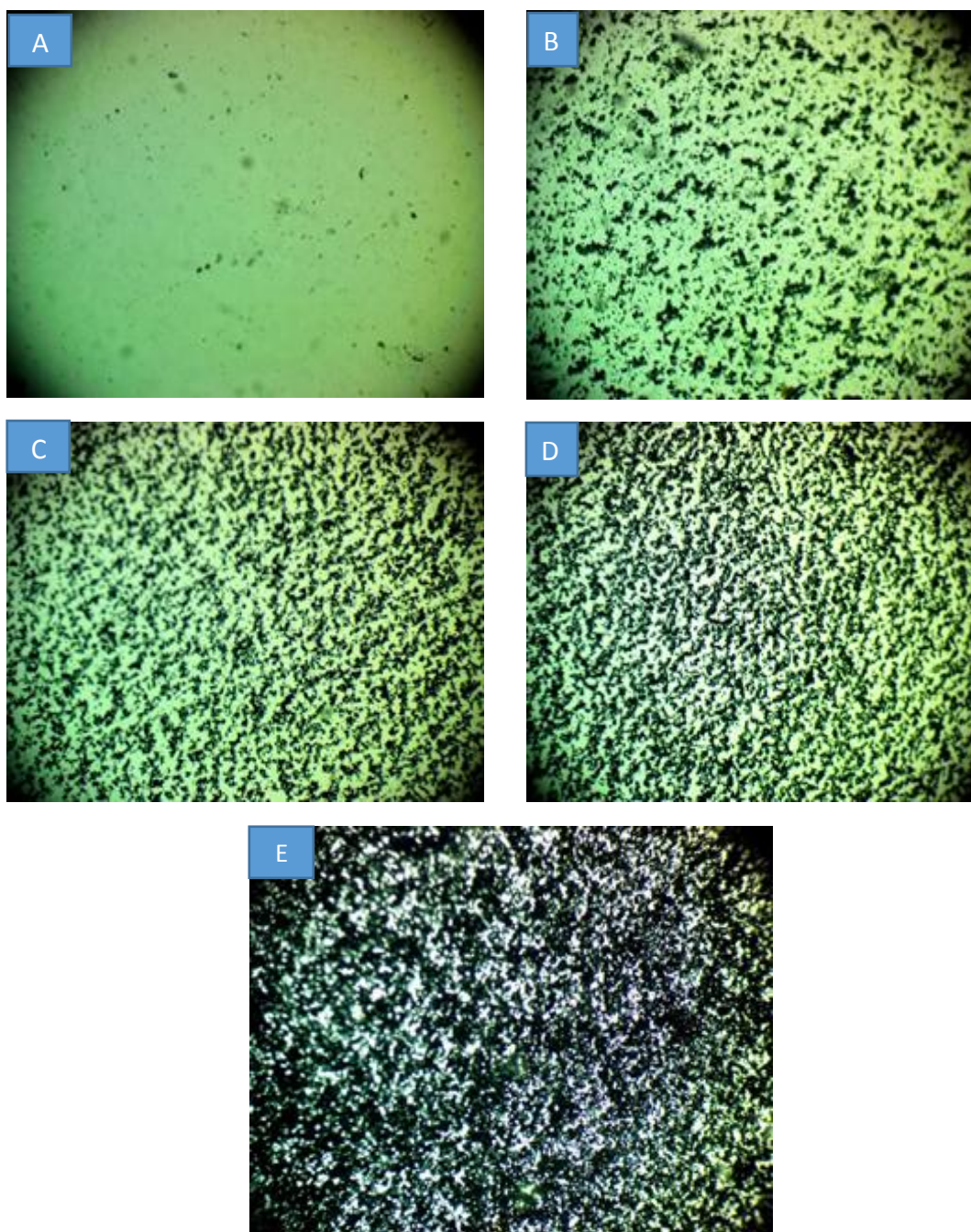


**Fig. (4.1).** Photomicrographs (10X) for (PVA-PVP-  $\text{Co}_2\text{O}_3$ ) nanocomposites: (A) for pure (PVA-PVP), (B) for 1.6 wt%  $\text{Co}_2\text{O}_3$ , (C) for 3.2 wt%  $\text{Co}_2\text{O}_3$ , (D) for 4.8 wt%  $\text{Co}_2\text{O}_3$ , (E) for 6.4 wt%  $\text{Co}_2\text{O}_3$ .

### 4.2.2 Fourier Transform Infrared Rays

FTIR spectroscopy has been used to analyze the interactions among atoms or ions in (PVA-PVP-Co<sub>2</sub>O<sub>3</sub>) nanocomposites, these interactions can include changes in the vibrational modes of the nanocomposites. The (FTIR) transmittance spectra of (PVA-PVP-Co<sub>2</sub>O<sub>3</sub>) nanocomposites films with the different ratio of (Co<sub>2</sub>O<sub>3</sub>) nanoparticles are shown in figure (4.2) are recorded at room temperature in the region (400-4000) cm<sup>-1</sup>. From the spectra, the FTIR spectrum of (PVA-PVP) films shows broad band about 3300 cm<sup>-1</sup> is assigned to the stretching vibration of hydroxyl group (OH) of PVA, which may be due to the intermolecular or intra molecular type of hydrogen bonding of the polymer and the nanoparticles. The band corresponding to CH<sub>2</sub> asymmetric stretching vibration occurs at about 2930 cm<sup>-1</sup>. The peaks at 1710 and 1652 cm<sup>-1</sup> have been attributed to the C=O, C=C stretching mode. The absorption peak at 1240 cm<sup>-1</sup> has been assigned to the wagging (CH) group. The band about 1105 cm<sup>-1</sup> corresponds to C-O stretching of carbonyl groups present on the PVA backbone. While the absorption band about 962 cm<sup>-1</sup> is assigned to out of plane rings C-H bending. Table (4.1) shows the links in polyvinyl alcohol. The band relating to the pyrrolidone C=O group is located at 1698 cm<sup>-1</sup>. The vibrational band at 1698 cm<sup>-1</sup> corresponds to C=O stretching of PVP polymer film, C-H asymmetric stretching of CH<sub>2</sub> absorption band located at 2987 cm<sup>-1</sup>. The bands at 931 cm<sup>-1</sup>, 1260 cm<sup>-1</sup> and 1427 cm<sup>-1</sup> are attributed to C-C stretching vibration, C-N stretching vibration and C-H bending vibration of pure respectively. Table (4.2) shows the links in polyvinyl pyrrolidone. In case of (PVA-PVP-Co<sub>2</sub>O<sub>3</sub>) with different (Co<sub>2</sub>O<sub>3</sub>) ratio, FTIR spectra show shift in peak position as well as the change in shape and intensity comparing with pure (PVA-PVP) films. This indicates decoupling between the corresponding vibrations due to interaction between (Co<sub>2</sub>O<sub>3</sub>) nanoparticles and the two

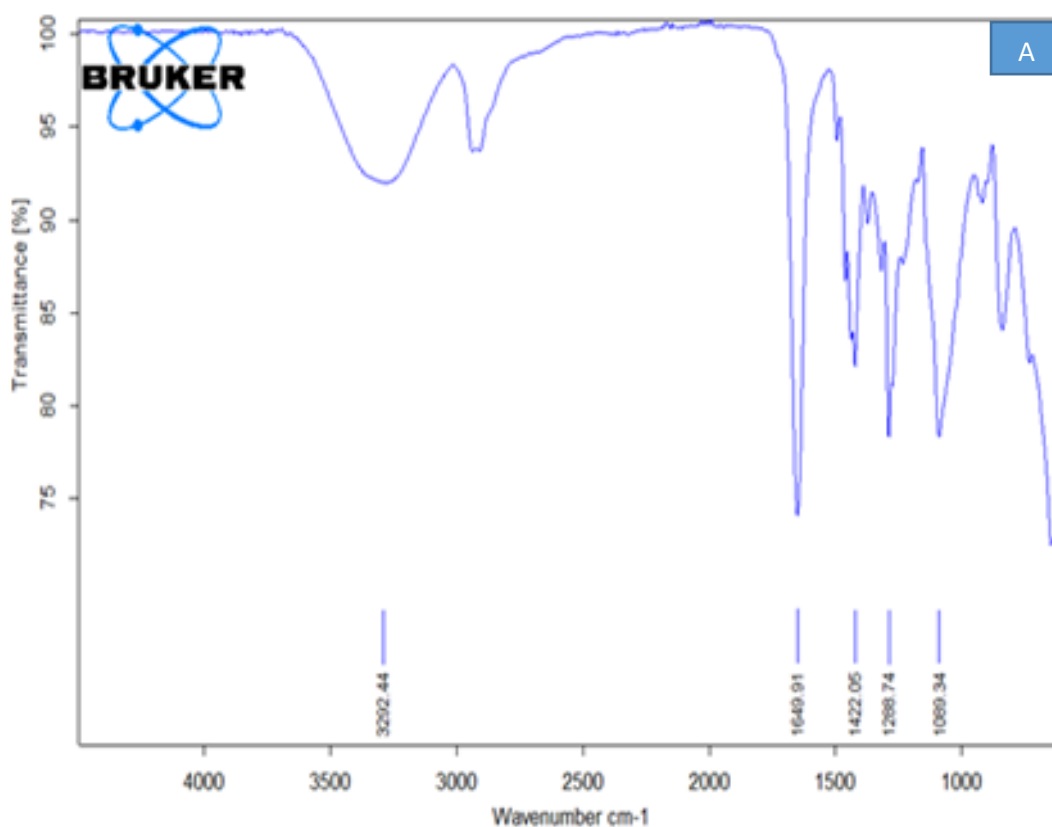
polymers [115], and this noticed that there is a decrease in transmittance at increasing the amount of weight percent of cobalt oxide nanoparticles. The increased density of the films, means an increase of atoms and ions in the light path and increase the absorbance at UV contrary the IR, as shown in the figure (4.2 A-B-C-D and E) [115,116].

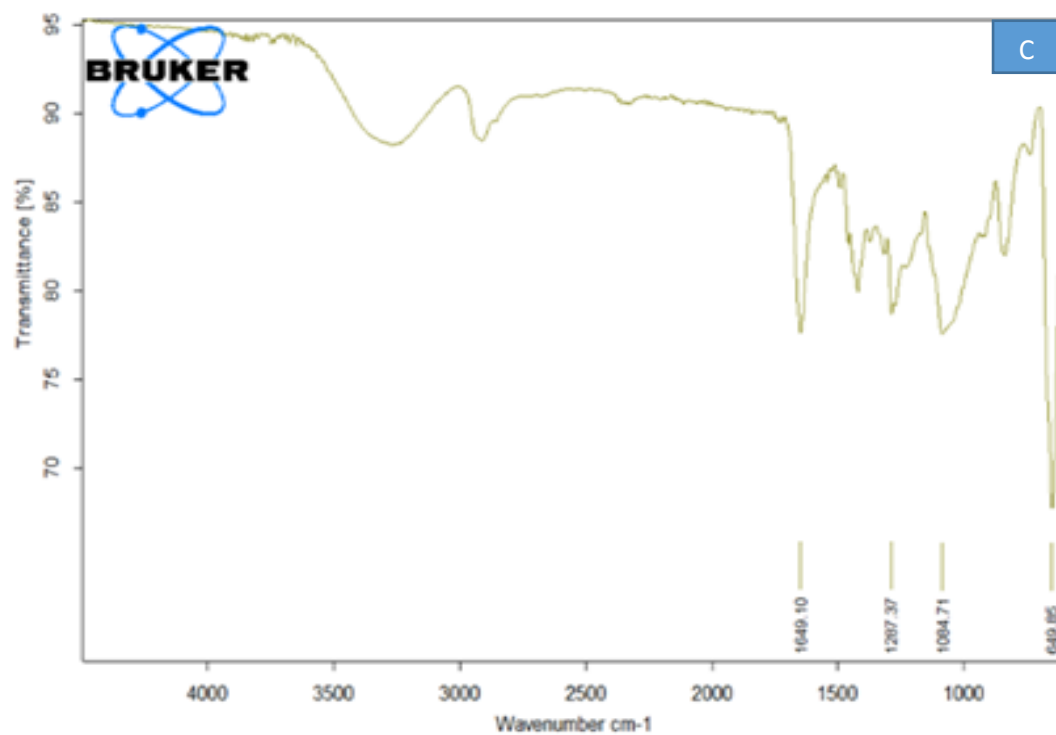
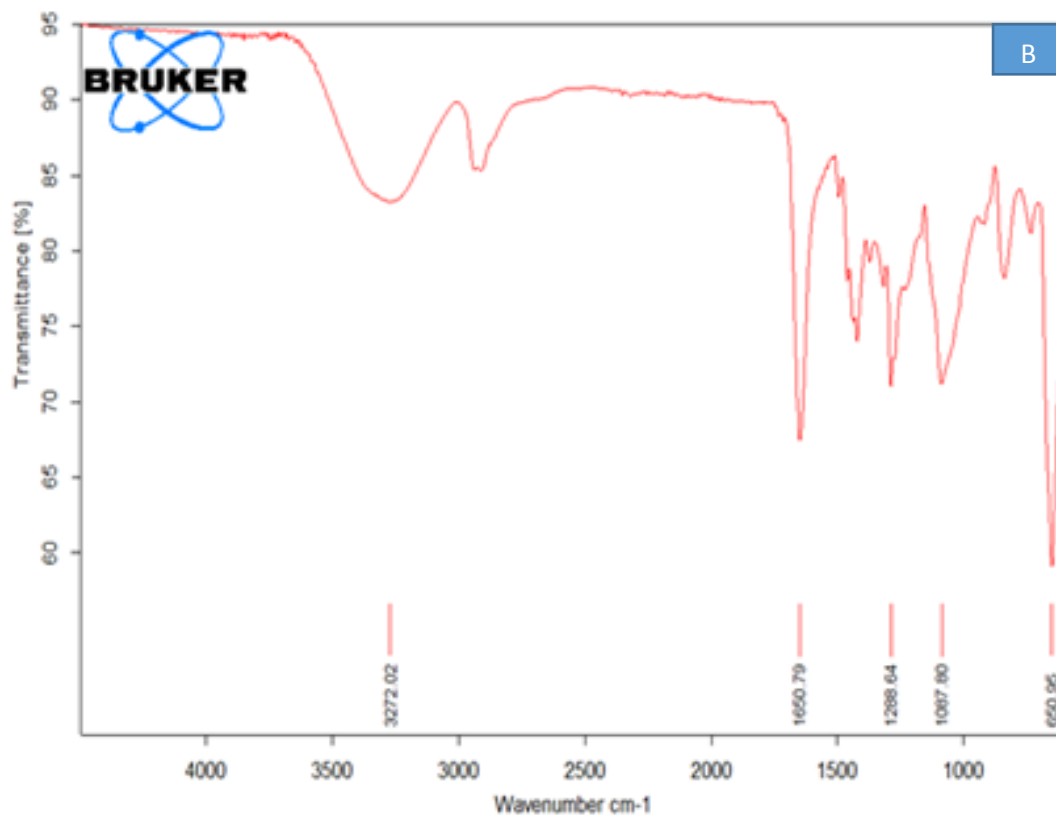
**Table (4.1): FTIR Transmittance bands positions and their assignments for pure PVA.**

Wavenumber (cm <sup>-1</sup> )	Band assignment
3300	OH stretching
2930	CH <sub>2</sub> asymmetric stretching
1652	C=C stretching
1710	C=O stretching
1429	Symmetric bending of CH <sub>2</sub>
1326	(CH+OH) bending
1241	Wagging of (CH)
1105	C-O stretching
963	Out of plane rings C-H bending
845	CC stretching vibrations
663	Wagging mode of (OH) groups
481	Bending mode of (CO)
421	Wagging of (CO)

**Table (4.2): FTIR Transmittance bands positions and their assignments for pure PVP.**

Wavenumber (cm <sup>-1</sup> )	Band assignment
1698	C=O stretching
2987	C-H stretching
931	C-C stretching
1260	C-N stretching
1427	C-H bending





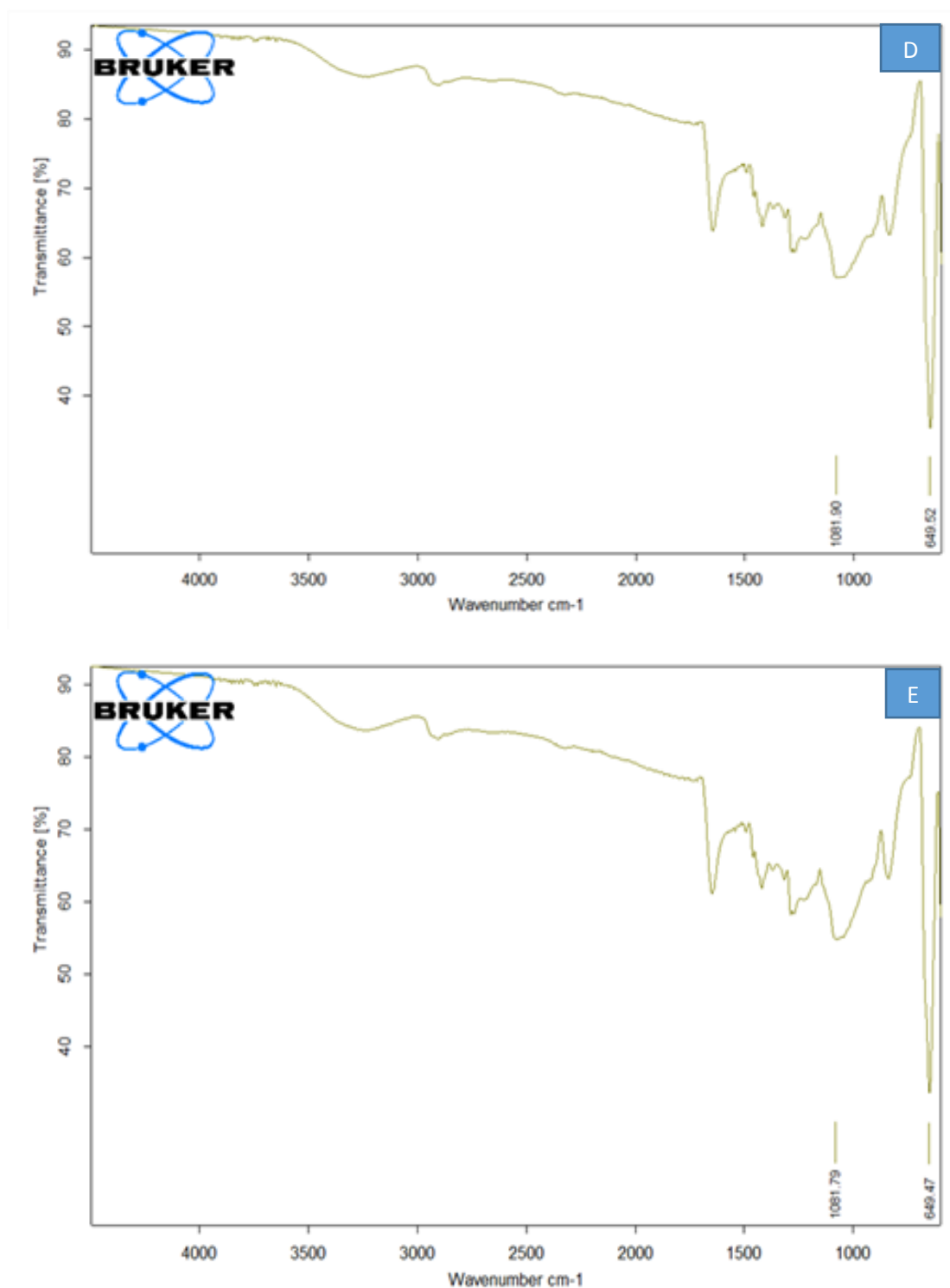


**Fig. (4.2).** FTIR spectra for (PVA-PVP-Co<sub>2</sub>O<sub>3</sub>) nanocomposites films : (A) PVA-PVP, (B) 1.6 wt% Co<sub>2</sub>O<sub>3</sub>, (C) 3.2 wt% Co<sub>2</sub>O<sub>3</sub>, (D) 4.8 wt% Co<sub>2</sub>O<sub>3</sub> , (E) 6.4 wt% Co<sub>2</sub>O<sub>3</sub>.

### 4.2.3 Scanning Electron Microscopy (SEM)

SEM is used to investigate fully the effect of cobalt oxide nanoparticles content and to examine the dispersion of nanocomposites particles in the polymers matrix. Figures (4.3) show SEM images of the (PVA-PVP-Co<sub>2</sub>O<sub>3</sub>) nanocomposites films with different concentrations of cobalt oxide nanoparticles content. Image (A) in figure (4.3) for polymers is found to be softer, homogenous and coherence. One can noticed from the figures that the addition of cobalt oxide nanoparticles in (PVA-PVP-Co<sub>2</sub>O<sub>3</sub>) nanocomposites leads to changes in the surface morphology. It can be seen from the images that the grain aggregates with increasing cobalt oxide nanoparticles ratio. The surface morphology of the (PVA-PVP-Co<sub>2</sub>O<sub>3</sub>) nanocomposites films show many aggregates or chunks randomly distributed on the top surface [117]. The results show an increase in the number of white dots on the surface with increasing concentration of cobalt oxide nanoparticles.

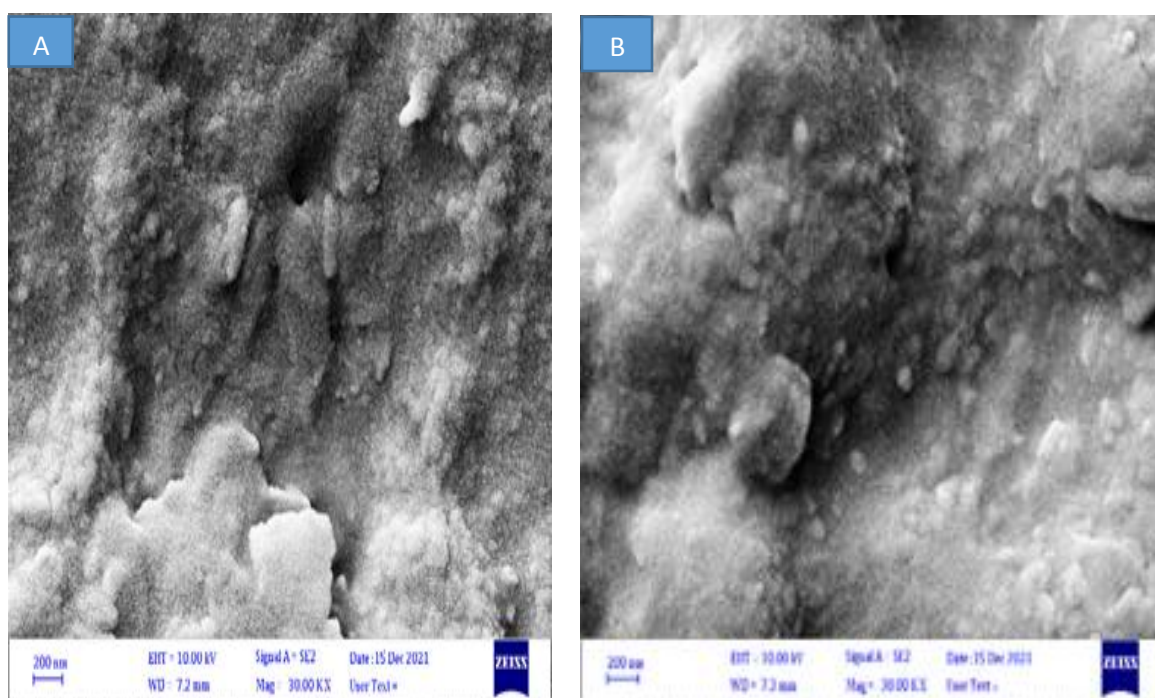




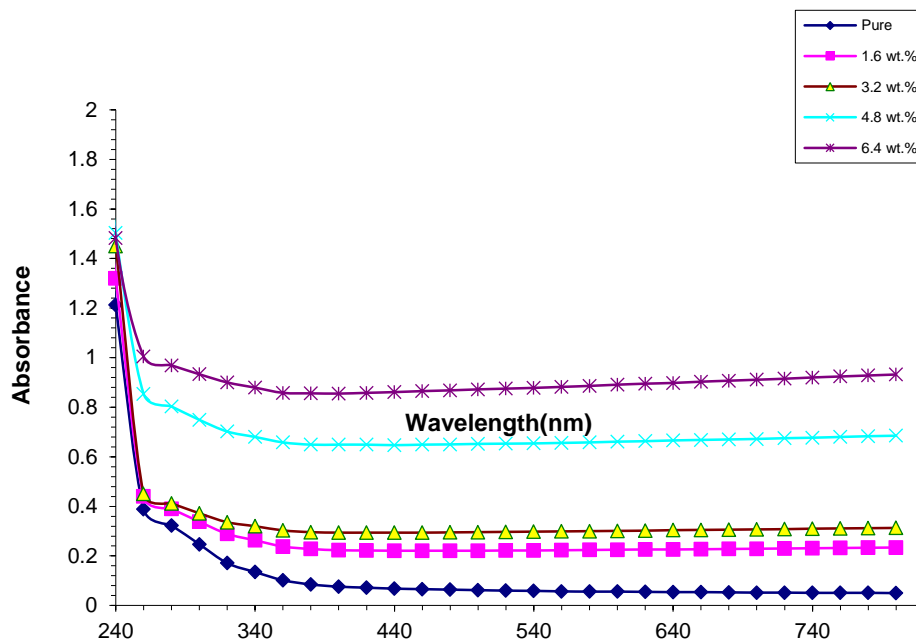
**Fig. (4.3).** SEM images for (PVA-PVP- $\text{Co}_2\text{O}_3$ ) nanocomposites : (A) for (PVA-PVP), (B) for 1.6 wt%  $\text{Co}_2\text{O}_3$ , (C) for 3.2 wt%  $\text{Co}_2\text{O}_3$ , (D) for 4.8 wt%  $\text{Co}_2\text{O}_3$ , (E) for 6.4 wt%  $\text{Co}_2\text{O}_3$ .

### **4.3 The Optical Properties**

The main purpose of studying the optical properties of the (PVA-PVP- $\text{Co}_2\text{O}_3$ ) nanocomposites is to identify the effect of adding Cobalt oxide nanoparticles on the optical properties of (PVA-PVP) films. The research covers the recording of the spectrum of absorbance for the (PVA-PVP- $\text{Co}_2\text{O}_3$ ) films at room temperature and calculating the absorption coefficient, extinction coefficient, and other optical constants, as well as identifying the types of electronic transitions and calculating energy gaps.

#### **4.3.1 The Absorbance (A)**

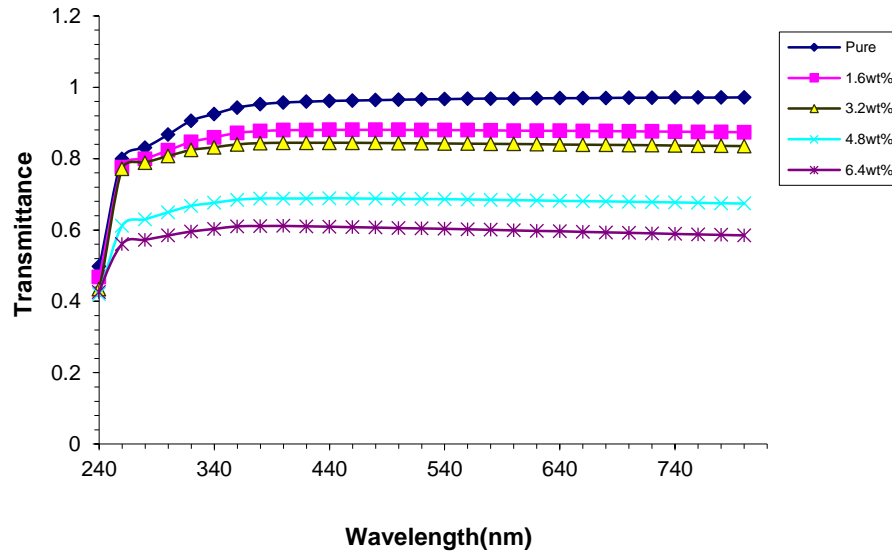
The absorption spectrum of (PVA-PVP- $\text{Co}_2\text{O}_3$ ) nanocomposites as a function of wavelength of the incident light is depicted in figure (4.4). It is seen in the figure that the absorbance of all films is highest at a wavelength (220 nm) in the vicinity of a fundamental absorption edge, then the absorbance decreases as the wavelength increases. In general, films have a low absorbance in near-the infrared and the visible ranges. This demeanor is explained by the following: at high wavelength the incident photon doesn't have enough energy to interact with atoms, thus the electron will be transmitted, when the wavelength decreases (at the neighborhood of the fundamental absorption edge), the interaction between incident photon and material will occur, and then absorbance will increase [118]. To put it another way, incident light is absorbed by free electrons. As a result, the absorbance is raised by increasing the weight percentages of cobalt oxide nanoparticles.



**Figure(4.4).** The absorption of (PVA-PVP- $\text{Co}_2\text{O}_3$ ) nanocomposites as a function of wavelength.

### 4.3.2 Transmittance Spectrum

The optical transmittance spectrum of (PVA-PVP- $\text{Co}_2\text{O}_3$ ) films is shown in figure (4.5) as a function of wavelength of incident light when varied rates of ( $\text{Co}_2\text{O}_3$ ) nanoparticles are added. The figure demonstrates that transmittance reduces as the concentration of ( $\text{Co}_2\text{O}_3$ ) nanoparticles increases, This is due to the addition of ( $\text{Co}_2\text{O}_3$ ) nanoparticles having electrons in their outer orbits that can absorb the electromagnetic energy of incident light and move to upper energy levels, this procedure does not result in the emission of radiation because the electrons that have moved to upper levels have filled vacant energy band positions, As a result, a portion of incident ray is absorbed by material and does not pass through it, In addition, pure (PVA and PVP) have a high transmittance due to the absence of free electrons (i.e. electrons are covalently bound to atoms), this is because the process of breaking the electron's bond and transferring it to the conduction band requires a high energy photon [119].

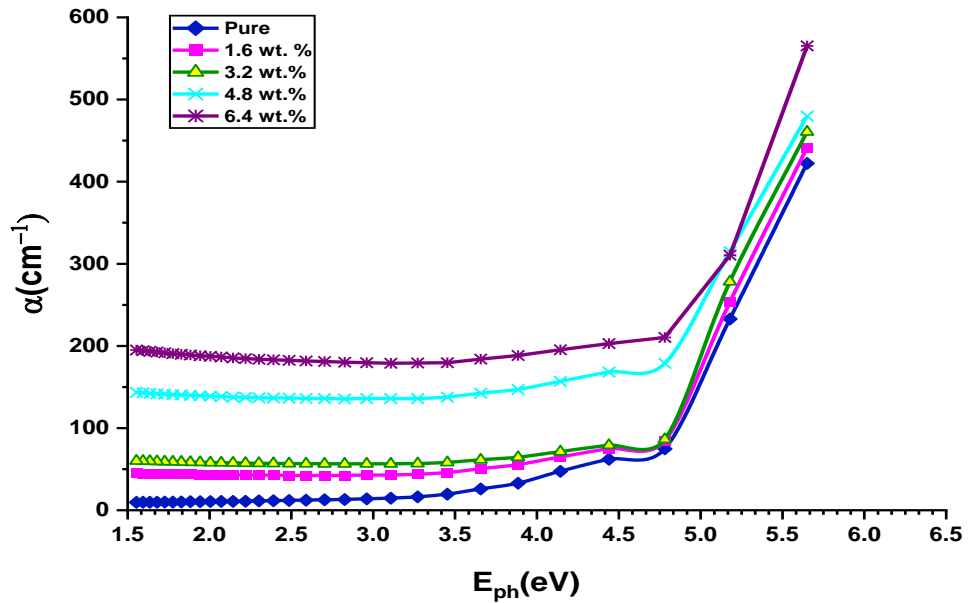


Figuer(4.5). The relationship between transmittance of (PVA-PVP-CO<sub>2</sub>O<sub>3</sub>) and wavelength

### 4.3.3 Absorption Coefficient ( $\alpha$ )

The absorption coefficient ( $\text{cm}^{-1}$ ) is found by using the equation: (2.13), The absorption coefficient ( $\text{cm}^{-1}$ ) as a function of photon energy for (PVA-PVP-CO<sub>2</sub>O<sub>3</sub>) nanocomposites is depicted in figure (4.6). It can be noted that at high wavelengths and low energies, the absorption coefficient is the smallest, This signifies that the possibility of an electron transition is low, as the incident photon's energy is insufficient to transfer the electron from (V.B) to the (C.B) ( $h\nu < E_g^{opt}$ ) [120]. At greater energies, the absorption is greater, implying a greater possibility of electron transitions, The incident photon's energy is sufficient to transfer the electron from the valence band to the conductive band, this indicates that the incident photon's energy is higher than the prohibited energy gap. This demonstrates the value of the absorption coefficient in determining the type of electron transfer, if absorption coefficient ( $\alpha > 10^4$ )  $\text{cm}^{-1}$  is large at high energy, electrons are predicted to undergo a direct transition, the photons and electrons retain the energy and

moment, but indirect transition of electrons are expected to occur since the values of the absorption coefficient are low ( $10^4$ )  $\text{cm}^{-1}$  at low energies, and the phonon assists in maintaining the electronic momentum [120], among other findings, the absorbance coefficient of the (PVA-PVP- $\text{Co}_2\text{O}_3$ ) nanocomposites is lower than ( $10^4$   $\text{cm}^{-1}$ ), indicating that the electron transition is indirect.



Figure(4.6). The relationship between the absorption coefficient of (PVA-PVP- $\text{Co}_2\text{O}_3$ ) and the photon energy.

#### 4.3.4 Optical Energy Gaps of The Indirect Transition (Allowed and Forbidden)

The energy gap for the allowed and forbidden indirect transition bands has been determined using equation (2.4), The variation of the absorption edge  $(\alpha h\nu)^{1/2}$  of (PVA-PVP- $\text{Co}_2\text{O}_3$ ) nanocomposites with the photon energy is depicted in figure (4.7), the energy gap of allowed indirect transition can be obtained by way of drawing a direct line from upper part of the curve

towards to x axis at the value  $(\alpha h\nu)^{1/2} = 0$ . The values obtained are listed in table (4.3).

The energy gap values are lower as the concentration of cobalt oxide nanoparticles increases. This is ascribed to the formation of localized energy levels within the forbidden energy gap [120], in this situation, the transition occurs in two steps, with the electrons moving from the valence band to the local levels and finally to the conduction band as a result of increasing the concentration of cobalt oxide nanoparticles, this demeanor is related to the heterogeneous nature of nanocomposites (i.e. the electronic conduction depends on added concentration), with increasing concentrations of ( $\text{Co}_2\text{O}_3$ ) nanoparticles, the density of the localized state increased.

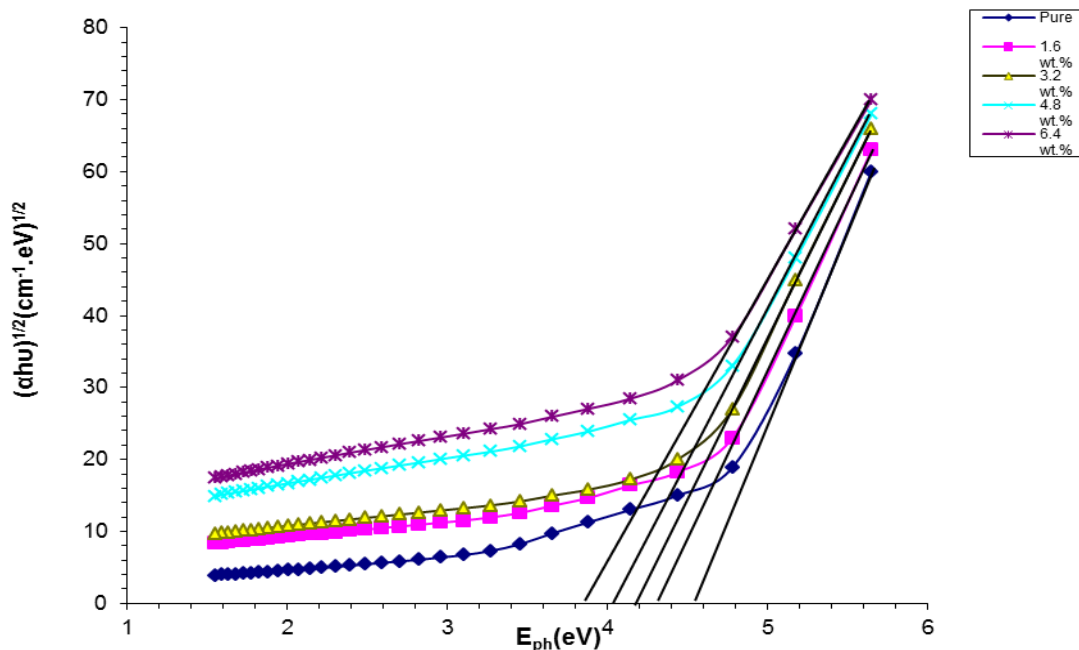
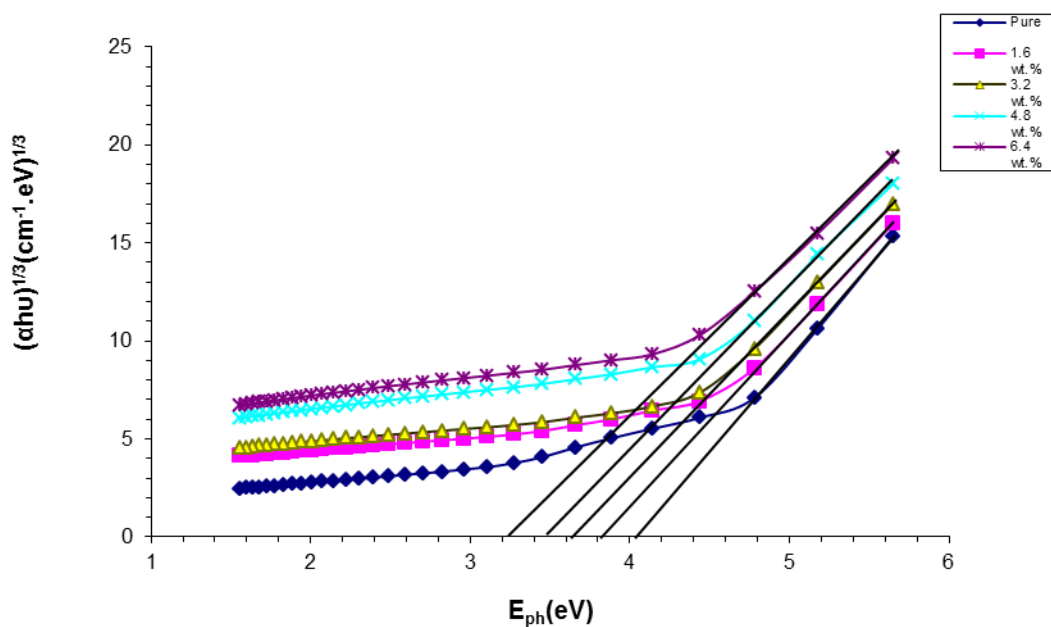


Figure (4.7).The relationship between  $(\alpha h\nu)^{1/2} (\text{cm}^{-1}.\text{ev})^{1/2}$  and allowed photon energy of (PVA-PVP- $\text{Co}_2\text{O}_3$ ) nanocomposites.

The same way is used to determine the forbidden transition of indirect energy gap. The forbidden transition of the (PVA-PVP-Co<sub>2</sub>O<sub>3</sub>) nanocomposites' indirect energy gap is depicted in figure (4.8).



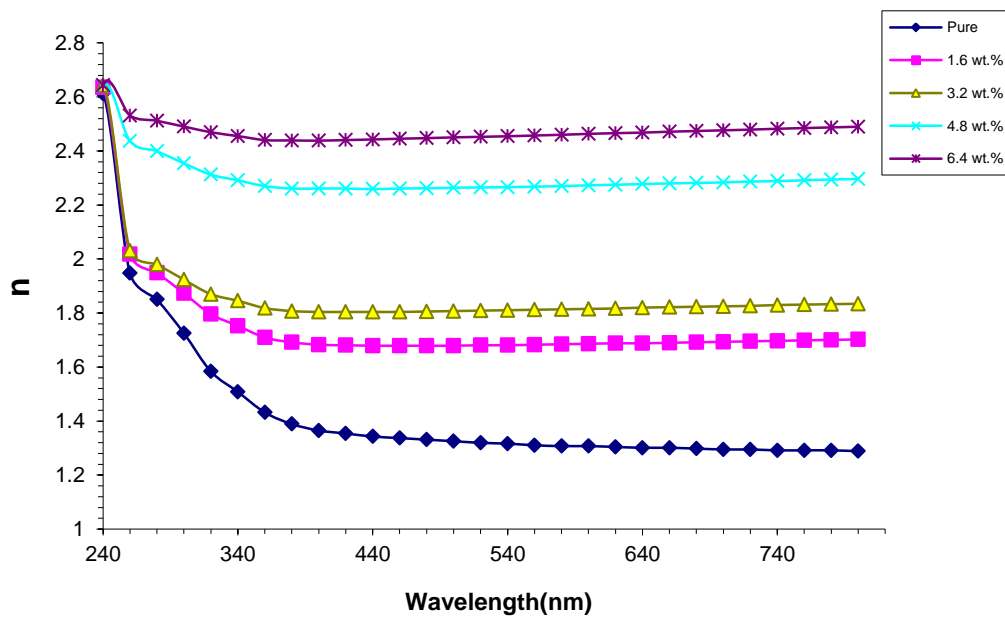
Figure(4.8). The relationship between  $(\alpha h\nu)^{1/3} (\text{cm}^{-1}.\text{eV})^{1/3}$  and the forbidden photons energy of the (PVA-PVP-Co<sub>2</sub>O<sub>3</sub>) nano-composites.

Table (4.3): The energy gap for the allowed and forbidden indirect transition for (PVA-PVP-Co<sub>2</sub>O<sub>3</sub>) nanocomposites.

Cobalt oxide nanoparticles wt. %	The optical energy gap of the indirect transition (eV)	
	allowed	forbidden
0	4.5	4.1
1.6	4.3	3.8
3.2	4.2	3.6
4.8	4.1	3.5
6.4	3.9	3.2

### 4.3.5 Refractive Index ( $n$ )

The refractive index ( $n$ ) of a material can be calculate using equation (2.16). The figure (4.9) show the relationship between the refractive index of (PVA-PVP- $\text{Co}_2\text{O}_3$ ) nanocomposites and the wavelength. As shown in the figure, the refractive index increase as the weight % of ( $\text{Co}_2\text{O}_3$ ) nanoparticles in (PVA and PVP) increases due to the growing density of nanocomposites. In the UV region, it is possible to observe that the refractive index is extremely high due to the region's low transmittance, while in the visible region, low values were observed due to the region's high transmittance [121].

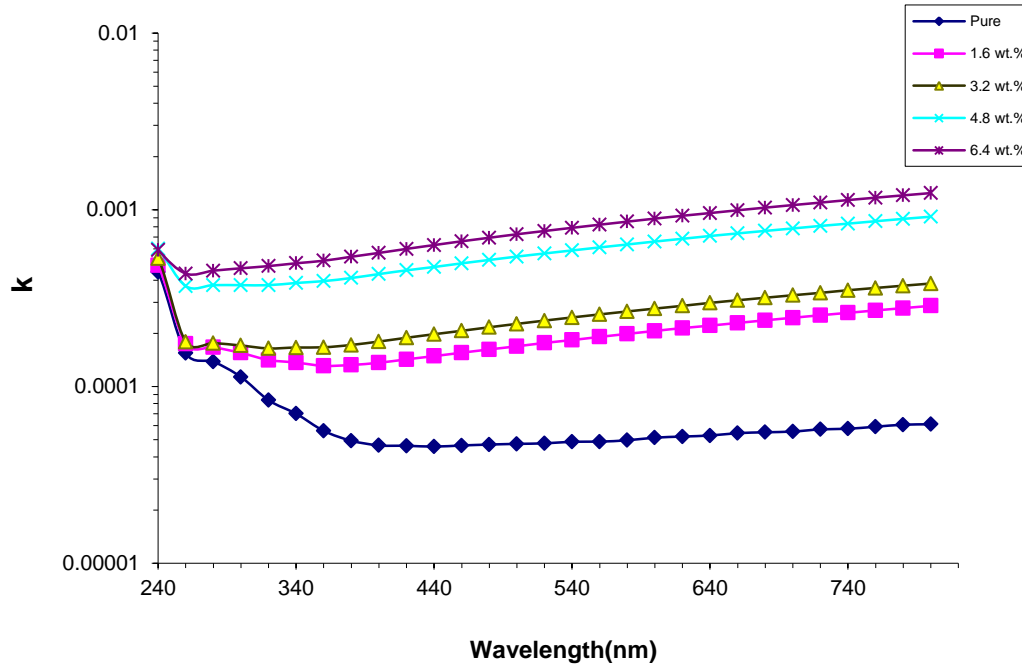


Figure(4.9). The relationship between refractive index of (PVA-PVP- $\text{Co}_2\text{O}_3$ ) and wavelength

### 4.3.6 Extinction Coefficient ( $k$ )

Extinction coefficient ( $k$ ) is determined by an equation (2.18), figure (4.10) depicts the relationship between the extinction coefficient of (PVA-PVP- $\text{Co}_2\text{O}_3$ ) nanocomposites and the wavelength . As can be observed, ( $k$ ) is smaller at low concentrations and increases as the concentration of

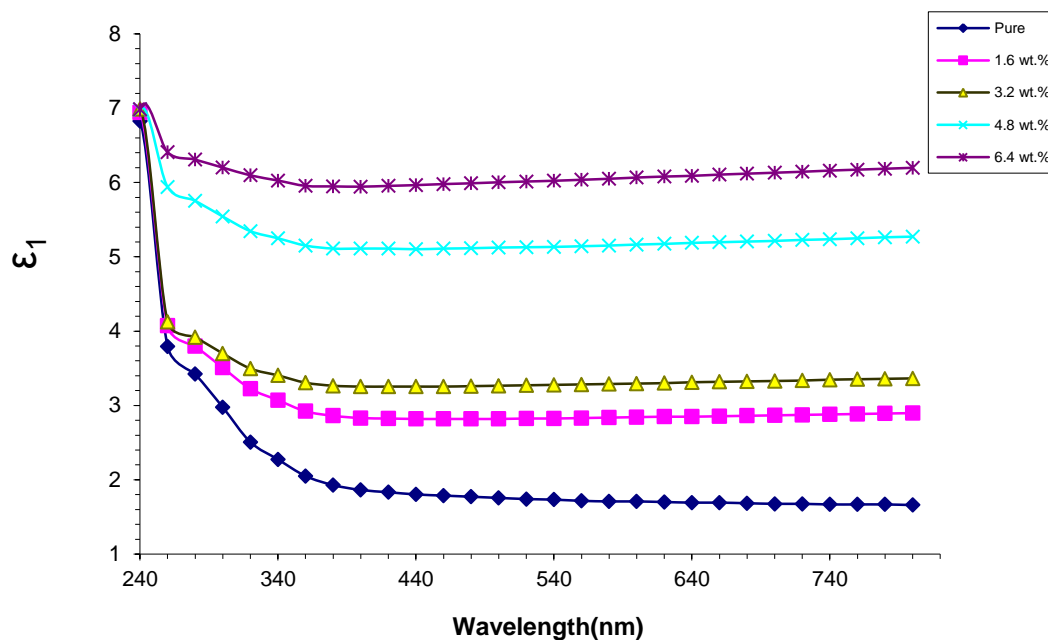
(Co<sub>2</sub>O<sub>3</sub>) nanoparticles increases. This is due to the fact that the absorption coefficient increases as the percentage of (Co<sub>2</sub>O<sub>3</sub>) nanoparticles increases. This finding shows that the host polymer's structure will be altered by the atoms of (Co<sub>2</sub>O<sub>3</sub>) nanoparticles [122].



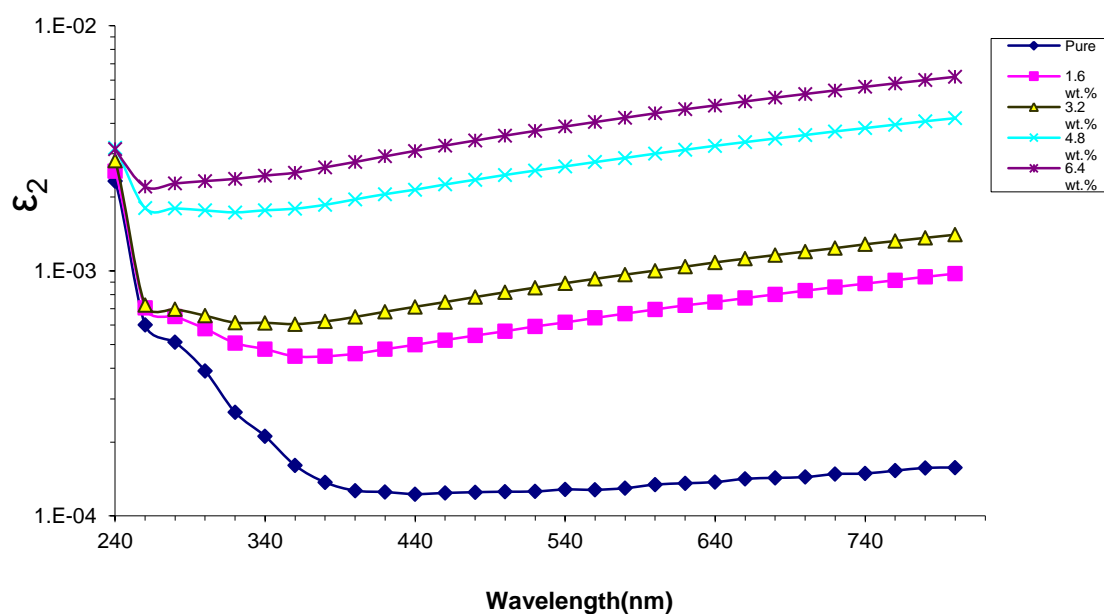
**Figure(4.10). Relationship between extinction coefficient of (PVA-PVP-Co<sub>2</sub>O<sub>3</sub>) and wavelength.**

#### 4.3.7 Real and Imaginary Parts of Dielectric Constant ( $\epsilon_1$ , $\epsilon_2$ )

The dielectric constants for two portions (real and imaginary) of (PVA-PVP-Co<sub>2</sub>O<sub>3</sub>) nanocomposites were determined using equations (2.22) and (2.23) sequentially. Figure (4.11 ) shows the relationship between ( $\epsilon_1$ ) and wavelength. As showed in the figure, ( $\epsilon_1$ ) is very dependent on ( $n^2$ ) because of the low value of ( $k^2$ ), the real dielectric constant increases as the concentrations of (Co<sub>2</sub>O<sub>3</sub>) nanoparticles increase[123]. Figure (4.12 ) shows the relationship between ( $\epsilon_2$ ) and wavelength. As seen in the figure, ( $\epsilon_2$ ) is dependent on ( $k$ ) values, which vary with the absorption coefficient because of the relationship between ( $k$ ) and ( $\alpha$ ) [124].



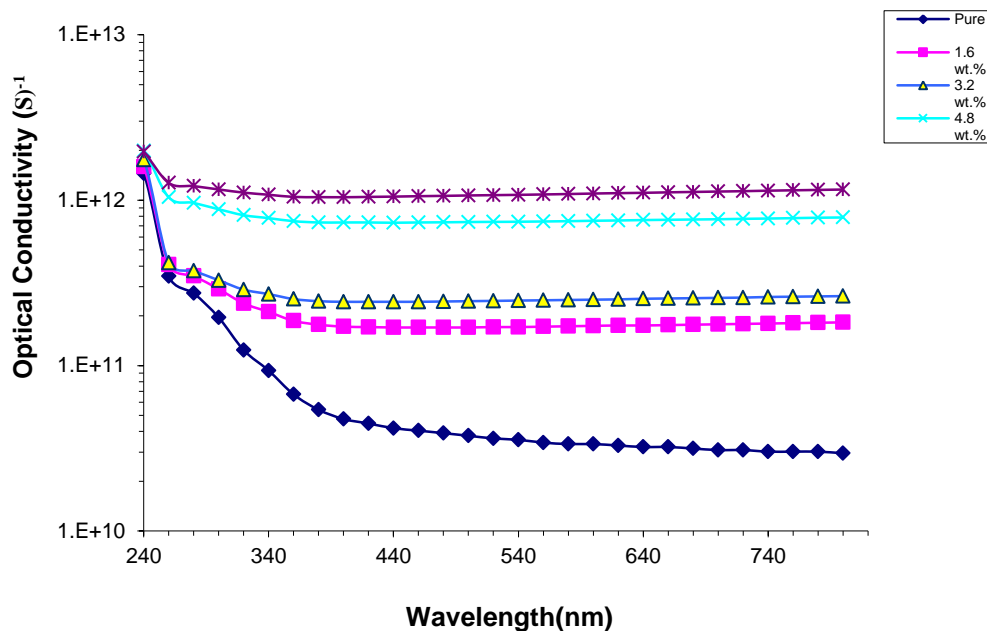
Figure(4.11). The relationship between the real dielectric constant of (PVA-PVP- $\text{Co}_2\text{O}_3$ ) and the wavelength.



Figure(4.12). The relationship between the imaginary dielectric constant of (PVA-PVP- $\text{Co}_2\text{O}_3$ ) and the wavelength.

### 4.3.8 Optical Conductivity ( $\sigma_{op}$ )

The optical conductivity is determined by an equation (2.24). The variation in optical conductivity as a function of wavelength is depicted in figure (4.13). It was discovered that the optical conductivity of (PVA-PVP) increases when the percentages of  $\text{Co}_2\text{O}_3$  in the material increase to (6.4 wt.% ). As a result of the new levels being created in the band gap, electrons are more easily able to move from the valence band to these local levels and finally the conduction band as a result, the band gap narrows and conductivity increase this conclusion agree with Berada *et.al* [125].



Figure(4.13). The relationship between optical conductivity of (PVA-PVP- $\text{Co}_2\text{O}_3$ ) and the wavelength.

### 4.4 - The A.C Electrical Properties of (PVA-PVP- $\text{Co}_2\text{O}_3$ )

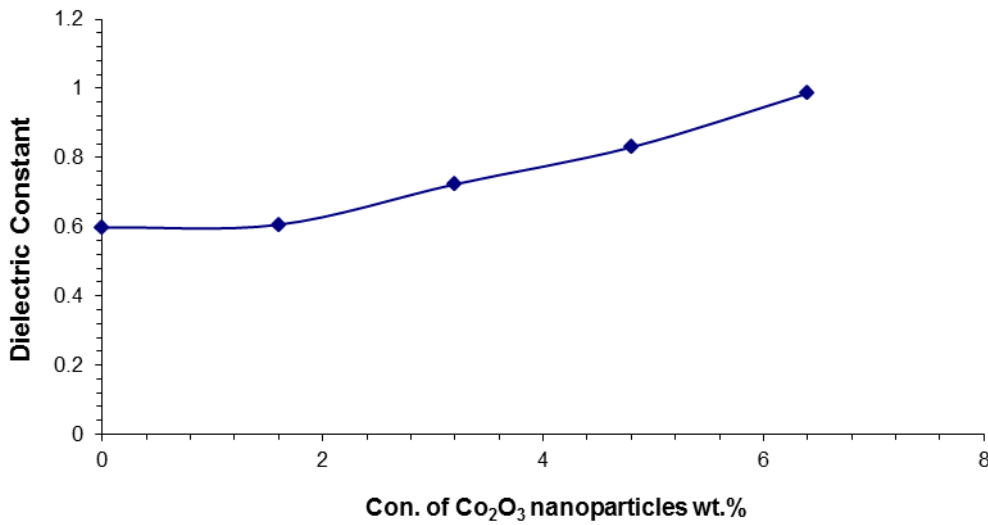
#### Nanocomposites

The (PVA-PVP- $\text{Co}_2\text{O}_3$ ) nanocomposites were investigated for their alternating current (A.C) electrical properties between 100Hz and 5MHz at

room temperature. In order to identify the dielectric constant, that is the most essential of A.C characteristic, we used the equation (2.47). The dielectric loss can be calculated by the dielectric constant and  $(\tan\delta)$ , using the equation (2.41), while A.C electrical conductivity ( $\sigma_{AC}$ ) can be calculated by equation (2.48) by substituting the values of  $(\epsilon'')$ .

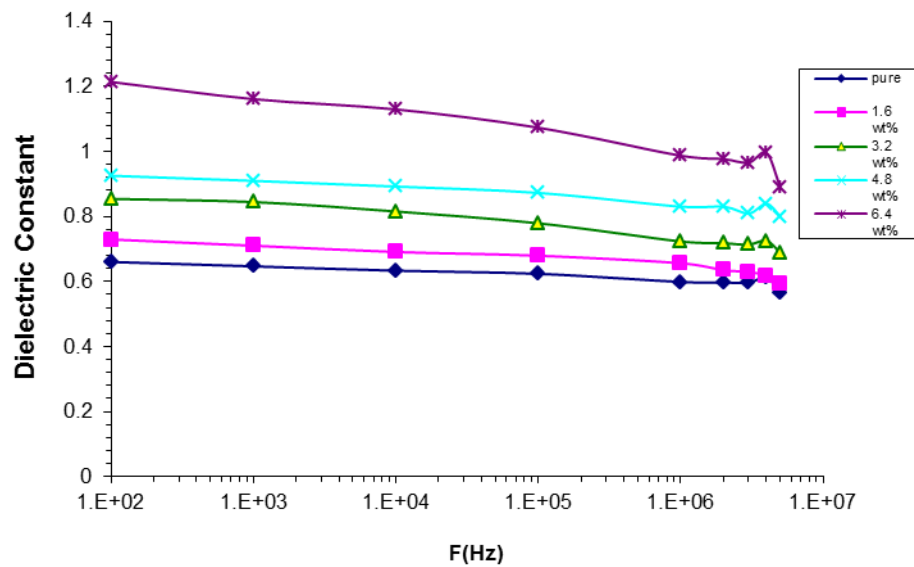
#### 4.4.1 - The dielectric constant for (PVA-PVP- $\text{Co}_2\text{O}_3$ ) nanocomposites

Figure (4.14) shows an increase in the dielectric constant with an increase in the concentration of cobalt oxide. This increase in dielectric constant values is due to an increase in charge carriers and also the creation of a continuous network of  $(\text{Co}_2\text{O}_3)$  ions within the composite [126], This was clearly demonstrated in the microscopic pictures taken for films of (PVA-PVP- $\text{Co}_2\text{O}_3$ ) nanocomposites at various concentrations [127]. When the concentration of the additive is little (1.6wt%), it takes the form of single aggregates and as a result, the dielectric constant decreases. On other hand, when cobalt oxide nanoparticles are present in high concentrations (6.4wt %) , they create a continuous network inside the nanocomposites, increasing the dielectric constant according to the density rate of the cobalt oxide nanoparticles this conclusion agree with Kadaji *et.al* [128].



**Figure (4.14):** The relationship between dielectric constant of (PVA-PVP- $\text{Co}_2\text{O}_3$ ) nanocomposites with a concentration of ( $\text{Co}_2\text{O}_3$ ) nanoparticles

Figure (4.15) shows the variation of the dielectric constant of (PVA-PVP- $\text{Co}_2\text{O}_3$ ) nanocomposites with frequency. The figure shows that the dielectric constant values decrease with increasing applied frequency, the increase of frequencies result in decreasing of space charge polarization to the total polarization. The space charge polarization becomes the more contributing type of polarization at low frequencies, and less contributing with the increase of frequency; this would result in the decrease of dielectric constant values for all samples of (PVA-PVP- $\text{Co}_2\text{O}_3$ ) nanocomposites with the increase of the electric field frequency. The other types of polarizations appear at subsequent frequencies, the ionic polarization reacts slightly to the variation in the field frequencies compared with electronic polarization, this is due to the mass of ion is greater than that of electron. The electrons respond to even the high frequencies of the field vibrations. The low mass of electron makes the electronic polarization was the only type of polarization at higher frequencies. This makes the dielectric constant approximately constant for all samples at high frequencies this conclusion agree with Kadaji *et.al* [128].

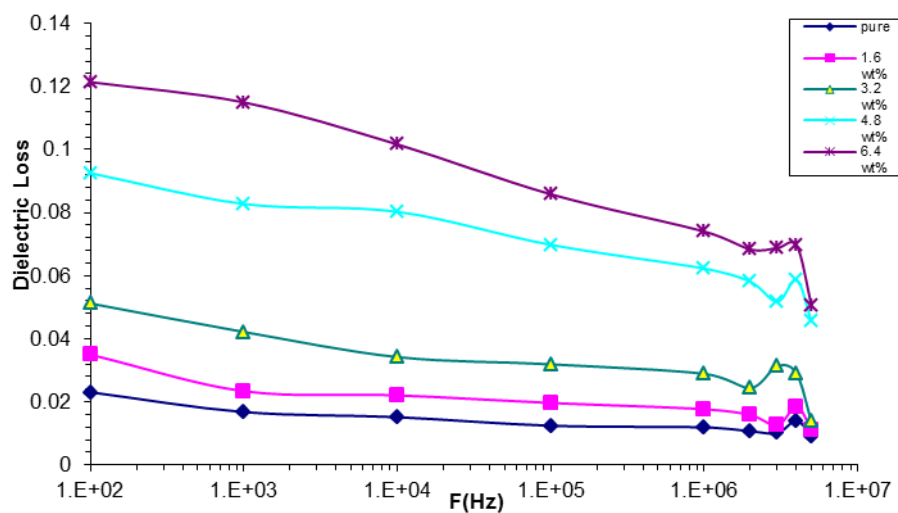


**Figure (4.15):** Variation of the dielectric constant with frequency for (PVA-PVP- $\text{Co}_2\text{O}_3$ ) nanocomposites

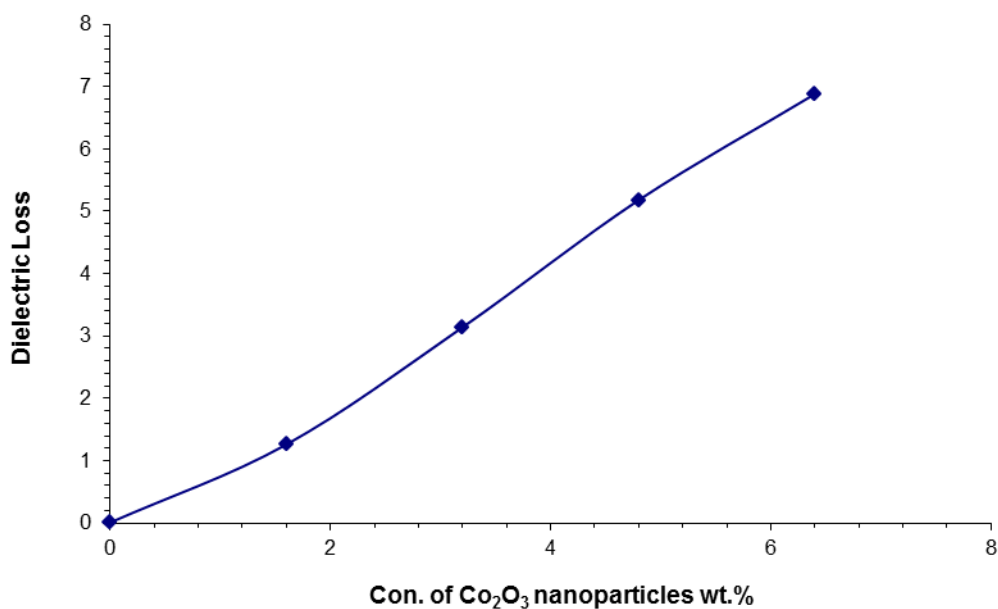
#### 4.4.2 The Dielectric Loss of (PVA-PVP- $\text{Co}_2\text{O}_3$ ) Nanocomposites

Figure (4.16) shows the dielectric loss as a function of the frequency of (PVA-PVP- $\text{Co}_2\text{O}_3$ ) nanocomposites. It is obvious from the figure that the values of dielectric loss are high at low applied frequency but they decrease with increasing of frequency. This attributed to the decrease of the space charge polarization contribution when increasing the frequency. The highest value of the dielectric loss at  $f=100\text{Hz}$  for (PVA-PVP- $\text{Co}_2\text{O}_3$ ) nanocomposites, this value represents the highest dielectric loss at certain frequency, that is the highest absorption of applied field. The absorption happens due to the Maxwell-Wagner phenomenon which is caused by A.C current due to the different of dielectric constant and conductivity of the phases in the nanocomposites [129]. When the frequency is increasing to 2MHz, the dielectric loss is approximately constant for (PVA-PVP- $\text{Co}_2\text{O}_3$ ) nanocomposites. This attributed to the mechanism of other types of polarization that occurs at high frequencies. The value of dielectric loss is

increasing by increasing the concentration of ( $\text{Co}_2\text{O}_3$ ) nanoparticles due to the increase of the charge carriers caused by the increase of ( $\text{Co}_2\text{O}_3$ ) nanoparticles concentration, as shown in figure (4.17).



**Figure (4.16):** Variation of the dielectric loss with frequency for (PVA-PVP- $\text{Co}_2\text{O}_3$ ) nanocomposites



**Figure (4.17):** Variation of dielectric loss with a concentration of ( $\text{Co}_2\text{O}_3$ ) nanoparticles for (PVA-PVP- $\text{Co}_2\text{O}_3$ ) nanocomposites

### 4.4.3 The A.C Electrical Conductivity of (PVA-PVP-Co<sub>2</sub>O<sub>3</sub>) Nanocomposites

Figure (4.18) shows the variation of A.C conductivity of (PVA-PVP-Co<sub>2</sub>O<sub>3</sub>) nanocomposites with Cobalt oxide concentration at 100Hz. The conductivity is increasing with the increase of Cobalt oxide nanoparticles concentration. This increase is due to the effect of the space charge and the formation of a continuous network from Cobalt oxide nanoparticles inside the nanocomposites [130].

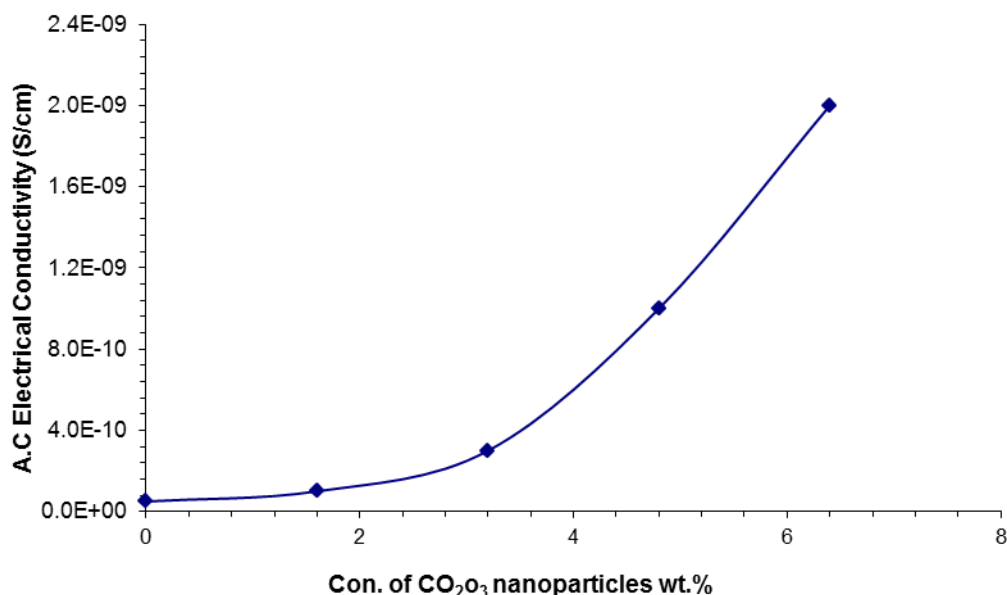


**Figure (4.18):** Variation of the A.C electrical conductivity with different concentrations for (PVA-PVP-Co<sub>2</sub>O<sub>3</sub>) nanocomposites.

Figure (4.19) shows the variation of the A.C conductivity for (PVA-PVP-Co<sub>2</sub>O<sub>3</sub>) nanocomposites with frequency. The figure shows that A.C conductivity increases considerably with the increase of frequency, this attributed to the space charge polarization that occurs at low frequencies, and to the motion of charge carriers by hopping process. The increasing of the conductivity is small at high frequencies, because the electronic polarization

and the charge carriers that travel by hopping process [131]. Consequently, The conductivity is increasing when increasing the frequency for all different rates of Cobalt oxide nanoparticles for (PVA-PVP- $\text{Co}_2\text{O}_3$ ) nanocomposites [132].

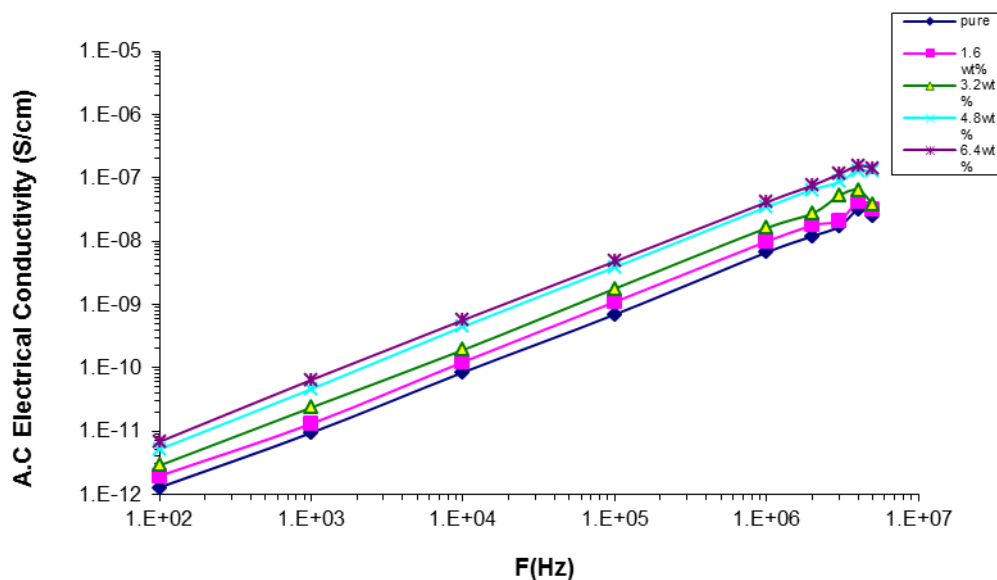
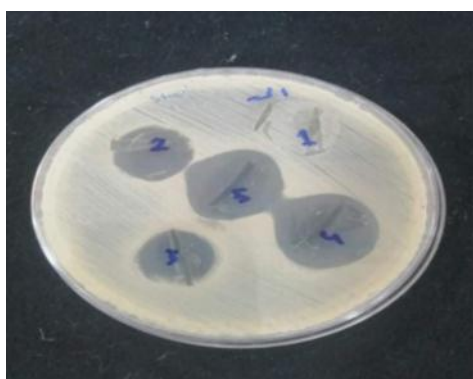


**Figure (4.19):** Variation of the A.C electrical conductivity with frequency for (PVA-PVP- $\text{Co}_2\text{O}_3$ ) nanocomposites.

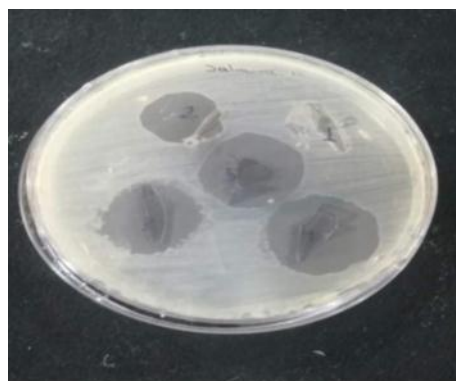
#### 4.5 Application of (PVA-PVP- $\text{Co}_2\text{O}_3$ ) nanocomposites for antibacterial activity.

The (PVA-PVP- $\text{Co}_2\text{O}_3$ ) nanocomposites were tested against gram-positive (*Staphylococcus aureus*) and gram-negative (*Escherichia coli*) bacteria, and the results are shown in figures ( 4.20,4.21,and 4.22 ). The diameter of the inhibition zone grows in proportion to the increase in  $\text{Co}_2\text{O}_3$  content in the polymer matrix, reaching its maximum (26 mm) in the case of a Gram-negative (*Escherichia coli*) compound at the highest ( $\text{Co}_2\text{O}_3$ ) content (6.4 wt percent) in the polymer matrix. Nanocomposite films appear to inhibit the growth of *Escherichia coli* and *Staphylococcus aureus*. The antibacterial activity of nanocomposites films by nanoparticles may be caused primarily

by oxidative stress caused by reactive oxygen species (ROS). Oxidative stress (ROS) includes radicals like  $O_2$ , hydroxyl radicals ( $-OH$ ), and hydrogen peroxide ( $H_2O_2$ ), which may be responsible for damaging bacteria's proteins and DNA ( $^1O_2$ ). The (PVA-PVP- $Co_2O_3$ ) nanocomposites have been shown to have the strongest antibacterial activity against *S. aureus* and *E. coli*, which is attributed to the high antibacterial activity of ( $Co_2O_3$ ) nanoparticles [133,134].



(Staph)



(E.coli)

**Figure (4.20):** Image for inhibition zones of (PVA-PVP- $Co_2O_3$ ) nanocomposite films on *S. aureus* and *E. coli*.

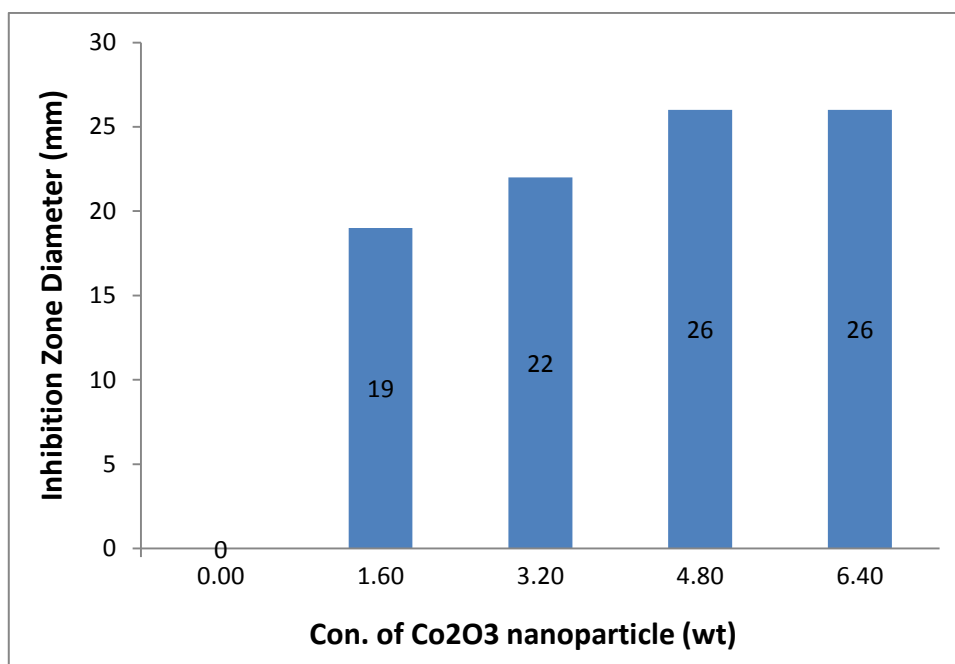


**Figure (4.21):** Variation inhibition zone diameter of (PVA-PVP-Co<sub>2</sub>O<sub>3</sub>) nanocomposite films on *E. coli* with Co<sub>2</sub>O<sub>3</sub> concentration

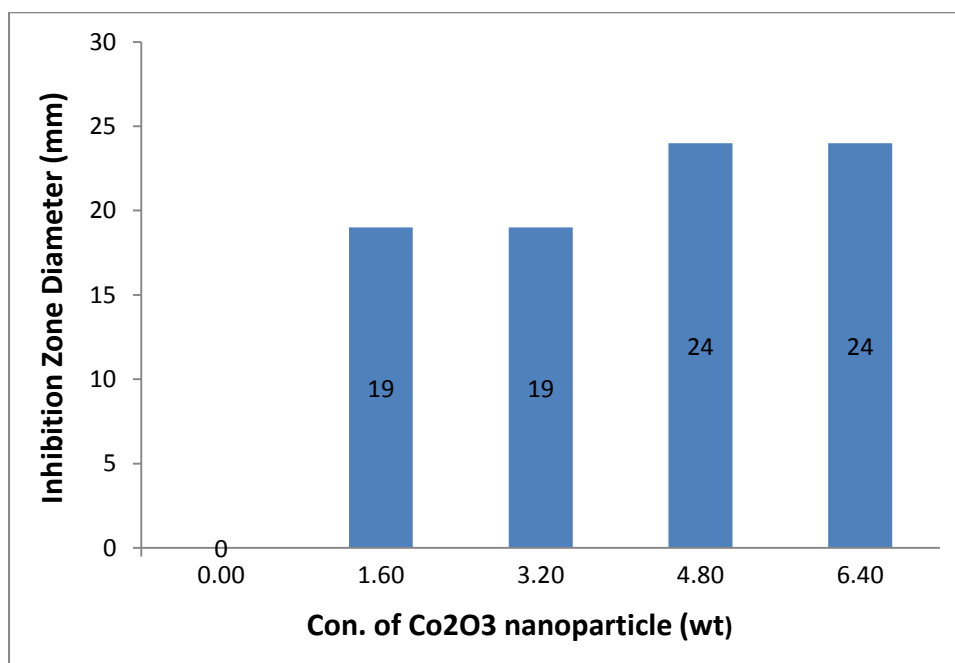


**Figure (4.22):** Variation inhibition zone diameter of (PVA-PVP-Co<sub>2</sub>O<sub>3</sub>) nanocomposite films on *S. aureus* with Co<sub>2</sub>O<sub>3</sub> concentration.

## 4.6 Conclusions

From the obtained results and discussions, the following points are concluded:

1- The optical microscope images show that Cobalt oxide nanoparticles form a continuous network inside the polymers when the ratio of (6.4)wt.%

2-FTIR spectra show a shift in some bands and change in the intensities of other bands comparing with pure (PVA-PVP-Co<sub>2</sub>O<sub>3</sub>) films, this indicates there is no interaction between the polymers and the added nanoparticles.

3- SEM shows the surface morphology of the (PVA-PVP-Co<sub>2</sub>O<sub>3</sub>) nanocomposites films with many aggregates or chunks randomly distributed on the top surface, homogeneous and coherent.

4- The absorbance and absorption coefficient of (PVA-PVP-Co<sub>2</sub>O<sub>3</sub>) nanocomposites increase with the increasing of the concentrations of the (Co<sub>2</sub>O<sub>3</sub>) nanoparticles. The absorption coefficient for all films is less than (10<sup>4</sup>) cm<sup>-1</sup>. Refractive index, extinction coefficient, and dielectric constant (real, imaginary) are increasing with the increasing of concentrations of (Co<sub>2</sub>O<sub>3</sub>) nanoparticles, while the energy gap for indirect transition (allowed, forbidden) decreases with the increasing of the concentrations of (Co<sub>2</sub>O<sub>3</sub>) nanoparticles, the optical conductivity increases as the concentrations of (Co<sub>2</sub>O<sub>3</sub>) in the (PVA-PVP) increase to (6.4 wt.%), these properties can be used for films in solar cells, coatings, and microsensors.

5- The dielectric constant, dielectric loss and A.C electrical conductivity for (PVA-PVP-Co<sub>2</sub>O<sub>3</sub>) nanocomposites are increasing with the increasing (Co<sub>2</sub>O<sub>3</sub>) nanoparticles concentration and decreasing with the increase of frequency of the applied electric field, on the other hand, the A.C electrical conductivity increases with the increase of frequency, these properties can be used for films in capacitors, transistor, and electronic circuits.

6- The inhibition zone diameter increases with the increase in  $\text{Co}_2\text{O}_3$  nanoparticles concentrations .

#### **4.7 Future works**

1- Study the thermal and mechanical properties of (PVA-PVP- $\text{C}_2\text{O}_3$ ) nanocomposites.

2- Study the effect of radiation on some physical properties of (PVA-PVP- $\text{C}_2\text{O}_3$ ) nanocomposites.

3- Study the rheological properties of (PVA-PVP- $\text{Co}_2\text{O}_3$ ) nanocomposites.

### References

- [1] L. Qian , "Application of Nanotechnology for high performance textiles", J. of textile and apparel ,Technology and management ,Vol. 4,No. 1, pp.12-23,( 2004).
- [2] A. H. Doulabi, K. Mequanint, and H. Mohammadi," Blends and Nanocomposite Biomaterials for Articular Cartilage Tissue Engineering", Materials, Vol. 7, No. 7, pp.5327-5355, (2014).
- [3] G.Cao, "Nanostructures and Nanomaterials, Synthesis, Properties and Applications", Imperial College Press, (2004).
- [4] N .Taniguchi," Proc.of International Conference on Precision Engineering", Tokyo, Part II, Japan Society of Precision Engineering, pp.18-23 (1974).
- [5] B.M Baraker, Preeti B Hammannavar and Blaise Lobo\*, "Optical, Electrical, Thermal Properties Of Cadmium Chloride Doped PVA – PVP Blend", Journal of Rheology Special Issue:Associating Polymers,(2015).
- [6]A. J. Hassan, "Study of Optical and Electrical Properties of Nickel Oxide (NiO) Thin Films Deposited by Using a Spray Pyrolysis Technique", Journal of Modern Physics, Vol. 5,pp. 2184-2191, (2014).
- [7] M. Richardon, " Polymer Engineering Composites" , I<sup>st</sup> Ed. Applied Science Publishers Ltd. London , (1977) .
- [8] A.C. Long, "Composites forming technologies", Cambridge England, (2007).
- [9] F. A. Mustafa, "The Structural and Optical Characteristics of polyvinyl Pyrrolidone Doped with Nano Crystal NaF Films", Natural and Applied Sciences Vol. 4, pp.125-141, (2013).
- [10]O. Robert, "Polymer Science and Technology ", Department of Chemical ,Engineering University of Benin, Benin city, Nigeria, (1996).
- [11] G. Al - Adam and H. A , "Technology and Polymer Chemistry", College of Sci., University of Basrah, (1983).
- [12]K. Gabur , " Preparation and Study The Electrical and Optical Properties of (PS-Ni)Composites", M.Sc .Thesis, College of Science, Babylon University, (2010).
- [13] G. Akovali , "Hand book of composites fabrication" , Ankara , (2001).

## References

---

- [14] D. I. Bower, "An Introduction to Polymer Physics", Cambridge University Press, United States of America New York, (2001)
- [15] F. M. AL Jubouri, "Study of the Electrical Properties of (PMMA-Ag) and (PMMA-Ti) nanocomposites," M.Sc. thesis, College of Education for Pure Sciences, University of Babylon, (2013).
- [16] F. Haaf, A. Sanner, and F. Straub, "Polymers of N-vinyl Pyrrolidone: Synthesis, Characterization and Uses", *Polymer Journal*, Vol. 17, No. 1, pp. 143-152, (1985).
- [17] F. Hussain, M. Hojjati, M. Okamoto, and R. E. Gorga, "Polymer-Matrix Nanocomposites, Processing, Manufacturing, and Application: An Overview", *Journal of Composite Materials*, Vol. 40, No. 17, pp. 1511-1575, (2006).
- [18] A. Adeniyi, O. Agboola, E. R. Sadiku, M.O. Durowoju, P.A. Olubambi, A. B. Reddy, I. D. Ibrahim and W. K. Kupolati, "Chapter2-thermoplastic-thermoset nanostructured polymer blends", pp. 1-23, (2016).
- [19] R. Muthuraj, M. Misra and A. K. Mohanty, "Biodegradable compatibilized polymer blends for packaging applications: A literature review ", *Journal of Applied Polymer Sciences*, Vol. 135, No. 24, pp. 1-35, (2017).
- [20] A. H. O. Alkhayatt, A. H. Al-Azzawi and Z. Alakayashi, "Rheological and optical characterization of polyvinyl pyrrolidone (PVP) - polyethylene glycol (PEG) polymer blends", *IOSR Journal of Applied Physics*, Vol. 8, No.1, pp. 11-18, (2016).
- [21] S. P. Masti and R. B. Chougale, "Influence of polyvinyl pyrrolidone on binary blend films made from polyvinyl alcohol/chitosan", *International Research Journal of Environment Sciences*, Vol. 3, No. 3 , pp.11-13, (2014).
- [22] M. A. Kader and A. K. Bhowmick, "Effect of filler on the mechanical, dynamic mechanical, and aging properties of binary and ternary blends of acrylic rubber, fluorocarbon rubber, and polyacrylate", *Journal of applied polymer science*, Vol. 90, No. 1, pp. 278-286, (2003).
- [23] A. Y. Ban, "Development and characterization of ternary thermosetting polymer blends", Ph. D thesis, University of technology, (2010).

## References

---

- [24] M. N. Subramanian, "Basics of polymers fabrication and processing technology", India, Printed in the United States of America, Momentum Press, LLC, pp. 5-108, (2015).
- [25] S. A. Jabbar, F. L. Rashid, A. Hadi, M. A. Habeeb and A. Hashim "Enhancement of optical properties for poly vinyl alcohol by addition of biomaterial", Journal of Chemical and Pharmaceutical Sciences, Vol. 10, No.1, pp. 0974-2115, (2017).
- [26] A. Khan, "CdS nanoparticles with a thermoresponsive polymer: synthesis and properties", J. Nanomater,(2012).
- [27] A. Nikalje, "Nanotechnology and its Applications in Medicine, Medicinal chemistry, and morphological evaluation of gamma radiation irradiated polyp role-based nanocomposites", J Adv Mater Lets Vol. 3,No. 5, pp. 426–432. (2015).
- [28] M. Arifitekhar, "Introduction to Composite Materials", BMEn 5001, (1999).
- [29] M. Dahshan," Introduction to Material Science and engineering", 2nd ,(2002).
- [30] M. Richardson, " Polymer Engineering Composites" , Ist Ed. Applied Science Publishers Ltd. London , (1977).
- [31] B. Hussien, "D.C and A.C Electrical Properties of (PMMA-Al<sub>2</sub>O<sub>3</sub>) Composites", European Journal of Scientific Research, Vol. 52, No. 2,pp. 236-242, (2011).
- [32] B.G.Stereeman, "Solid State Electronic Devices", 2nd Ed. , Practice Hall, Inc. Engle wood Cliffs, N.J. (1980).
- [33] C. J. F. Bottcher, "Theory of Electric Polarization", 2nd Ed., Elsevier Science B.V., Amsterdam, (1993).
- [34] R.M,Mohammed, A.Habbeeb,A.Hashim,"Study Effect of Antimony oxide Nanoparticles on Structural, Optical, and AC Electrical properties of (PEO-PVA) Blend for Antibacterial Applications", international J. of Emerging Trends in Engineering Research,Vol.8,No.8, (2020).
- [35] Sk. M. Begum , M. C. Rao and R. V. S. S. N. Ravikumar, "Cu<sup>2+</sup> doped PVA passivated ZnSe nanoparticles-preparation, characterization and properties", Journal of Inorganic and Organometallic Polymers and Materials, Vol. 23 , No. 2, pp. 350-356, (2013).

## References

---

- [36] N. B. R. Kumar, V. Crasta and B. M. Praveen, "Advancement in microstructural, optical, and mechanical properties of PVA (Mowiol 10-98) doped by ZnO nanoparticles", *Physics Research International*, Vol. 2014, pp. 1-9, (2014).
- [37] N. Othman, N. Azlen and H. Ismail, "Thermal properties of polyvinyl alcohol (PVOH)/Corn starch blend film", *Malaysian Polymer Journal*, Vol. 6, No. 6, pp. 147-154, (2011).
- [38] A. A. M. Shehab, E. Y. Abid and S. H. Salman, "Studying the structural and optical properties of PVA doped with CuO and FeCl<sub>3</sub> composites films", *Engineering & Technology Journal*, Vol. 33, No. 9, pp. 1712-1722, (2015).
- [39] J. Selvi, S. Mahalakshmi and V. Parthasarathy, "Synthesis, structural, optical, electrical and thermal studies of poly(vinyl alcohol)/CdO nanocomposite films", *Journal of Inorganic and Organometallic Polymers and Materials*, Vol. 27, pp. 1918-1926, (2017).
- [40] S. K. Das, M. Hasan, J. M. M. Islam, M. A. Khan, Md. A. Gafur and E. Hoque, "Characterization of solution casting derived carbon nanotube reinforced poly(vinyl alcohol) thin films", *International Journal of Plastics Technology*, Vol. 21, No. 2, pp. 338-350, (2017).
- [41] P. Kanakasabai, A. P. Deshpande, S. Varughese, "Novel polymer electrolyte membranes based on semi-interpenetrating blends of poly (vinyl alcohol) and sulfonated poly (ether ether ketone)", *Journal of Applied Polymer Science*, Vol. 127, No. 3, pp. 2140-2151, (2013).
- [42] A. Chaturvedi, A. K. Bajpai, J. Bajpai, "Preparation and characterization of polyvinyl alcohol Cryogel-silver nanocomposites and evaluation of blood compatibility, cytotoxicity, and antimicrobial behaviors", *Polymer Composites*, Vol. 36, No.11, pp. 1983-1997, (2015).
- [43] EM. Abdelrazek, AM. Abdelghany and AE. Tarabih, "Characterization and physical properties of silver/PVA nano- composite", *Research Journal of Pharmaceutical, Biological and Chemical Sciences*, Vol. 3, No. 4, pp. 448-459, (2012).
- [44] P. Jayakrishnan and M. T. Ramesan, "Synthesis, characterization, electrical conductivity and materialn properties of magnetite/ polyindole /poly(vinyl alcohol) blend nanocomposites", *Journal of Inorganic and Organometallic Polymers and Materials*, Vol. 27, No.1, pp. 323-333, (2017).

## References

---

- [45] F.L.Martien,"Encyclopedia of Polymer Science and Engineering", Wiley, New York, (1986).
- [46] Z.Ping,Q.T.Nguyen,A.Essamri,and J.Ne'el, *Macromol. Chem. Phys, Polym. Adv. Technol*, No. 195,pp.21,(1994).
- [47] M.T. Razzak, Zainuddin, Erizal, S.P. Dewi, H. Lely, E. Taty ,and Sukirno, "The Characterization of Dressing Component Materials and Radiation Formation of PVA-PVP Hydrogel", *Radiat. Phys. Chem.*, Vol. 55,No. 2, pp.153–165,(1999).
- [48] D.C.Liu,C.H.Tasil,D.Liaw,J.H.Ho,B.Y. Liaw ,and T.L.Ho,"Effects of Gamma Radiation on Various Polyimides", *J.of the Chinese Chemical Society*, Vol.47,pp.583-588,(2000).
- [49] S. S. Kanakillam, B. Krishnan, D. A.Avellaneda, & S. Shaji, "A simple synthesis of ZnO: Co<sub>2</sub>O<sub>3</sub> nanocomposites by pulsed laser irradiation in liquid". *Materials Today: Proceedings*, Vol.33,pp. 1444-1452,(2020).
- [50] R.J. Sengwa, S. Sankhla, and S. Choudhary, “ studied dielectric characterization of solution intercalation and melt intercalation poly(vinyl alcohol)-poly(vinyl pyrrolidone) blend-montmorillonite clay nanocomposite films”, *India Journal of Pure/Applied Physics*. Vol.48, pp.196-204, (2010).
- [51] K. Sivaiah, K. Kumar, V. Naresh and S. Buddhudu, "Structural and Optical Properties of Li<sup>+</sup>: PVP & Ag<sup>+</sup>: PVP Polymer Films," *Materials Sciences and Applications*, Vol. 2, No. 11, pp. 1688-1696, (2011).
- [52] X. Zhu, J. Wang, D. Nguyen, J. Thomas, R. A. Norwood, and N. Peyghambarian, “Linear and nonlinear optical properties of Co<sub>3</sub>O<sub>4</sub> nanoparticle-doped polyvinyl-alcohol thin films,” *Opt. Mater. Express*, Vol. 2, No. 1, pp. 103, (2012).
- [53] M. Ghanipour,and D. Dorrnian,"Effect of Ag-Nanoparticles Doped in Polyvinyl Alcohol on the Structural and Optical Properties of PVA Films", *J.of Nanomater*.Vol. 2013,pp. 1-10, (2013).
- [54] ] M. A. Habeeb,"Effect of Nanosilver Particles on Thermal and Dielectric Properties of (PVA-PVP) Films",*International J. of Applied and Natural Sciences (IJANS)*, Vol. 2,No. 4, pp. 103-108,(2013).
- [55] H.N.Chandrakala, Shivakumaraiah, H. Somashekarappa, R. Somashekar,S. Chinmayee and Siddaramaiah," Polyvinyl Alcohol/Zincoxide-Ceriumoxide Nanocomposites: Electrical, Optical,

## References

---

Structural and Morphological Characteristics", *Indian Journal of Advances in Chemical Science*, Vol. 2, pp. 103-106,(2014).

[56] K. J. Kadhim, I. R. Agool and A. Hashim , "Enhancement in Optical Properties of (PVA-PEG-PVP) Blend By the Addition of Titanium Oxide Nanoparticles for Biological Application", *Advances in Environmental Biology*, Vol.10, pp.81-87,(2016).

[57] M. Karpuraranjith, and S. Thambidurai, "Chitosan/zinc oxide-polyvinyl pyrrolidone (CS/ZnO-PVP) nanocomposite for better thermal and antibacterial activity", *International Journal of Biological Macromolecules*, Vol. 104, pp. 1753-1761, (2017).

[58] F.M. Ali, R. M. Kershi, M. A. Sayed, Y. M. AbouDeif "Evaluation of structural and optical properties of Ce<sup>3+</sup> ions doped (PVA/PVP) composite films for new organic semiconductors" *Physica B: Condensed Matter*, Vol. 538, pp. 160-166, (2018).

[59] H. Khalid, H. Al-Attiyah<sup>1</sup>, A. Hashim, "Fabrication of novel (carboxymethylcellulose–polyvinyl Pyrrolidone –polyvinyl alcohol)/lead oxide nanoparticles nanocomposites have high attenuation coefficients for gamma rays shielding applications", *International Journal of Plastics Technology*,(2019).

[60] Q. Jebur, A. Hashim, , & M. Habeeb, " Fabrication, Structural and Optical properties for (Polyvinyl Alcohol–Polyethylene Oxide–Iron Oxide) Nanocomposites", *Egyptian Journal of Chemistry*, Vol. 63, No. 2, pp. 611-623, (2020).

[61] A. A. Abid, Sameer H. Al-nesrawy and A. R. Abdulridha, "New Fabrication (PVA-PVP-C.B) Nanocomposites: Structural and Electrical Properties " *Journal of Physics: Conference Series* , Vol. 1804 , pp. 012037, (2021).

[62] Y. Cao, C. Shen, Z. Yang, Z. Cai, Z. Deng, & D. Wu, "Polycaprolactone/polyvinyl pyrrolidone nanofibers developed by solution blow spinning for encapsulation of chlorogenic acid". *Food Quality and Safety*,(2022).

[63] Q. Feng, Zhimin Dang, Na Li and Xiaolong Cao "Studied the preparation and dielectric property of Ag/PVA nano-composite", *Materials Sci. and Eng. B*, Vol. 99, pp. 325-328 (2003).

## References

---

- [64] T.O. Owolabi, M.A. Abd Rahman, "Modeling the Optical Properties of a Polyvinyl Alcohol-Based Composite Using a Particle Swarm Optimized Support Vector Regression Algorithm", *Polymers*, Vol. 13, No. 16, pp. 2697, (2021).
- [65] R. Khaleel, "Electrical and Optical Properties Modification of Poly (Vinyl Chloride) by Zinc, Copper and Nickel EthylXanthate Chelate Complexes", M. Sc. Thesis, University of Mustansiriah, Collage of Science, (2004).
- [66] S. Shekhar, V. Prasad, S. V. Subramanyam, "Structural and electrical properties of composites of polymer-iron carbide nanoparticle embedded in carbon" *J. Els., Sci.*, Vol.18, (2006).
- [67] O.Stenz," The physics of thin film optical spectra", *An Introduction*, Winzerlaer Str. 10, 07745 Jena Germany, pp.71-72, (2005).
- [68] C. Mwolfe, N. Holouyak and G. B. Stillman, "Physical properties of semiconductor", prentice Hall, New York,(1989).
- [69] H. R. A. AL-Dawodi," A study of the structural and optical properties of obliquely deposited (CdS) thin films", M.Sc. Thesis, University Al-Mustansiriyah, College of Science,(2010).
- [70] A. G. Nilens, "deep imparity in semiconductors" , Wiley -Interscience pub., (1973).
- [71] Q. Li1, Q. Z. Xue, X. L. Gao, Q. B. Zheng, "Temperature dependence of the electrical properties of the carbon nanotube/polymer composites", *Express Polym., Lett.*3, Vol.12, pp. 769–777, (2009).
- [72] S. S. Chiad, N. F. Habubi, S. F. Oboudi and M. H. Abdul-Allah, "Effect of Thickness on The Optical Parameters of PVA: Ag", *Diyala Journal for pure Sciences*, Vol. 7, No. 3, (2011).
- [73] A. Hashim, "Experimental Study of Electrical Properties of (PVA-CoNO<sub>3</sub>, AgCO<sub>3</sub>) Composites", *American J. of Sci., Res.*, 68, pp. 56- 61, (2012).
- [74] T. R. Dhakal, Mishra, R. Sanjay, Glenn, Zachery, Rai, K. Binod "Synergistic Effect of PVP and PEG on the Behavior of Silver Nanoparticle-Polymer Composites", *J. of Nanoscience and Nanotechnology*, Vol.12, pp. 6389-6396, (2012).

## References

---

- [75] S. M. Hassan, "Optical Properties of Prepared Polyaniline and Polymethyl methacrylate blends", *International Journal of Application or Innovation in Engineering & Management (IJAIEM)*, Vol. 2, No. 9, pp. 232-235, (2013).
- [76] M. Sauer, J. Hofkens and J. Enderlein, *Handbook of Fluorescence Spectroscopy and Imaging, from Single molecules to Ensembles*, Wiley-VCH Verlag GmbH & Co. KGaA, Weinheim, Germany, (2011).
- [77] M. A. Al-Alousi, "The Effect of Substrate Temperature and The Annealing Time on the Optical Properties of The AgInS<sub>2</sub> Thin Films Prepared by chemical spray Pyrolysis Technique", *J. of University of Anbar for pure science* 4, (2010).
- [78] M. Abdelaziz and E. M. Abdelrazek, Effect of Dopant Mixture on Structural, Optical and Electron Spin Resonance Properties of Polyvinyl Alcohol, *Physica B*, Vol. 390, pp. 1-9, (2007).
- [79] H. N. Najeeb, G. A. Wahab Ali, A. K. Kodeary, J. Ali, "Doping Effect on Optical Constants of Poly-Vinyl Chloric (PVC)", *Academic Research International*, Vol.4, pp. 53-62, (2013).
- [80] M. I. Baker, S. Walsh, Z. Schwartz and B. D. Boyan, A Review of Polyvinyl Alcohol and its Uses in Cartilage and Orthopedic Applications, *Journal of Biomedical Materials Research: Applied Biomaterials* 9999B, (2012).
- [81] M. Meyyappa, *Nanotechnology Measurement Handbook, A Guide to Electrical Measurements for Nanoscience Applications*, 1st Edition, Keithley Instruments, Inc., USA, (2007).
- [82] M. Tyagi and D. Tyagi, "Polymer Nanocomposites and their Applications in Electronics Industry", *International Journal of Electronics and Electrical Engineering*, Vol. 7, pp. 603-608, (2014).
- [83] N. K. Abbas, M. A. Habeeb, and A. J. K. Algidsawi, "Influence of Prepared Chloropenta Amine Cobalt (III) Chloride Nanoparticles on The Dielectric Properties of PVA Film", *Australian Journal of Basic and Applied Sciences*, Vol. 9, pp. 26-34, (2015).
- [84] N. A. Azahari, N. Othman and H. Ismail, "Biodegradation Studies of Polyvinyl Alcohol/Corn Starch Blend Films in Solid and Solution Media", *Journal of Physical Science*, Vol. 22, pp.15-31, (2011).

## References

---

- [85] N. B. R. Kumar, V. Crasta, R. F. Bhajantri and B. M. Praveen, "Microstructural and Mechanical Studies of PVA Doped with ZnO and WO<sub>3</sub> Composites Films", *Journal of Polymers*, Vol. 2014, (2014).
- [86] N. C. Jeevan, B. R. N. Babu, and K. Chandrashekara, "Characteristic Analysis of Mechanical Properties on Carbon Fiber Reinforced Plastic", *International Journal of Research in Engineering & Advanced Technology (IJREAT)*, Vol. 3, pp. 305-308, (2015).
- [87] N. E. Hill, W. E. Vaughan, A. H. Price, and M. Davis, "Dielectric Properties and Molecular Behavior", Van Nostrand, London, (1969).
- [88] N. Saba, M. Tahir and M. Jawaid, A Review on Potentiality of Nano Filler/Natural Fiber Filled Polymer Hybrid Composites, *Polymers*, Vol. 6, pp. 2247-2273, (2014).
- [89] S. Wen and D. D. L. Chung, "Electric Polarization in Carbon Fiber-Reinforced Cement", *Cement and Concrete Research*, Vol. 31, pp.141-147, (2001).
- [90] L. Solymar and D. Walsh, "Electrical Properties of Materials, 7<sup>th</sup> Edition", Oxford University Press, Oxford, New York, (2004).
- [91] D. J. Griffith, Introduction to Electrodynamics 3<sup>rd</sup> Edition, Prentice Hall, Inc., New Jersey, USA, (1999).
- [92] S. O. Gladkov Dielectric Properties of Porous Media, Springer- Verlag Berlin Heidelberg, New York, USA, (2003).
- [93] T. I. Zohdi, Electromagnetic Properties of Multiphase Dielectrics, A Primer on Modeling, Theory and Computation, Springer-Verlag Berlin, Heidelberg, Berkeley, USA, (2012).
- [94] W. Gao and N. M. Sammes, An Introduction to Electronic and Ionic Materials, World Scientific Publishing Co. Pte. Ltd., Singapore, (1999).
- [95] A. Chelkowski, "Dielectric physics", 1st edition, pwin-polish sci. Pub. (1980).
- [96] O. G. Abdullah, S. A. Hussien, and A. Alani, "Electrical Characterization of Polyvinyl Alcohol Films Doped with Sodium Iodide", *Asian Transactions on Science & Technology*, Vol. 1, No. 4, (2011).
- [97] L. A. Prystaj, Effect of Carbon filler Characteristics on the Electrical Properties of Conductive Polymer Composites Possessing Segregated

## References

---

Network Microstructures, MSc. Thesis, The Academic Faculty, Georgia Institute of Technology, (2008).

[98]H. I. Jafar, N. A. Ali and A. Shawky, "Study of A.C Electrical Properties of Aluminum-Epoxy Composites", *Journal of Al-Nahrain University*, Vol.14, pp.77-82, (2011).

[99]T. Seghier and F. Benabed, Dielectric Properties Determination of High Density Polyethylene (HDPE) by Dielectric Spectroscopy, *International Journal of Materials, Mechanics and Manufacturing* 3, (2015).

[100]T. Blythe and D. Bloor, *Electrical Properties of Polymers*, 2<sup>nd</sup> Edition, Cambridge University Press, UK, (2005) .

[101]R. C. Dorf, *The Electrical Engineering Hand Book*, CRC Press LLC, 2<sup>nd</sup> Edition, Piscataway, New Jersey, USA, (2000).

[102]R. S. A. Al-Khafaji, Study the Effect of Iraqi Bentonite Clay addition on the Properties of Porcelain Body Prepared from Local Clays, PhD. Thesis, College of Education/Ibn Al-Haithem, University of Baghdad, (2009).

[103]C. V. S. Reddy, X. Han, Q. Y. Zhu, L. Q. Mai and W. Chen, "Dielectric Spectroscopy Studies on (PVP-PVA) Poly blend Film", *Microelectronic Engineering*, Vol. 83, pp. 281-285, (2006).

[104]I. Yucedag, A. Kayab, S. Altındalc and I. Uslu," Frequency and Voltage-Dependent Electrical and Dielectric Properties of Al/Co-doped PVA/p-Si Structures at Room Temperature", *Chin. Phys. B*, Vol. 23, pp. 047304, (2014).

[105] A. Azam, A. S. Ahmed, M. Oves, M. S. Khan, S. S. Habib and A. Memic, "Antimicrobial activity of metal oxide nanoparticles against gram-positive and gram-negative bacteria: A comparative study", *International Journal of Nanomedicine*, Vol. 7, pp. 6003-6009, (2012).

[106] Z. Si-Wei, G. Chong-Rui, H. Ying-Zhu, G. Yuan-Ru and P. Qing-Jiang , "The preparation and antibacterial activity of cellulose/ZnO composite: A review", *De Gruyter* , Vol. 16, No.1, pp. 9-20, (2018).

[107] N. Tran, A. Mir, D. Mallik, A. Sinha, S. Nayar and TJ. Webster, "Bactericidal effects of iron oxide nanoparticles on staphylococcus aureus", *International Journal of Nanomedicine* , Vol. 5, pp. 277-283, (2010).

## References

---

- [108] A. Azam, A. Ahmed, M. Oves, M. Khan and A. Memic, "Size-dependent antimicrobial properties of CuO nanoparticles against gram-positive and -negative bacterial strains", *International Journal of Nanomedicine*, Vol. 7, pp. 3527-3535, (2012).
- [109] KR. Raghupati, RT. Koodali and AC. Manna, "Size-dependent bacterial growth inhibition and mechanism of antibacterial activity of zinc oxide nanoparticles", *Langmuir*, Vol. 27, pp. 4020-4028, (2011).
- [110] M. Singh, S. Singh, S. Prasada and I. Gambhir, "Nanotechnology in medicine and antibacterial effect of silver nanoparticles", *Digest Journal of Nanomaterials and Biostructures*, Vol. 3, No. 3, PP. 115-122, (2008).
- [111] V. Monzillo, C. D. Valle, M. Corbella, E. Percivalle, D. Sasser, D. Scevola and P. Marone, "Antibacterial activity and cytotoxic effect of SIAB-GV3", *Journal New of Microbiology*, Vol. 37, pp. 535-541, (2014).
- [112] M. A. Ansari, H. M. Khan, A. A. Khan, A. Sultan, A. Azam, M. Shahid and F. Shujatullah, "Antibacterial activity of silver nanoparticles dispersion against mssa and mrsa isolated from wounds in a tertiary care hospital of north india", *International Journal of Applied Biology and Pharmaceutical Technology*, Vol. 2, No. 4, pp. 34-42, (2011).
- [113] S. A. Salman, Z. A. Al-Ramadhan and Z. F. Nazal, "Optical Properties Of Polyvinyl Alcohol (PVA) Films Doped With CoCH<sub>3</sub>COOH salt", *Diyala journal for pure sciences*, Vol. 10, No. 3, pp. 30-38, (2014).
- [114] S. Bhavani, M. Ravi, and V. V. R. N. Rao, "Studies on Electrical Properties of PVA: NiBr<sub>2</sub>Complexed Polymer Electrolyte Films for Battery Applications", *International Journal of Engineering Science and Innovative Technology (IJESIT)*, Vol. 3, pp. 426-434, (2014).
- [115] M. A. Habeeb and L. A. Hamza, "Structural, Optical and DC Electrical Properties of (PVA-PVP-Y<sub>2</sub>O<sub>3</sub>) Films and Their Application for Humidity Sensor," *J. Adv. Phys.*, Nol. 6, No. 1, pp. 1–9, (2017).
- [116] E. M. Abdelrazek, A. M. Abdelghany and A.E. Tarabih, "Characterization and Physical Properties of Silver/PVA nano- composite", *Research Journal of Pharmaceutical, Biological and Chemical Sciences*, Vol. 3, pp. 448-459, (2012).
- [117] S. M. Sze and Kwok, and K. Ng "Physics of semiconductor devices" 3rd, National Chiao Tung Uni., John Wiley and Sons, Inc, Publication, (2007).

## References

---

- [118] S. Mustafa, "Engineering Chemistry", Library of Arab society for publication and distribution, Jordan, (2008).
- [119]R. G. Kadhim, Study of Some Optical Properties of Polystyrene-Copper Nanocomposite Films, World Scientific News, Vol. 30, pp.14-25, (2016).
- [120]G. A. AL-Dahash, H. N. Najeeb, A. Baqer and R. Tiama," The Effect of Bismuth Oxide  $\text{Bi}_2\text{O}_3$  on Some Optical Properties of Poly vinyl Alcohol", British Journal of Science, Vol. 4, pp.117-124, (2012).
- [121]R. A. Abed and M. A. Habeeb," Preparation and Study Optical Properties of (PVA-PVP-CrCl<sub>2</sub>) Composites", Industrial Engineering Letters, Vol. 3, pp. 60-66, (2013).
- [122]H. Neama, N. AL-Khegani, "The Effect of Ferrous Chloride (FeCl<sub>2</sub>) on Some Optical Properties of Polystyrene", Academic Research International, Vol. 5, pp. 161-166, (2014).
- [123] Md J. Uddin, B. Chaudhuri, K. Pramanik, T. R. Middya and B. Chaudhuri ," Black tea leaf extract derived Ag nanoparticle-PVA composite film: Structural and dielectric properties", J. Materials science and Engineering B, Vol. 177 ,No.20, pp.1741- 1747, (2012).
- [124] T. S. Bachari, "Electric Properties of Polyvinyl Acetate (PVA)-Polyol and Prepared Sulfonated Phenol-formaldehyde Resin (SPF) Bulk Samples Composite", Asian Journal of Applied Science and Engineering, Vol. 3, pp. 33-44, (2014).
- [125] T. Beraada and G. al- Adam, " The Updated Chemistry of Large Molecules", University of Basrah, (1989).
- [126] T. H. C. Salsa, C. B. Lombello and M. Akira, "Electro spinning of Gelatin/Poly (Vinyl Pyrrolidone) Blend from Water/Acetic Acid Solutions", Materials Research, Vol. 18, pp. 509-518, (2015).
- [127] T. S. Gaza, A. Sulong, M. N. Akhtar, A. H. Kadhum, A. Mohamad, and A. A. Al-Amery, "Properties and Applications of Polyvinyl Alcohol, Halloysite Nanotubes and Their Nanocomposites", Molecules, Vol. 20, No.12, pp. 22833-22847, (2015).
- [128] V. G. Kadajji and G. V. Betageri, "Water Soluble Polymers for Pharmaceutical Applications", Polymers, Vol. 3, No.4, pp. 1972-2009, (2011).

## References

---

- [129] P. Raju and S. R. Murthy, "Microwave-hydrothermal Synthesis of CoFe<sub>2</sub>O<sub>4</sub>-TiO<sub>2</sub> Nanocomposites", *Advanced materials letters*, Vol.4, No.1, pp. 99-105, (2013).
- [130] Z. F. Nazzal, *Physical Properties of Polymer (PVA Doped With Cobalt Salts)*, M.Sc. Thesis, College of Sciences, University of Diyala, (2013).
- [131] G. Shui, J. Hu, M. Qiu, M. Wei, D. Xiao and J. Chinese chem. "Study of Dielectric Properties For (Calcium Oxide-poly-vinyl alcohol)Composites", *letters*, Vol. 15, No. 12, pp.1501-1504, (2004).
- [132] S. A. Salman, N. A. Bakr and M. H. Mahmood, "Preparation and Study of Some Electrical Properties of PVA-Ni(NO<sub>3</sub>)<sub>2</sub> Composites", *International Letters of Chemistry, Physics and Astronomy*, Vol. 40, pp. 36-42, (2015).
- [133] Y.T. Prabhu, K.V. Rao, B.S. Kumari, V.S.S. Kumar, and T. Pavani, "Synthesis of Fe<sub>3</sub>O<sub>4</sub> nanoparticles and its antibacterial application", *International Nano Letters*, Vol. 5, No. 2, pp. 85–92, (2015).
- [134] S.S. Behera, J.K. Patra, K. Pramanik, N. Panda, and H. Thatoi, "Characterization and Evaluation of Antibacterial Activities of Chemically Synthesized Iron Oxide Nanoparticles", *World Journal of Nano Science and Engineering*, Vol. 2, No. 4, pp. 196–200, (2012).